

2011

Three essays on commodity futures and options markets

Na Jin

Iowa State University

Follow this and additional works at: <https://lib.dr.iastate.edu/etd>

 Part of the [Economics Commons](#)

Recommended Citation

Jin, Na, "Three essays on commodity futures and options markets" (2011). *Graduate Theses and Dissertations*. 10377.
<https://lib.dr.iastate.edu/etd/10377>

This Dissertation is brought to you for free and open access by the Iowa State University Capstones, Theses and Dissertations at Iowa State University Digital Repository. It has been accepted for inclusion in Graduate Theses and Dissertations by an authorized administrator of Iowa State University Digital Repository. For more information, please contact digirep@iastate.edu.

Three essays on commodity futures and options markets

by

Na Jin

A dissertation submitted to the graduate faculty
in partial fulfillment of the requirements for the degree of

DOCTOR OF PHILOSOPHY

Major: Economics

Program of Study Committee:

Dermot Hayes, Co-major Professor

Sergio Lence, Co-major Professor

Ananda Weerasinghe

Chad Hart

Helle Bunzel

Iowa State University

Ames, Iowa

2011

Copyright © Na Jin, 2011. All rights reserved.

DEDICATION

To Li Yu, Fiona and Olivia

TABLE OF CONTENTS

LIST OF TABLES	vi
LIST OF FIGURES	vii
ACKNOWLEDGEMENTS	ix
CHAPTER 1. OVERVIEW	1
CHAPTER 2. The Long-Term Structure of Commodity Futures	3
2.1 Introduction	3
2.2 Schwartz's Model and A Generalization	6
2.2.1 <i>Price Mean Reversion</i>	8
2.2.2 <i>Seasonality</i>	9
2.3 Futures Pricing	10
2.4 Empirical Analysis	11
2.4.1 <i>Description of the Data</i>	13
2.4.2 <i>Empirical Method</i>	13
2.5 Estimation Results	16
2.5.1 <i>Lean Hog Market</i>	16
2.5.2 <i>Soybean Market</i>	19
2.5.3 <i>Comparison Among Models</i>	23
2.5.4 <i>95 Percent Credible Band of Futures Prices</i>	24
2.6 Conclusion	27
2.7 Appendix	28
2.7.1 Appendix A	28
2.7.2 Appendix B	29

2.7.3	Appendix C	30
2.7.4	Appendix D	31
CHAPTER 3. Price Mean Reversion, Seasonality, and Options Markets		36
3.1	Introduction	36
3.2	Graphical examples	39
3.3	Schwartz's model and generalization	41
3.3.1	<i>Price mean reversion</i>	42
3.3.2	<i>Seasonality</i>	44
3.4	Futures and option pricing	45
3.4.1	<i>Futures pricing</i>	45
3.4.2	<i>Option pricing</i>	46
3.5	Empirical analysis	49
3.5.1	<i>Empirical model</i>	49
3.5.2	<i>Description of the data</i>	51
3.5.3	<i>Empirical method</i>	52
3.6	Estimation results	55
3.6.1	<i>Lean hog market</i>	55
3.6.2	<i>Soybean market</i>	60
3.6.3	<i>Crude oil market</i>	64
3.7	Conclusion	67
3.8	Appendix	68
3.8.1	Appendix A	68
3.8.2	Appendix B	70
CHAPTER 4. Test of Samuelson Hypothesis in Commodity Futures Market: An Analysis		
Using Term Structure Models		73
4.1	Introduction	73
4.2	Term Structure of Futures Return Volatility and Empirical Model	75
4.3	Description of the Data	79

4.4	Empirical Results	80
4.4.1	<i>Energy Market</i>	83
4.4.2	<i>Livestock Market</i>	83
4.4.3	<i>Metal Market</i>	84
4.4.4	<i>Grain Market</i>	86
4.5	<i>Seasonality Effect on the Futures Return Volatility</i>	88
4.6	Conclusion	93
CHAPTER 5. SUMMARY AND DISCUSSION		96
5.1	Summary of Methods and Contributions	96

LIST OF TABLES

2.1	Parameter estimates for the lean hog futures market.	17
2.2	Parameter estimates for the soybean futures market.	22
2.3	Deviance results for the lean hog and soybean futures prices.	24
2.4	Gelman-Rubin test statistics for the lean hog and soybean futures markets. . .	30
3.1	Parameter Estimates: Lean Hogs	56
3.2	Parameter Estimates: Soybeans (Futures data Only)	61
3.3	Parameter Estimates: Soybeans (Futures and Options)	62
3.4	Parameter Estimates: Crude Oil	65
4.1	One Regressor OLS Regression Results	81
4.2	Regression Results of Our Model	82
4.3	Seasonality Effect on Futures Return Volatility	89

LIST OF FIGURES

2.1	Projection of lean hog futures prices on January 15, 2010.	18
2.2	Projection of lean hog futures prices on December 16, 2002.	19
2.3	Projection of soybean futures prices on January 15, 2010.	21
2.4	Projection of soybean futures prices on November 15, 2000.	21
2.5	95 percent credible band of futures prices predicted by Model 3 for soybean market on January 15, 2010.	25
2.6	95 percent credible band of futures prices predicted by Model 3 for lean hog market on January 15, 2010.	26
2.7	Posterior distributions of selected parameters for Model 3, corresponding to lean hog futures prices.	31
2.8	Posterior distributions of selected parameters for Model 3, corresponding to soybean futures prices.	32
3.1	Behavior of x_t , conditional expectations, and 95% confidence intervals under Black's model	39
3.2	Behavior of x_t , conditional expectations, and 95% confidence intervals under Schwartz's model	40
3.3	Behavior of x_t , conditional expectations, and 95% confidence intervals under our model	41
3.4	Projection of lean hog futures prices on Jan. 15, 2010	58
3.5	Projection of lean hog futures prices on Dec. 16, 2002	59
3.6	Projection of normalized at-the-money call option prices: lean hogs	60
3.7	Projection of normalized at-the-money call option prices: soybeans	64
3.8	Projection of normalized at-the-money call option prices: crude oil	66
4.1	Three different patterns on futures return volatility	74
4.2	Model implied and historical volatility of futures return	77

4.3	Model fitted and historical volatility of futures return on energy market	84
4.4	Model fitted and historical volatility of futures return on livestock market	85
4.5	Model fitted and historical volatility of futures return on metal market	86
4.6	Model fitted and historical volatility of futures return on grain market	87
4.7	Seasonality effect in the grain market	90
4.8	Seasonality effect in the energy market	91
4.9	Seasonality effect in the meat market	92
4.10	Seasonality effect in the metal market	92

ACKNOWLEDGEMENTS

I would like to express my gratitude to all those who gave me the possibility to complete this dissertation. I am deeply indebted to the guidance from my supervisors, Dr. Sergio Lence and Dr. Dermot Hayes and my committee member Dr. Chad Hart. We have been meeting and discussing on this project almost every week for more than three years. They provided me time, patience, and energy in my work and I am deeply grateful for their helpful advice, continued support and encouragement. The completion of the dissertation would have been impossible without their knowledge and assistance.

I wish to express my sincere gratitude to my committee members Dr. Helle Bunzel, Associate Professor at Iowa State University and Dr. Ananda Weerasinghe, Professor at Iowa State University for their constructive comments and invaluable insights to the dissertation. I also have been benefitted a lot from taking their inspiring courses.

Lastly, I would like to give my special thanks to my family for their understanding and endless love through the duration of my studies, to my daughters Fiona and Olivia for bringing us a lot of joys and happiness throughout my work.

CHAPTER 1. OVERVIEW

This dissertation consists of three essays investigating the pricing issue in and properties of commodity futures and options markets.

Chapter 2 focus on commodity futures markets. Futures markets on agricultural commodities typically trade with maximum maturity dates of less than four years. If these markets did trade with maturities eight or ten years distant, futures prices would have value as price forecasts and as a way to structure long-term swaps and insurance contracts. Agricultural commodity markets generally exhibit mean reversion in spot prices and convenience yields. Spot markets also exhibit seasonality. We develop and implement a procedure to generate long-term futures curves from existing futures prices. Data on lean hogs and soybeans are used to show that the method provides plausible and statistically significant results.

An option pricing model is proposed in Chapter 3. Options on agricultural commodities with maturities exceeding one year seldom trade. One possible reason to explain the lack of trading is that we do not have an accurate option pricing model for products where mean reversion in price levels can be expected. Standard option pricing models assume proportionality between price variance and time to maturity. This proportionality is not a valid assumption for commodities whose supply response brings prices back to production costs. The model proposed here incorporates mean reversion in price levels and includes a correction for seasonality. Mean reversion and seasonality are both observed in agricultural markets. We use futures prices from crude oil and lean hog market as well as futures and options data from soybean market to fit our model. The empirical analysis lends strong support to our model.

Chapter 4 investigates the relationship between futures price return volatility and the contract's time to maturity. The Samuelson hypothesis predicts that futures price return volatility will increase as the futures contract approaches its expiration date. In prior tests of this hypothesis, researchers have used linear regression to show this this relationship generally holds. In Chapter 4, we develop a term structure

model that predicts that this pattern is generally non-linear, if the Samuelson effect exists. We use data on ten commodities to test the hypothesis using our model and the linear model. The evidence suggests that our model can better explain the term structure of futures return volatility on metals, livestock and energy markets. However, there is no significant improvement in the grain market. A seasonal effect is also proposed and estimated but does not change these findings.

The remainder of this dissertation is organized as follows. Chapter 2 and Chapter 3 are developed to get more accurate pricing formulas for commodity futures and options markets, especially for renewable agricultural commodities. Chapter 4 tests Samuelson hypothesis using the term structure model based on the futures pricing formula that we proposed in Chapter 2. Finally, in Chapter 5, we summarize the contributions in this dissertation.

CHAPTER 2. The Long-Term Structure of Commodity Futures

2.1 Introduction

Futures contracts on agricultural commodities have a limited number of maturity dates. For example, the most distant maturity date for corn, soybeans and wheat is at most four years. For futures contracts on livestock products, the furthest maturity date is about two years. This situation is unfortunate for two reasons. First, futures markets have long been known to be more accurate in predicting future prices than large-scale econometric models (Just and Rausser (1981)).¹ This suggests that longer-maturity contracts would have public value as predictors of future prices. Second, the agricultural sector has not participated in the development of swap contracts to the extent that is common in other markets and sectors. We hypothesize that some market participants might be willing to use these contracts if there was an inexpensive way to find the fair value of the long-term contracts given the information implicit in the short-term contracts that do trade.

One key piece of information needed to successfully construct a swap is the long-term futures curve. For crude oil and Eurodollars, maturity dates as far as ten years in the future are available. For other markets, such as gold, stock indices and exchange rates, the futures curve can be determined by simple arbitrage formulae (e.g., cost of carry for gold, interest rate minus dividend for stocks, and the interest rate differential for currencies). However, the long-term futures curve cannot be obtained from current futures contracts in agriculture due to the lack of long-term maturities.

To see why it might be useful to introduce long-term swaps in agriculture, consider the circumstances faced by a farmer who is about to purchase land or build a livestock facility, or a soybean

¹It could be argued that the method we propose here is in fact an econometric model, and therefore subject to the failings of these models. While it is true that the method we propose depends on econometric estimation, the purpose of this estimation is to use the term structure of existing short-term futures to estimate the long-term futures curve. This philosophy is very different from the long-run supply and demand parameters that are typically used to drive results in structural econometric models of the type evaluated by Just and Rausser.

processor who plans to construct a new crushing plant. These investments will typically not provide a return that covers costs for a decade or more. We are not aware of any long-term swaps or forward contracts that are routinely used in agriculture to mitigate these long-term risks. Firms making these investments might be willing to forgo the benefits associated with price volatility and instead sign long-term swaps or forward contracts to ensure a return on investment, but they cannot do this because the long-term futures curve is not available.² It is also likely that the interest paid on funds that are borrowed to make these long-term investments would be lower if exposure to long-term price risk could be mitigated.

One challenge in estimating the long-term futures curve in agriculture is that commodity supply will typically respond to prices if producers are given enough time. This means that long-term futures contracts, if they did exist, would exhibit a trend toward expected production costs in the absence of risk premia.³ Equivalently, the market would exhibit mean reversion. The speed of mean reversion will depend on the commodity in question, as well as on particular market circumstances, such as the distance of current spot price from production costs, expected production costs for future periods, the level of carryover stocks, current and expected weather patterns, livestock productivity, or the level of convenience yield. These circumstances will be known to market participants and will be used by them in buying and selling the futures and options contracts that do trade. But these relationships are complex and far more difficult to understand than the simple no-arbitrage relationships that exist for investment commodities such as gold, stock indices, or currency.

This chapter develops and implements a procedure for extracting the commodity- and time-specific parameters required to construct long-term futures curves where mean reversion exists. A number of studies report evidence of mean reversion in commodity cash prices (e.g., Peterson, Ma, and Ritchey (1992); Allen, Ma, and Pace (1994); Walburger and Foster (1995)). Our model builds on an influential paper by Schwartz (1997). In an out-of-sample forecasting exercise, Bernard *et al.* (2008) show

²As pointed out by an anonymous reviewer, even though multi-year rollover hedges might seem appealing in the absence of long-term futures, rollover strategies do not allow one to lock in current futures prices for crops to be harvested one or more years later. Lence and Hayenga (2001) provide a theoretical model explaining the failure of multiyear rollover hedging strategies, and empirical evidence supporting their model.

³Under the risk-neutral measure, futures prices for a fixed maturity are martingales. The risk-neutral measure and the physical measure differ to the extent that there are risk premia. Thus, if the spot price exhibits mean reversion in the physical measure and there are no risk premia, the futures curve must show a tendency for long-term futures to revert back to the spot price's long-term mean.

that Schwartz or Schwartz and Smith (2000) type state-space models greatly outperform other models according to an RMSE criterion.

Schwartz recognized that periods of temporary scarcity in commodity markets, as indicated by a positive convenience yield, would eventually be resolved by market forces. He constructed a model where convenience yield exhibits mean reversion and he used it to create a futures curve for crude oil. The spot price in Schwartz's two-factor model is assumed to be trending rather than mean reverting. When convenience yield is a constant, the spot price in Schwartz's model exhibits geometric Brownian motion. Our problem is more complex because we expect mean reversion both in the convenience yield and the price level. In our setup, the spot price is allowed to exhibit mean reversion in both the historical and risk-neutral measures.⁴ For example, if lean hog supplies are plentiful and prices are below production costs, the market might show a very normal convenience yield, but we will expect a contraction in supply and a reversion in the price level to production costs.

A second feature of our model is that we recognize that agricultural markets exhibit seasonality, and that these seasonal patterns will be evident in the futures contracts that do trade and in the long-term futures curve that we want to estimate. Sørensen (2002) modeled seasonality in agricultural commodity futures by adding a deterministic seasonal component to the commodity spot price. He derived a closed-form futures pricing formula based on his one-factor model with seasonality. Richter and Sørensen (2002) proposed a three-factor model to explore the seasonality patterns in both spot price level and volatility in commodity markets. However, closed-form solutions for futures pricing formulas are not available for their model setup.

Seasonality is introduced into our model by allowing the parameters in the drift terms of the two factors (spot price and convenience yield) to be a periodical function of calendar time. The evaluation of futures pricing expressions can be reduced to the problem of solving ordinary differential equations (Duffie, Pan, and Singleton (2000)). Adding seasonality into the model makes the solution more involved, because the corresponding stochastic differential equations are inhomogeneous in time as the drift coefficients are functions of calendar time. However, we are able to derive closed-form expressions for futures formulas, which greatly facilitate the empirical work.

As Schwartz recognized, a negative relationship between supply/inventories and convenience yields

⁴Futures prices are risk-neutral expectations of future spot prices, and are martingales in the risk-neutral measure.

is predicted by the theory of storage. Thus, when inventory is low and supply is scarce the convenience yield from marginal storage is high, and the opposite is true when inventory is high and supply is large. Since commodity supply exhibits seasonality, the convenience yield is also assumed to behave as a mean-reverting process with seasonality. The present empirical work suggests that the speed of mean reversion is higher in the lean hog market than in the soybean market. Seasonal patterns are clear in the estimation results for both agricultural commodities. The impact of our two modeling innovations (mean-reverting spot prices and seasonality) is shown by comparing Schwartz's model to ours.

Similar to the partially overlapping time series (POTS) model introduced by Smith (2005), our estimation relies on data for all of the futures contracts being traded on a particular date. However, our study differs from Smith's in a number of important aspects. In particular, Smith focused on capturing the volatility dynamics of commodity futures, whereas our main interest is in estimating the long-term futures curve. Hence, even though the POTS model may prove quite useful for pricing options on futures contracts, it cannot be employed to estimate the futures price of long-term non-traded contracts, which is essential for the present exercise. Another important difference between the POTS model and ours is that our theoretical framework prices the entire futures curve by imposing no-arbitrage restrictions across all contracts.⁵ In contrast, the POTS model does not impose any theory-based restriction among the prices of futures contracts for different maturities.

The rest of this chapter is organized as follows. In the next section, we generalize Schwartz's two-factor model, and seasonality is introduced into the proposed model. In the third section, futures pricing formulas are derived. Section four describes the empirical specification, the data set, and the estimation method. The econometric results and their analysis are discussed in section five. The last section concludes the chapter.

2.2 Schwartz's Model and A Generalization

Schwartz advanced a path-breaking model of commodity prices, by incorporating Kaldor's (1939) fundamental insight that commodity markets are characterized by convenience yields. Schwartz postulated that the convenience yield net of storage cost (net convenience yield), c_t , follows the Ornstein-

⁵In fact, it is this restriction which allows us to estimate long-term futures prices from the prices of short-term futures contracts.

Uhlenbeck stochastic process

$$dc_t = (u_c - k_c c_t)dt + \sigma_c dw_c(t), \quad (2.1)$$

where u_c/k_c is the long-term mean of the net convenience yield, $k_c > 0$ is the net convenience yield's speed of mean reversion, and $dw_c(t)$ is a Wiener process. However, Schwartz assumed that the process of the commodity spot price, S_t , is not mean reverting. Instead, he assumed it to behave as a geometric Brownian motion when net convenience yield (c_t) is a constant,

$$dS_t = (u_s - c_t)S_t dt + \sigma_s S_t dw_s(t), \quad (2.2)$$

where $dw_s(t)$ is a Wiener process, and $dw_c(t)dw_s(t) = \rho_{sc}dt$. By defining $x_t \equiv \ln(S_t)$, application of Ito's Lemma yields the stochastic process for x_t ,

$$dx_t = (u_x - c_t)dt + \sigma_x dw_x(t), \quad (2.3)$$

where $u_x \equiv u_s - \sigma_s^2/2$, $\sigma_x \equiv \sigma_s$, $dw_x(t) \equiv dw_s(t)$, and $\rho_{xc} \equiv \rho_{sc}$.

The expected total rate of return to the commodity holder consists of the expected relative price change ($E(dS_t/S_t) = u_s - c_t$) plus the net convenience yield (c_t). In equilibrium, the expected rate of return to the commodity holder must equal the risk-free rate (r) plus the risk premium associated with the stochastic process dx_t (λ_x), i.e., $u_s - c_t + c_t = r + \lambda_x$. Therefore, the corresponding risk-neutral processes are

$$dc_t = (u_c - k_c c_t - \lambda_c)dt + \sigma_c dw_c^Q(t), \quad (2.4)$$

$$dS_t = (r - c_t)S_t dt + \sigma_s S_t dw_s^Q(t), \quad (2.5)$$

where λ_c is the market price for the risk associated with the stochastic process of c_t , and $dw_c^Q(t)$ and $dw_s^Q(t)$ are the Wiener processes under the equivalent martingale measure. By application of Ito's lemma, the risk-neutral process of dx_t can be shown to be

$$dx_t = (r - \sigma_x^2/2 - c_t)dt + \sigma_x dw_x^Q(t). \quad (2.6)$$

Note that $dw_x^Q(t) = dw_s^Q(t)$ and $dw_c^Q(t)dw_x^Q(t) = \rho_{xc}dt$. For convenience, this model is labeled Model 1.

2.2.1 Price Mean Reversion

A stylized fact of commodity markets is that convenience yields are positively associated with spot prices. Typically, when a commodity is in relatively short supply, its price is high and its convenience yield is high as well. Therefore, the net convenience yield is postulated to consist of a linear function of the logarithm of the spot price ($k_x x_t$) plus a stochastic component (y_t):

$$c_t = y_t + k_x x_t. \quad (2.7)$$

The dynamics of y_t is given by the Ornstein-Uhlenbeck stochastic process

$$dy_t = (u_y - k_y y_t)dt + \sigma_y dw_y(t), \quad (2.8)$$

with $dw_x(t)dw_y(t) = \rho_{xy}dt$. Hence, the corresponding spot price stochastic process is

$$dS_t = [u_s - y_t - k_x \ln(S_t)]S_t dt + \sigma_s S_t dw_s(t), \quad (2.9)$$

and Ito's Lemma yields the Ornstein-Uhlenbeck stochastic process for the logarithm of the spot price

$$dx_t = (u_x - y_t - k_x x_t)dt + \sigma_x dw_x(t). \quad (2.10)$$

In equilibrium, the instantaneous expected total return to commodity holders must equal the risk-free rate plus the associated market price of risk:

$$r + \lambda_x = (u_x - y_t - k_x x_t) + (y_t + k_x x_t) \quad (2.11)$$

$$\Rightarrow (u_x - y_t - k_x x_t) - \lambda_x = r - (y_t + k_x x_t). \quad (2.12)$$

Therefore, the risk-neutral process of dS_t may be written as:

$$dS_t = [r - (y_t + k_x x_t)]S_t dt + \sigma_s S_t dw_s^Q(t). \quad (2.13)$$

Then, application of Ito's lemma yields

$$dx_t = [r - \sigma_x^2/2 - (y_t + k_x x_t)]dt + \sigma_x dw_x^Q(t). \quad (2.14)$$

Denoting the market price for the y_t risk as λ_y , the risk-neutral process of dy_t is

$$dy_t = (u_y - k_y y_t - \lambda_y)dt + \sigma_y dw_y^Q(t), \quad (2.15)$$

where $dw_x^Q(t)dw_y^Q(t) = \rho_{xy}dt$.

This generalized model is referred to as Model 2. It is clear that Model 1 is a special case of Model 2, because the two models are identical if k_x is restricted to equal zero, in which case $c_t = y_t$. The key difference between Models 1 and 2 is that, when c_t is a constant, the logarithm of the spot price in Model 1 behaves like a Geometric Brownian motion. In contrast, when y_t is a constant, the logarithm of the spot price in Model 2 satisfies an Ornstein-Uhlenbeck stochastic process. Empirically, testing whether k_x is equal to zero or not allows us to determine whether the spot prices are mean reverting in a given market.

2.2.2 Seasonality

The models considered so far assume that all parameters are constant throughout the year. Most commodity markets differ from the markets for stocks, bonds, and other conventional financial assets, in that they typically exhibit seasonal patterns. For example, prices for annual crops are high in the pre-harvest season and low at peak-harvest, and pork prices are usually high during the barbecue months. To capture this feature, the periodicity in the corresponding parameters is represented by a truncated Fourier series. Seasonality is added into the model by setting u_x in equation (2.10) to be a periodic deterministic function of time:

$$u_x(t) = u_{x,0} + \sum_{h=1}^H [u_{x,h,\cos} \cos(2\pi ht) + u_{x,h,\sin} \sin(2\pi ht)], \quad (2.16)$$

where H determines the number of terms in the sum, and $u_{x,0}$, $u_{x,h,\cos}$ and $u_{x,h,\sin}$ are constant seasonality parameters. Based on the Akaike Information Criterion (AIC) (see, e.g., Harvey 1981), H is selected to be equal to 2. Note that if $u_{x,h,\cos} = u_{x,h,\sin} = 0$, for $\forall h \geq 1$, $u_x(t) = u_{x,0}$, then the model does not exhibit seasonality.

The long-term mean parameter of the first component of the net convenience yield in equation (2.15), $u_y(t)$, is similarly generalized to allow for seasonality by assigning to it a functional form analogous to (2.16). In addition, the risk premia λ_x and λ_y in the previous section are also assumed to be analogous periodic function of calendar time,

$$\lambda_i(t) \equiv \lambda_{i,0} + \sum_{h=1}^H [\lambda_{i,h,\cos} \cos(2\pi ht) + \lambda_{i,h,\sin} \sin(2\pi ht)], \quad (2.17)$$

for $i = x, y$. For simplicity, Model 2 augmented with seasonality is referred to as Model 3. The risk-neutral processes (2.14) and (2.15) incorporating seasonality provide us the basic foundations for pricing futures contracts on commodity markets, which is done in the next section.

2.3 Futures Pricing

Commodity spot prices and net convenience yields are modeled in continuous time as a system of stochastic differential equations in an affine term structure class. The key advantage of affine models is that they are tractable for asset pricing purposes. We rely on the traditional no-arbitrage approach to price commodity derivatives. The seasonality component makes the derivation more complicated. However, closed-form solutions for the futures pricing formula can still be obtained. The following paragraphs show the process of valuation of commodity futures contracts in the presence of mean-reversion and seasonality.

The risk-neutral process of the two latent variables defined in the previous section for the advocated model can be written as

$$\begin{bmatrix} dx_t \\ dy_t \end{bmatrix} \sim N \left(\begin{bmatrix} r - \sigma_x^2/2 - k_x x_t - y_t \\ u_y(t) - \lambda_y(t) - k_y y_t \end{bmatrix} dt, \begin{bmatrix} \sigma_x^2 & \rho_{xy} \sigma_x \sigma_y \\ \rho_{xy} \sigma_x \sigma_y & \sigma_y^2 \end{bmatrix} dt \right). \quad (2.18)$$

This may be expressed more compactly as

$$d\mu_t = (\kappa_0(t) - \kappa_1 \mu_t) dt + V dw^Q(t), \quad (2.19)$$

by defining $\mu_t \equiv [x_t, y_t]'$, $\kappa_0(t) \equiv [r - \sigma_x^2/2, \psi(t)]'$, $\psi(t) \equiv u_y(t) - \lambda_y(t) \equiv \psi_0 + \sum_{h=1}^H [\psi_{h,\cos} \text{Cos}(2\pi ht) + \psi_{h,\sin} \text{Sin}(2\pi ht)]$, $\psi_0 \equiv u_{y,0} - \lambda_{y,0}$, $\psi_{h,\cos} \equiv u_{y,h,\cos} - \lambda_{y,h,\cos}$, $\psi_{h,\sin} \equiv u_{y,h,\sin} - \lambda_{y,h,\sin}$, $\kappa_1 \equiv \begin{bmatrix} k_x & 1 \\ 0 & k_y \end{bmatrix}$,

$V \equiv \begin{bmatrix} \sigma_x^2 & \rho_{xy} \sigma_x \sigma_y \\ \rho_{xy} \sigma_x \sigma_y & \sigma_y^2 \end{bmatrix}$, and ' is the transpose operator.

Duffie, Pan, and Singleton (2000) analyzed a set of stochastic processes that includes processes like (2.19). By applying the method they proposed, a closed-form solution for the futures price at date t

maturing at time T can be obtained as follows:

$$\begin{aligned} F(t, T) &= E_t^Q[S(T)] \\ &= E_t^Q\{\exp[\phi_0 + \phi \mu(T)]\} \end{aligned} \quad (2.20)$$

$$\begin{aligned} &= \exp[\alpha(t, T) + \beta(t, T)\mu(t)] \\ \Rightarrow f_{t, T} \equiv \ln(F(t, T)) &= \alpha(t, T) + \beta(t, T)\mu(t), \end{aligned} \quad (2.21)$$

where $E_t^Q[\cdot]$ is the expectation operation under the risk-neutral probability measure. Since the first factor is defined to be the logarithm of the spot price ($x_t \equiv \ln(S(t))$), it must be the case that $\phi_0 = 0$ and $\phi' = [1, 0]$.⁶ To prevent arbitrage, coefficients $\alpha(t, T)$ and $\beta(t, T)$ need to satisfy the following ordinary differential equations (ODEs)

$$\frac{\partial \beta(t, T)}{\partial t} = \kappa_1 \beta(t, T) \text{ and} \quad (2.22)$$

$$\frac{\partial \alpha(t, T)}{\partial t} = -\kappa_0(t)\beta(t, T) - \frac{1}{2}\beta'(t, T)V\beta(t, T), \quad (2.23)$$

with boundary conditions $\beta(T, T) = \phi$ and $\alpha(T, T) = \phi_0$. Closed-form solutions for $\alpha(t, T)$ and $\beta(t, T)$ are shown in Appendix A.

2.4 Empirical Analysis

In the advocated model, we employ the logarithm of the spot price and the net convenience yield as the two latent state variables. Recall equation (2.19) and define $\Lambda(t) \equiv [\lambda_x(t), \lambda_y(t)]'$. Then, the historical process of the two latent variables can be written in matrix form as

$$d\mu_t \sim N((\kappa_0(t) - \kappa_1\mu_t + \Lambda(t))dt, Vdt). \quad (2.24)$$

We apply the first-order Euler discretized version of the continuous time model (2.24) with discretization interval $\Delta = \frac{1}{12}$ to reflect monthly data. The discretized empirical model is

$$\mu_{t+\Delta} = \mu_t + (\kappa_0(t) - \kappa_1\mu_t + \Lambda(t))\Delta + \sqrt{\Delta}\varepsilon_t, \quad \varepsilon_t \sim N(\mathbf{0}_{(2 \times 1)}, V). \quad (2.25)$$

⁶This restriction on ϕ_0 and ϕ follows from (2.20) and the fact that the spot price is the same as the futures price with instantaneous maturity (i.e., $S(t) = F(t, t)$). To see this, note that application of (2.20) yields $x_t \equiv \ln(S(t)) = \ln(F(t, t)) = \ln(E_t^Q\{\exp[\phi_0 + \phi \mu(t)]\}) = \ln(\exp[\phi_0 + \phi \mu_t]) = \phi_0 + \phi [x_t, y_t]'$, which can only be satisfied if $\phi_0 = 0$ and $\phi' = [1, 0]$.

The likelihood of observing the latent factors can be calculated from equation (2.25). In addition, we also observe futures prices from the markets, and the likelihood of observing the market prices can be inferred from the following empirical futures models.

According to equation (4.1), $f_{t,T} \equiv \ln(F(t,T)) = \alpha(t,T) + \beta(t,T)\mu(t)$. Following Chen and Scott (1993), we assume that all but two futures contract prices are observed with measurement error. Suppose we have a historical data set consisting of $M > 2$ series of (logarithms of) futures prices with M different times to maturity. Assume that among the M futures contracts with distinct maturity dates, two of the prices are perfectly correlated with the state variables μ_t , and the remaining $(M - 2)$ prices are observed with normally distributed errors e_t . Denote the vector with the two perfectly correlated futures prices as $f_t^\circ \equiv [f_{t,T_1^\circ}, f_{t,T_2^\circ}]'$ and their maturity dates $[T_1^\circ, T_2^\circ]'$. Similarly, let $f_t^\bullet \equiv [f_{t,T_1^\bullet}, f_{t,T_2^\bullet}, \dots, f_{t,T_{M-2}^\bullet}]'$ represent the $(M - 2)$ imperfectly correlated futures and $[T_1^\bullet, \dots, T_{M-2}^\bullet]'$ be their maturity dates, respectively. Then,

$$f_t^\circ = \alpha^\circ(t) + \beta^\circ(t)\mu_t, \quad (2.26)$$

$$f_t^\bullet = \alpha^\bullet(t) + \beta^\bullet(t)\mu_t + e_t, \quad (2.27)$$

where $\alpha^\circ(t) \equiv [\alpha(t, T_1^\circ), \alpha(t, T_2^\circ)]'$, $\beta^\circ(t) \equiv \begin{bmatrix} \beta_1(t, T_1^\circ) & \beta_2(t, T_1^\circ) \\ \beta_1(t, T_2^\circ) & \beta_2(t, T_2^\circ) \end{bmatrix}$, $\alpha^\bullet(t) \equiv [\alpha(t, T_1^\bullet), \alpha(t, T_2^\bullet), \dots, \alpha(t, T_{M-2}^\bullet)]'$, and $\beta^\bullet(t) \equiv \begin{bmatrix} \beta_1(t, T_1^\bullet) & \beta_2(t, T_1^\bullet) \\ \beta_1(t, T_2^\bullet) & \beta_2(t, T_2^\bullet) \\ \dots & \dots \\ \beta_1(t, T_{M-2}^\bullet) & \beta_2(t, T_{M-2}^\bullet) \end{bmatrix}$. The vector of errors associated with the log-

futures not perfectly correlated with the state variables is assumed to be multivariate normally distributed, i.e., $e_t \sim N(\mathbf{0}_{((M-2) \times 1)}, \sigma_e^2 \Omega)$, where $\mathbf{0}_{((M-2) \times 1)}$ is an $(M - 2)$ vector of zeros, $\sigma_e^2 > 0$ is a scalar, Ω is an $(M - 2) \times (M - 2)$ matrix with the i, j th element equal to $\rho^{|i-j|}$ for $\rho \in (-1, 1)$, and $\alpha(t, T)$ and $\beta(t, T)$ are defined in Appendix A.

Since the two latent factors are not observed, direct estimation of the historical evolution equation (2.25) is not feasible. However, given equation (2.26), the factors can be solved for as $\mu_t = [\beta^\circ(t)]^{-1}[f_t^\circ - \alpha^\circ(t)]$, provided the (2×2) matrix $\beta^\circ(t)$ is invertible. In this way, the value of the state variables can be exactly filtered out at each sample date, by inversion based on the two contract prices observed without errors.

2.4.1 Description of the Data

Futures prices for two agricultural commodities, soybeans and lean hogs, are employed to estimate the models. The futures prices involved are the settlement prices at the Chicago Mercantile Exchange (CME) for the 15th calendar day of each month from January 1978 through January 2010, for a total of 385 observation dates.⁷ If the 15th of the month is a holiday, the nearest trading day's settlement price is used. The settlement prices observed on days with zero trading volume are discarded, because they are set by the CME administration for the purpose of calculating margins. In other words, these prices are not actual trading prices. The price units are cents/bushel and cents/pound for soybean futures and lean hogs futures, respectively.

Since the longest maturity in the soybean (lean hog) futures sample is 34 (19) months, the ideal data set would consist of a panel of $385 \times 34 = 13,090$ ($385 \times 19 = 7,315$) observations. However, futures for some maturities are not traded. Soybean futures currently have only seven maturity months: January, March, May, July, August, September, and November. Lean hog futures have eight maturity months: February, April, May, June, July, August, October, and December. In addition, data with far-away maturities are often missing because they are not traded. For example, for January 1980 only seven prices are observed for soybean futures. They are the 2nd, 4th, 6th, 7th, 8th, 10th, and 12th elements of the 25th row of our data set, which correspond to the expiration dates of March, May, July, August, September, and November of 1980 and January of 1981. Letting the i, j th element of our data set be the price of the futures contract that expires j months after date i , this means that all of the elements in the 25th row of our soybean data set are missing except the 2nd, 4th, 6th, 7th, 8th, 10th, and 12th columns. All of the other elements for this data row are recorded as unobserved in our data set. Hence, given the futures contract specifications, the total number of observations available for soybean (lean hog) futures prices is 3,157 (3,032).

2.4.2 Empirical Method

Bayesian Markov chain Monte Carlo (MCMC) methods are employed to estimate the model parameters. Bayesian techniques have been used quite often over the past decade to analyze state-space

⁷In 1997, the hogs futures contract switched from live hogs to lean hogs. Live hog prices were converted to lean hog prices using the standardized conversion rate $LeanHogPrice = LiveHogPrice/0.74$. This conversion rate was the accepted rate at the time and has remained the accepted conversion rate between live and lean hog prices.

models (see Hore *et al.* (2010) and Durbin and Koopman (2000)). A recent article by Harvey and Koopman (2009) highlights that the two main approaches to estimate state-space models are maximum likelihood and Bayesian methods. Given that one of the key issues in the development of longer-term futures is the confidence market players have in constructing long-term futures curves, we chose to develop an estimation procedure that would allow us to separate the variation in projections between the parameter uncertainty (model uncertainty) and observational errors. The Bayesian framework does this more naturally than the maximum likelihood approach. Also, the proposed framework provides a streamlined way to produce credible intervals for nonlinear functions of the estimated parameters,⁸ such as the projections for the futures curves.

The empirical method described below is designed for Model 3. Models 1 and 2 can be easily retrieved by imposing the corresponding parameter restrictions into the procedure. We assume a constant risk-free rate of $r = 5$ percent.⁹ We adopt non-informative priors for $\vec{u}_x, \vec{u}_y, k_x, k_y, V, \rho, \vec{\lambda}_x,$ and $\vec{\lambda}_y,$ where $\vec{u}_i \equiv [u_{i,0}, u_{i,1,cos}, u_{i,1,sin}, u_{i,2,cos}, u_{i,2,sin}]$ and $\vec{\lambda}_i \equiv [\lambda_{i,0}, \lambda_{i,1,cos}, \lambda_{i,1,sin}, \lambda_{i,2,cos}, \lambda_{i,2,sin}]$ for $i = x, y.$ As such, the posterior distributions for these parameters are effectively the likelihoods for the parameters under the model specification. The exception is $\sigma_e^2,$ for which we impose the conjugate prior $\sigma_e^2 \sim Inv-\chi^2(\bar{v}_e, \bar{\sigma}_e^2).$ This prior is equivalent to the addition of \bar{v}_e data points with a sample variance of $\bar{\sigma}_e^2.$ For this study, \bar{v}_e is set at 4 and $\bar{\sigma}_e^2$ is set at 0.0005. For several of the parameters, explicit posterior distributions cannot be derived. For those cases, algorithms have been derived to sample from the unspecified distributions based on their proportionality with the model likelihoods.

Defining the set of parameters for the j th iteration as $\Phi^{(j)} \equiv \{V^{(j)}, \vec{\lambda}_y^{(j)}, \vec{\lambda}_x^{(j)}, \vec{\psi}^{(j)}, k_x^{(j)}, k_y^{(j)}, \rho^{(j)}, \sigma_e^{2(j)}\},$ and letting $\Phi_{-z}^{(j)}$ denote all of the components of $\Phi^{(j)}$ except for $z,$ the advocated MCMC iteration steps are as follows.

Step 1. Specify starting values for parameter and missing observations $\Phi^{(0)}.$

Step 2. Given $[V^{(j)}, \vec{\lambda}_y^{(j)}, \vec{\lambda}_x^{(j)}, \sigma_e^{2(j)}],$ estimate $[\vec{\psi}^{(j+1)}, k_x^{(j+1)}, k_y^{(j+1)}, \rho^{(j+1)}]$ by means of an

⁸Credible intervals are the Bayesian analogs of confidence intervals in frequentist statistics.

⁹For the period under analysis, the average annual interest rate corresponding to three-month treasury bills was 5.60 percent. It must be noted, however, that the interest rate does not change the analysis in any substantive way. As implied by (2.12) and (2.14), the main impact of adopting a different value for the interest rate (r) is to induce an equal change in the estimated y_t component of the net convenience yield, and a change of the same absolute value but opposite sign in the risk premium (λ_x). The model could be extended by explicitly modeling stochastic interest rates. However, Schwartz (1997) and Trolle and Schwartz (2009) show that for commodity futures the pricing error arising from ignoring the stochastic nature of interest rates is negligible.

effective adaptive, general purpose MCMC algorithm called t-walk developed by Christen and Fox (2010). The t-walk compares the likelihood of observing futures prices and state variables given (i.1) and (i.2) (i.e., the likelihood given existing parameter values) with (ii.1) and (ii.2), (i.e., the likelihood given proposed parameter values).

$$\begin{aligned}
\text{(i.1)} \quad & [f_t^{\bullet(j)} - \alpha^{\bullet(j)} - \beta^{\bullet(j)} \mu_t^{(j)}] \sim N(\mathbf{0}_{((M-2) \times 1)}, \sigma_e^{2(j)} \Omega^{(j)}), \\
\text{(i.2)} \quad & \left[\mu_{t+\Delta}^{(j)} - \mu_t^{(j)} - (\kappa_0(t)^{(j)} - \kappa_1^{(j)} \mu_t^{(j)} + \Lambda(t)^{(j)})/\Delta \right] / \sqrt{\Delta} \sim N(\mathbf{0}_{(2 \times 1)}, V^{(j)}), \\
\text{(ii.1)} \quad & [f_t^{\bullet(j)} - \alpha^{\bullet(prop)} - \beta^{\bullet(prop)} \mu_t^{(prop)}] \sim N(\mathbf{0}_{((M-2) \times 1)}, \sigma_e^{2(j)} \Omega^{(prop)}), \\
\text{(ii.2)} \quad & \left[\mu_{t+\Delta}^{(prop)} - \mu_t^{(prop)} - (\kappa_0^{(prop)}(t) - \kappa_1^{(prop)} \mu_t^{(prop)} + \Lambda(t)^{(j)})/\Delta \right] / \sqrt{\Delta} \sim N(\mathbf{0}_{(2 \times 1)}, V^{(j)}),
\end{aligned}$$

where $\mu_t^{(\cdot)}$ is computed from equation (2.26) using $\vec{\psi}^{(\cdot)}$, $k_x^{(\cdot)}$, and $k_y^{(\cdot)}$.¹⁰

Step 3. Given $[\vec{\psi}^{(j+1)}, k_x^{(j+1)}, k_y^{(j+1)}, \rho^{(j+1)}, \vec{\lambda}_y^{(j)}, \vec{\lambda}_x^{(j)}, \sigma_e^{(j)}]$, use the Metropolis-Hastings algorithm to generate $V^{(j+1)}$, as follows:

(a) Draw $V^{(prop)} \sim \text{Inv-Wishart}_{Nobs-3}((Nobs-3)V^{(j)})$ where $Nobs$ is the number of observations.

(b) Calculate the acceptance ratio, $R \equiv \frac{\text{Prob}(V^{(prop)} | \Phi_{-V, f_t}^j) \text{Prob}(V^{(prop)} | V^{(j)})}{\text{Prob}(V^{(j)} | \Phi_{-V, f_t}^j) \text{Prob}(V^{(j)} | V^{(prop)})}$.¹¹

(c) Draw a random variable ζ from a standard uniform distribution and set $V^{(j+1)} = V^{(prop)}$ if $\zeta < R$. Otherwise, set $V^{(j+1)} = V^{(j)}$.

Step 4. Given $[V^{(j+1)}, \vec{\psi}^{(j+1)}, k_x^{(j+1)}, k_y^{(j+1)}]$, update the unobserved futures prices to get $f_t^{(j+1)}$. In this step, we first compute $\mu_t^{(j+1)}$ from the estimated risk-neutral parameters and the futures observed with no errors using equation (2.26). Then, we update the unobserved futures from the estimated factors and the other corresponding parameters by means of equation (4.1).

Step 5. Given $[V^{(j+1)}, \vec{\psi}^{(j+1)}, k_x^{(j+1)}, k_y^{(j+1)}, \rho^{(j+1)}, \sigma_e^{(j)}]$, draw $\vec{\lambda}_y^{(j+1)}$ and $\vec{\lambda}_x^{(j+1)}$ from a multivariate normal distribution (see Appendix B for details).

Step 6. Given $[\vec{\lambda}_y^{(j+1)}, \vec{\lambda}_x^{(j+1)}, V^{(j+1)}, \vec{\psi}^{(j+1)}, k_x^{(j+1)}, k_y^{(j+1)}, \rho^{(j+1)}]$, draw $\sigma_e^{2(j+1)} | f_t^{(j+1)}, \Phi_{-\sigma_e}^{(j+1)} \sim \text{Inv-}\chi^2(\bar{v}_e + n_f, \frac{\bar{v}_e \bar{\sigma}_e^2 + n_f s_e^2}{\bar{v}_e + n_f})$, where n_f is the total number of observed futures prices and s_e^2 is the mean squared error of the observed futures prices.

¹⁰The perfectly correlated futures prices are selected to be among the observed data.

¹¹Calculating $\text{Prob}(V^{(prop)} | \Phi_{-V, f_t}^j)$ and $\text{Prob}(V^{(j)} | \Phi_{-V, f_t}^j)$ will again resort to the empirical equations (i.1) and (i.2).

Step 7. Set $j = j + 1$.

Step 8. If the maximum iteration is reached, stop. Otherwise, go to Step 2.

2.5 Estimation Results

The advocated Bayesian MCMC procedure is performed with four chains for each model and market. Each chain is started at a different initial value and run for two million iterations. The first one million iterations are discarded as a burn-in period, and the remaining one million iterations are tested for convergence by means of Gelman and Rubin (1992) tests. As evinced by the Gelman-Rubin test statistics reported in Appendix C, all of the chains converge adequately for the three models in both markets.

2.5.1 *Lean Hog Market*

Parameter estimates for the lean hog market are shown in table 2.1.¹² The posterior probability of parameter k_x being positive is estimated to be greater than 97.5% for both Models 2 and 3, which supports the postulation that the spot price in the lean hog market is mean reverting. This also implies that the convenience yield is positively related to the spot price. Comparing Model 1 with Model 2, the lower bound of the credible interval for the correlation coefficient between the two factors in Models 1 is larger than the upper bound of the corresponding credible interval estimated by Model 2, after we set the convenience yield to be a function of the logarithm of the spot price. The total expected return on the spot price (u_x), the long-term mean of net convenience yield, and the market prices of convenience yield risk are all negative at the median, but their 95% posterior density region contains zero except for λ_c in Models 1 and 2.

All of the seasonality parameters in Model 3 are estimated precisely enough to determine the sign with high probability. This indicates that the lean hog market exhibits a strong seasonal pattern. If the data exhibit seasonality but the model fails to incorporate it, the seasonal variability in the factors will be captured by the instantaneous volatility term. Hence, given a data set exhibiting seasonality, models not allowing for seasonality will estimate a significantly higher value of σ_x and σ_y than models allowing for it, which is confirmed by the values reported in table 2.1.

¹²See Appendix D for graphs of the posterior distributions of key parameters.

Table 2.1: Parameter estimates for the lean hog futures market.

Parameters	Model 1			Model 2			Model 3		
	2.5%	50%	97.5%	2.5%	50%	97.5%	2.5%	50%	97.5%
k_x				0.414	0.657	1.015	0.447	0.647	0.902
k_c/k_y	2.330	2.608	2.887	1.461	1.935	2.355	1.027	1.312	1.648
$\lambda_c/\lambda_{y,0}$	-0.449	-0.287	-0.126	-0.369	-0.225	-0.099	-0.208	-0.151	0.100
$\lambda_{y,1,sin}$							0.637	0.699	0.768
$\lambda_{y,1,cos}$							-0.485	-0.391	-0.301
$\lambda_{y,2,sin}$							-1.898	-1.758	-1.612
$\lambda_{y,2,cos}$							1.461	1.603	1.744
$u_{x,0}$	-0.061	-0.020	0.021	-0.049	-0.006	0.036	-0.004	0.018	0.038
$u_{x,1,sin}$							0.020	0.051	0.083
$u_{x,1,cos}$							0.068	0.093	0.117
$u_{x,2,sin}$							-0.128	-0.108	-0.089
$u_{x,2,cos}$							-0.267	-0.247	-0.226
$u_{c,0}/u_{y,0}$	-0.198	-0.085	0.027	-6.597	-5.254	-3.817	-4.230	-3.527	-2.887
$u_{y,1,sin}$							-0.457	-0.307	-0.155
$u_{y,1,cos}$							-2.277	-2.114	-1.945
$u_{y,2,sin}$							2.375	2.716	3.057
$u_{y,2,cos}$							2.908	3.260	3.613
σ_x	0.425	0.449	0.473	0.409	0.430	0.454	0.327	0.342	0.356
σ_y	1.282	1.447	1.612	0.931	1.107	1.304	0.532	0.617	0.702
$\rho_{x,y}$	0.868	0.884	0.898	0.608	0.728	0.803	0.508	0.628	0.726
ρ	0.156	0.190	0.225	0.161	0.196	0.231	0.061	0.099	0.137
σ_e	0.077	0.081	0.084	0.076	0.080	0.083	0.044	0.046	0.047

Note: The three quantities denote respectively the 2.5, 50 and 97.5 percentiles of the posterior probability band.

Seasonality may also significantly affect the model's ability to fit the market data. The estimates of σ_e describe the inferred standard deviation on the noise terms that allow for deviations between theoretical and observed log-futures prices. One source of this noise in our specific data set may be that the settlement prices are established by the CME administrators, which may not exactly match the market prices. Errors in data registration, price limits and handling of bid-ask spreads may also contribute to the noise term. As can be seen from table 2.1, the upper bound of the credible interval for σ_e in Model 3 is smaller than the lower bound of the corresponding credible interval estimated by Model 1 and 2, which signals a better fit of the observed data.

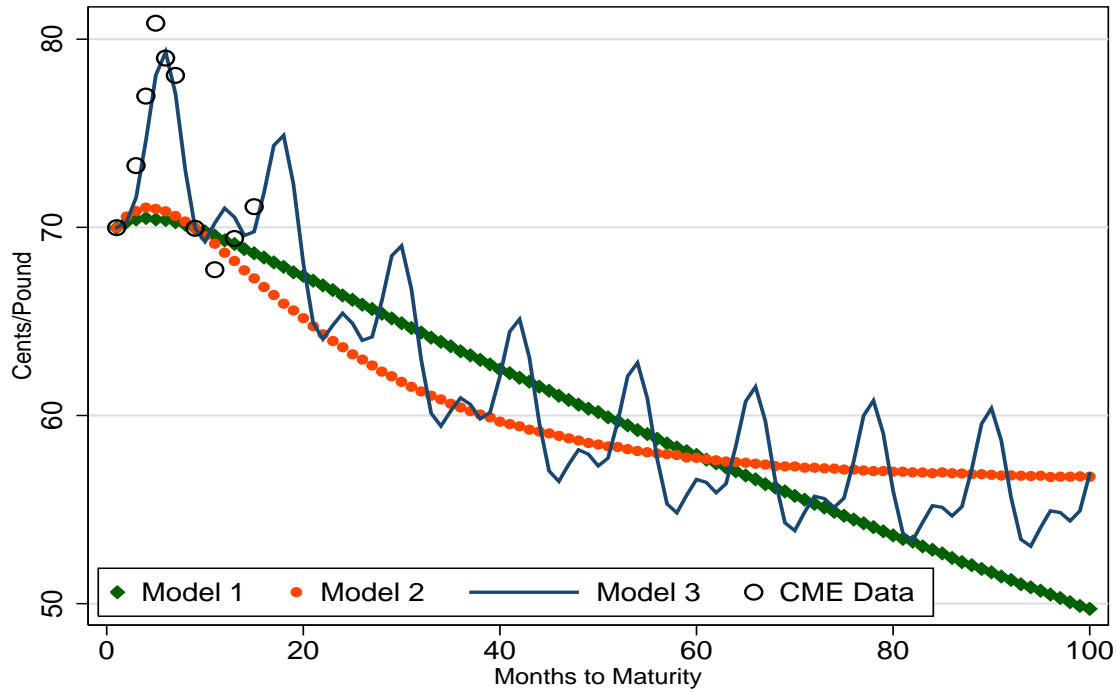


Figure 2.1: Projection of lean hog futures prices on January 15, 2010.

Figures 2.1 and 2.2 show the term structure of median lean hog futures prices implied by the three models on January 15, 2010 and December 16, 2002, respectively. On January 15, 2010, the spot price in the lean hog market was high relative to production costs. For the futures curve with a short time to maturity, the curvature depends on the relative value of the net convenience yield. However, in the long run, the futures curve implied by Schwartz's model (Model 1) depends on the risk-neutral drift of the spot price process. If we evaluate the drift at the risk-neutral long-term mean of the net convenience yield using posterior medians, it is negative. So, in the long run, the slope of the futures curve predicted by Model 1 is negative. Model 2 incorporates mean reversion in the spot price. So when the spot price is relatively high, the futures curve implied by Model 2 initially decreases at a faster rate than the futures curve implied by Model 1, and then flattens out as prices approach the market's estimate of production costs. This long-term futures price ($F(t, \infty)$) is independent of the current spot price and the net convenience yield. The futures curve implied by Model 3 follows the trend of Model 2, but with seasonality. It is clear that futures prices implied by Model 3 fit the observed prices more precisely compared to the models which ignore seasonality. A local maximum is observed when time to maturity

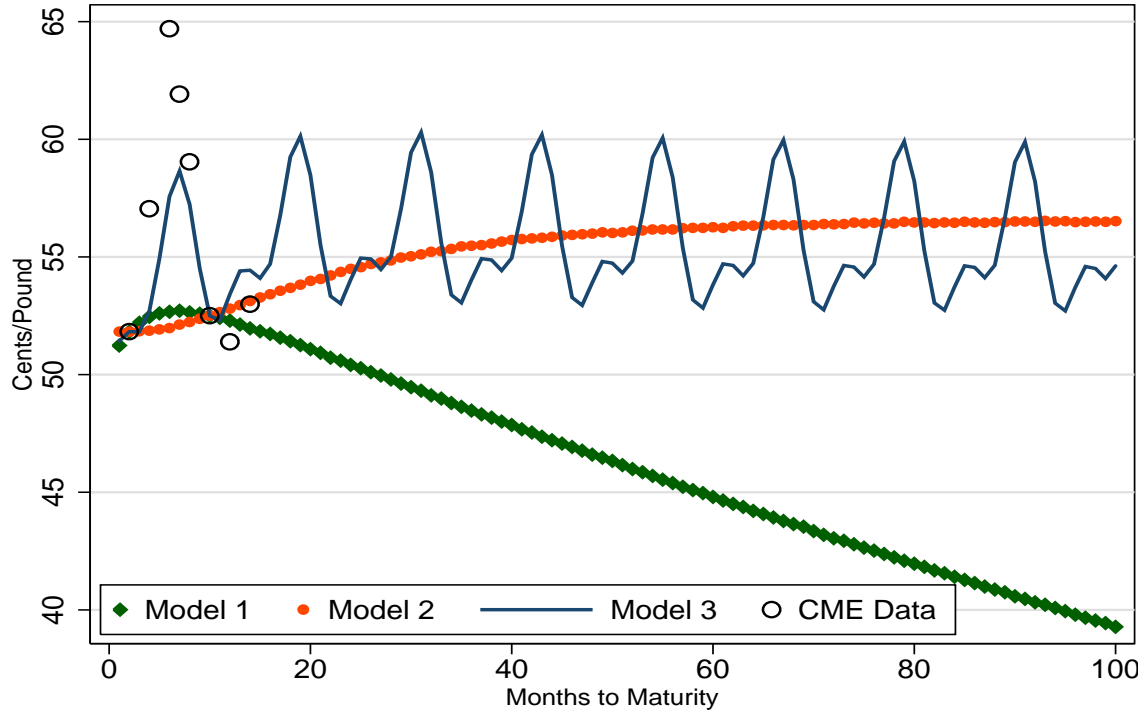


Figure 2.2: Projection of lean hog futures prices on December 16, 2002.

is six months, which corresponds to a July maturity date. July is the traditional barbecue season in the U.S. and the demand for lean hogs is the highest over the year, which is consistent with historical futures price patterns.

In contrast to January 15, 2010, the spot price for lean hogs was relatively low on December 16, 2002. With mean reversion embedded, Model 2 predicts that the futures curve will increase at a decreasing rate and will converge to the long-term futures price ($F(t, \infty)$). The curvature of the futures curve implied by Schwartz's model also depends on the relative level of the spot price and the net convenience yield on that date for short time maturities. However, for longer-term maturities the futures curve is predicted to be decreasing regardless of the fact that the spot price may have already been well below production costs.

2.5.2 Soybean Market

Model estimates for the soybean market are shown in table 2.2. The posterior probability of parameter k_x being positive is estimated to be greater than 97.5%, which provides empirical support for the postulation that the soybean spot price process is also mean reverting. Parameter u_x , which in

Schwartz's model describes the expected appreciation rate of the non-stationary state variable (the logarithm of the spot price), also has a posterior probability of being positive greater than 97.5%. The estimates in table 2.2 indicate that the net convenience yield mean-reversion parameters k_c and k_y are estimated to have a high probability of being positive in Model 1 and Model 2; hence, the state variable c_t in Schwartz's model and y_t in Model 2 are stationary for soybean. The median of the estimated k_c and k_y is about 1.06, corresponding to half-lives of 7.7 months.¹³ Compared to the lean hog market, the soybean market exhibits lower speeds of adjustment in the spot price (k_x) and the net convenience yield (k_y). One possible reason explaining this result is that lean hogs have a shorter production cycle, which allows producers to adjust supply faster. In Model 1, parameter u_c has an estimated posterior probability of being positive in excess of 97.5% , which implies that the long-term mean of the net convenience yield in the soybean market is positive. Parameter u_y is estimated to be negative with high probability in Models 2 and 3. However, net convenience yield in Models 2 and 3 is defined as $c_t = y_t + k_x x_t$. If we take the long-term mean of y_t and x_t to evaluate c_t , the latter is also positive.

All of the three models report similar instantaneous volatilities and instantaneous correlation coefficient between the two factors. Although for the soybean market k_x is estimated to have a posterior probability of being positive greater than 97.5%, its magnitude is small when compared to the lean hog market (for which $k_x = 0.65$ at the median), and it has little impact on the model's ability to fit the historical data. There is large overlap on the credible interval of σ_e for Models 1 and 2. The estimates of σ_e describe the inferred standard deviation on the noise terms that allow for some deviation between theoretical and observed log-futures prices.

Seasonality is important and significant in the soybean market. There is only one seasonality parameter ($\lambda_{y,1,cos}$) whose 95% posterior density region includes zero. Furthermore, the model with seasonality (Model 3) yields a credible interval of σ_e with an upper bound smaller than the lower bound of the corresponding credible interval generated by its counterpart without seasonality (Model 2). The non-seasonal part of risk premia associated with the net convenience yield process is estimated to have more than 97.5% posterior probability of being negative in all of the models.

Figures 2.3 and 2.4 show the term structure of median soybean futures prices implied by the three

¹³The half-life expresses the expected time it takes the impact from a given shock to the process to level off by half the size of the shock. The half-life in the Ornstein-Uhlenbeck process is calculated as $\ln(2)/k$. In our case $\ln(2)/1.07 = 0.65$ years, which is about 7.7 months.

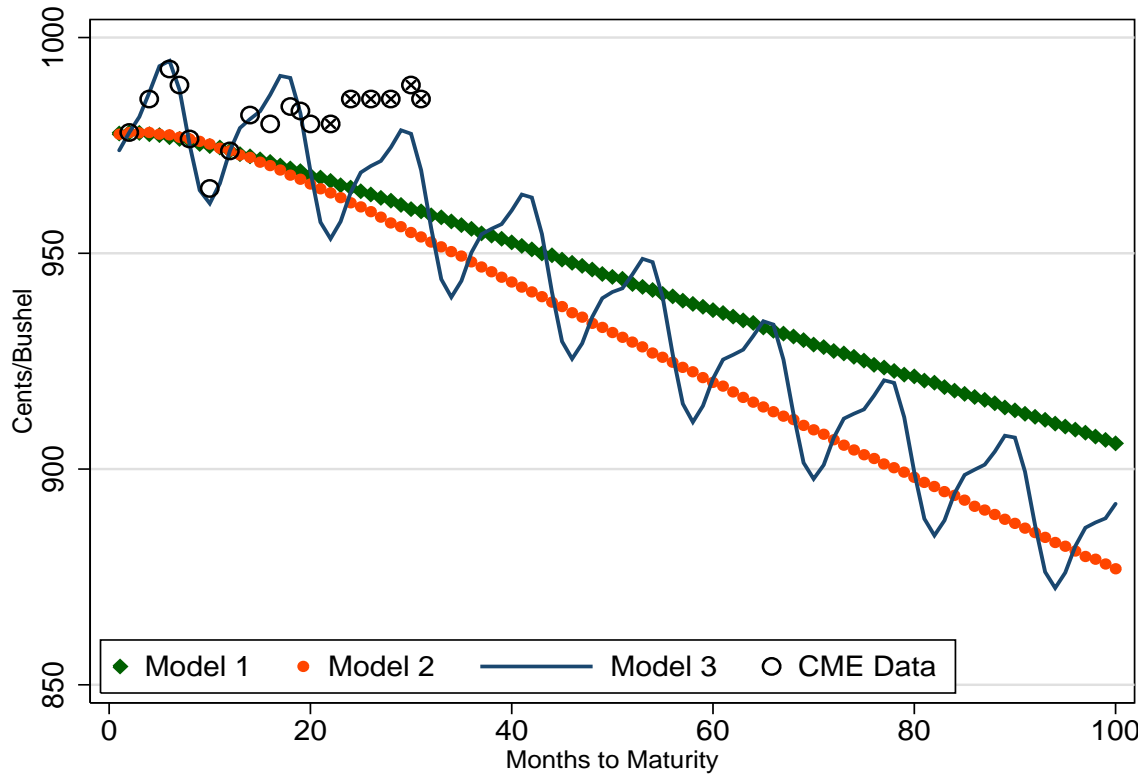


Figure 2.3: Projection of soybean futures prices on January 15, 2010.

Note: ⊗ represents CME data with zero volume.

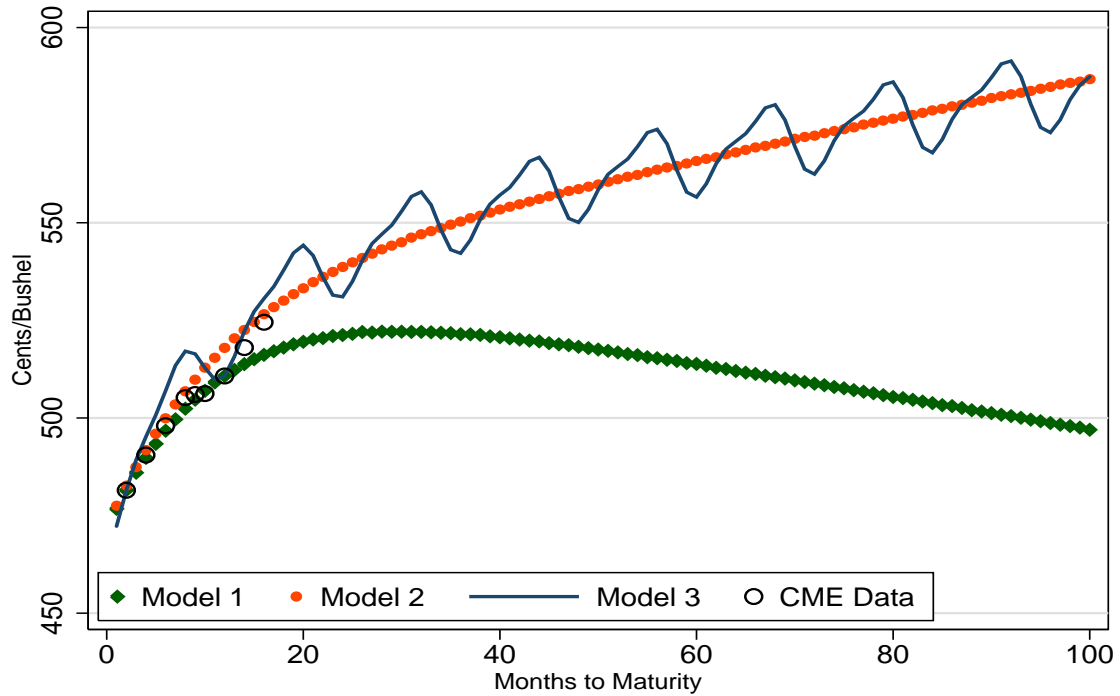


Figure 2.4: Projection of soybean futures prices on November 15, 2000.

Table 2.2: Parameter estimates for the soybean futures market.

Parameters	Model 1			Model 2			Model 3		
	2.5%	50%	97.5%	2.5%	50%	97.5%	2.5%	50%	97.5%
k_x				0.005	0.022	0.038	0.038	0.052	0.063
k_c/k_y	0.950	1.061	1.170	0.978	1.075	1.172	1.031	1.124	1.230
$\lambda_c/\lambda_{y,0}$	-0.061	-0.046	-0.033	-0.054	-0.040	-0.025	-0.038	-0.025	-0.013
$\lambda_{y,1,sin}$							0.183	0.200	0.218
$\lambda_{y,1,cos}$							-0.026	-0.008	0.010
$\lambda_{y,2,sin}$							-0.339	-0.245	-0.159
$\lambda_{y,2,cos}$							0.231	0.315	0.395
$u_{x,0}$	0.020	0.030	0.038	0.024	0.032	0.041	0.029	0.037	0.046
$u_{x,1,sin}$							0.079	0.091	0.103
$u_{x,1,cos}$							0.052	0.064	0.076
$u_{x,2,sin}$							-0.108	-0.096	-0.083
$u_{x,2,cos}$							-0.113	-0.102	-0.091
$u_{c,0}/u_{y,0}$	0.005	0.014	0.023	-0.249	-0.138	-0.018	-0.438	-0.361	-0.262
$u_{y,1,sin}$							0.203	0.249	0.289
$u_{y,1,cos}$							-0.651	-0.604	-0.559
$u_{y,2,sin}$							0.508	0.636	0.768
$u_{y,2,cos}$							0.223	0.356	0.501
σ_x	0.247	0.257	0.268	0.247	0.258	0.269	0.241	0.251	0.262
σ_y	0.245	0.263	0.281	0.246	0.262	0.279	0.241	0.256	0.275
$\rho_{x,y}$	0.669	0.700	0.729	0.647	0.682	0.716	0.625	0.662	0.696
ρ	0.076	0.107	0.138	0.080	0.109	0.140	0.084	0.115	0.148
σ_e	0.0305	0.0315	0.0332	0.0305	0.0313	0.0316	0.0247	0.0255	0.0263

Note: The three quantities denote respectively the 2.5, 50 and 97.5 percentiles of the posterior probability band.

models on January 15, 2010 and November 15, 2000, respectively. From figure 2.3, we can see that Model 3 precisely captures the seasonality feature of the CME data for maturities shorter than 20 months. For completeness, figure 2.3 also shows the settlement price for contracts with positive open interest but zero trading volume. These prices were set by the CME to calculate the margins that need to be posted, but are not prices at which trading actually occurred on January 15, 2010. The estimated futures curve suggests that such zero-volume settlement prices significantly understated the seasonality that characterizes the soybean market.

On January 15, 2010, the soybean price was relatively high. The futures curve implied by Model 3 shows a market expectation of a reduction in price levels to the market's estimate of production costs. For contracts with a short time to maturity, the curvature of the futures curve implied by Schwartz's model depends on the relative value of the net convenience yield. If we evaluate the drift at the risk-neutral long-term mean of the net convenience yield, it is negative. Consequently, the futures curve has a

constant negative slope in the long run. With a short time to maturity (e.g., less than 24 months), Models 1 and 2 predict similar futures prices. However, as time to maturity increases, the difference becomes noticeable, with Model 2 predicting a lower value of long-term futures prices. The futures curve implied by Model 3 follows the trend of Model 2 but with seasonality. We observe a local maximum when time to maturity is equal to 6 months, which corresponds to a maturity date of July 15, 2010. July is right before the U.S. harvest season. At that time, the supply is at the lowest point of the year. So it is not surprising to expect the spot price to be highest on that month.

Figure 2.4 shows the term structure of the futures curve predicted by Models 1 through 3 on November 15, 2000. Compared to January 2010, the soybean spot price was much lower on November 2000. The net convenience yield is also well below the long-term mean implied by Model 1. Since the stochastic process of the net convenience yield in Schwartz's model is assumed to be mean-reverting, the net convenience yield is expected to increase in the following months. And since the net convenience yield's speed of mean reversion is much lower in the soybean market than in the lean hog market, it takes a longer time for the net convenience yield to reach its long-term mean. As the net convenience yield recovers, the futures price is expected to increase at a decreasing rate. Finally, when the net convenience yield reaches its long-term mean, the risk-neutral process of the spot price has a negative risk-neutral drift. Consequently, the term structure of the long-term futures curve is expected to have a negative slope in Schwartz's model. On the other hand, price mean reversion is assumed in Model 2. On that date, a low value of the spot price and the net convenience yield is implied by Model 2, so both x_t and y_t are expected to increase. As a result, Model 2 predicts that futures prices will increase at a decreasing rate with time to maturity.

2.5.3 Comparison Among Models

Figures 2.1 through 2.4 suggest that Model 3 dominates Models 1 and 2 in terms of fitting historical data, at least for the dates selected. To provide a more rigorous comparison of the model specifications, we computed the Bayesian deviance information criterion (*DIC*) advocated by Spiegelhalter *et al.* (2002),

$$DIC \equiv D(\bar{\theta}) + 2p_D, \quad (2.28)$$

where $D(\theta) \equiv -2\log(\Pr(\text{data} | \theta))$, $p_D \equiv \overline{D(\theta)} - D(\bar{\theta})$ measures the complexity of the model, $\bar{\theta}$ represents the posterior means of the parameters, $\overline{D(\theta)}$ is the mean deviance, and $D(\bar{\theta})$ is the deviance of the means. *DIC* may be interpreted as a classical estimation of fit, $D(\bar{\theta})$, plus twice the effective number of parameters, p_D . Spiegelhalter *et al.* proposed that *DIC* inferences could follow similar guidelines to AIC tests, where differences of less than 2 show similar support among models, whereas differences greater than 3 indicate stronger support for one model over another.

Table 2.3: Deviance results for the lean hog and soybean futures prices.

Parameters	Lean Hogs			Soybean		
	Model 1	Model 2	Model 3	Model 1	Model 2	Model 3
\bar{D}	-6225.24	-6297.56	-9553.98	-14253.26	-14277.38	-15400.50
$D(\bar{\theta})$	-6233.04	-6307.04	-9576.64	-14261.18	-14288.16	-15425.34
p_D	7.80	9.48	22.66	7.92	10.78	24.84
<i>DIC</i>	-6217.44	-6288.08	-9531.32	-14245.34	-14266.60	-15375.66

The *DIC* comparison results are reported in table 2.3. Both the lean hog and soybean results are shown and the results are the same across the commodities. The differences between the *DIC*s of Models 1 and 2 exceed 20, which indicates strong statistical evidence for the inclusion of mean reversion in the spot price. The addition of seasonality parameters to the model is also strongly favored as can be seen by comparing the *DIC*s of Model 3 to those of Models 1 and 2. The *DIC* results parallel the inferences that can be drawn from figures 2.1 through 2.4.

2.5.4 95 Percent Credible Band of Futures Prices

Given the substantial uncertainty associated with long-term commodity prices, it is useful to look at the 95 percent credible band of the futures prices predicted by our model (Model 3). Figure 2.5 shows such a band for soybean futures on January 15, 2010. By construction, the predicted futures curve goes through the futures prices with 2 and 12 months until maturity, as those two futures prices were taken to be the ones perfectly correlated with the latent factors.

The band corresponding to parameter variability shows the 95 percent credible band of the futures curve induced by the uncertainty in model parameters only. It is observed that the 95 percent credible band is very tight for futures prices with a short time to maturity. As time to maturity increases, the

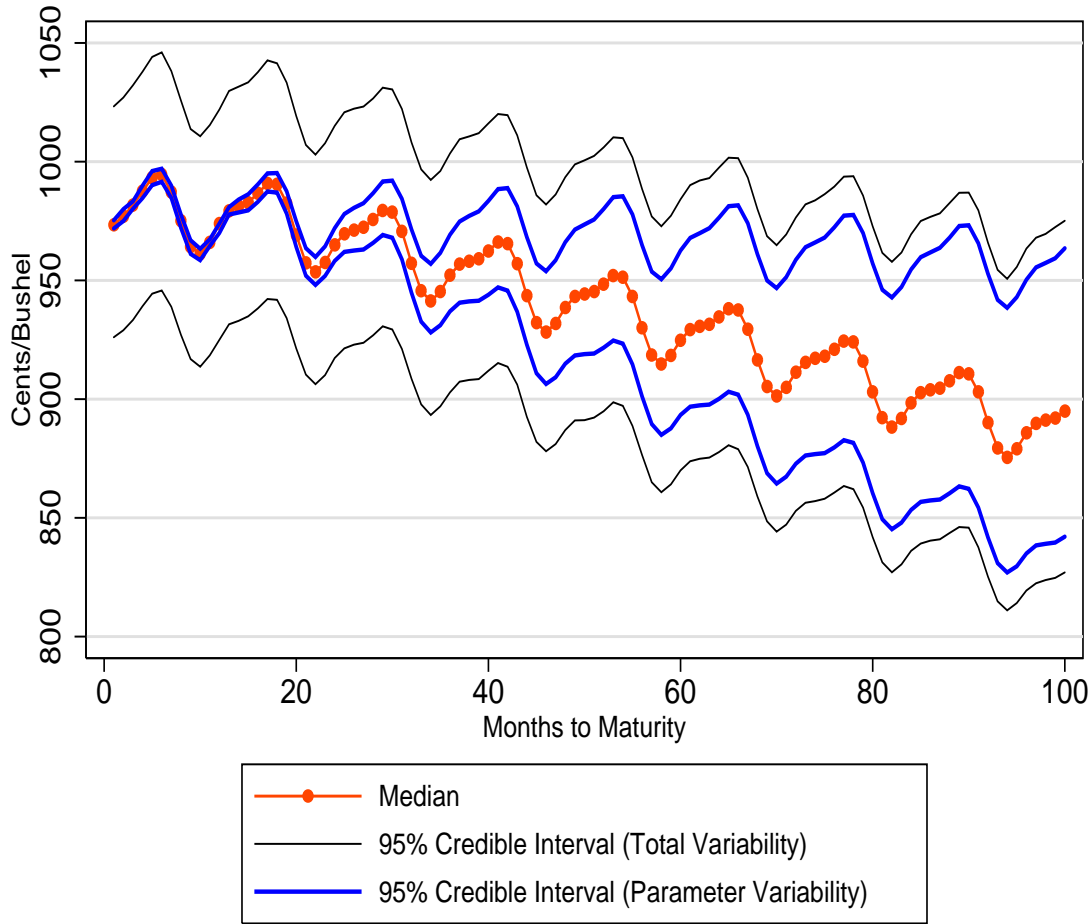


Figure 2.5: 95 percent credible band of futures prices predicted by Model 3 for soybean market on January 15, 2010.

variability in the Bayesian estimates leads to a wider 95 percent credible band. When time to maturity is near 100 months, the width of the band exceeds \$1/bushel.

The “total variability” band shows the 95 percent credible band of futures prices when we consider both the uncertainty in the model parameters and the observation errors. Allowing for observation errors has a negligible effect on the median value of the estimated futures prices, because errors are assumed to have zero mean. However, observation errors have a dramatic effect on the 95 percent credible band of futures prices. The total variability band is much wider than the parameter variability band for short maturities. As time to maturity increases, however, parameter uncertainty accounts for a larger share of the futures uncertainty relative to the observation errors.

Figure 2.6 for the lean hog market tells a similar story to its counterpart for the soybean market,

figure 2.5. The width of the 95 percent “parameter variability” credible band increases with time to maturity. One striking difference with figure 2.5 is that the 95 percent “total variability” credible band is slightly wider for short times to maturity. This result is somewhat counterintuitive at first glance. Note, however, that in equation (2.27) the error term is added to the logarithm of futures prices instead of futures prices themselves. Thus, when taking the exponential of the logarithm of futures prices including errors to compute futures prices, a wider band is obtained for larger values of the logarithm of futures prices. On this particular date (January 15, 2010), futures prices are decreasing with time to maturity (ignoring seasonal effects). As a result, in this instance the observation error volatility dominates the volatility in model parameters, which leads to a wider 95 percent credible band with short times to maturity.

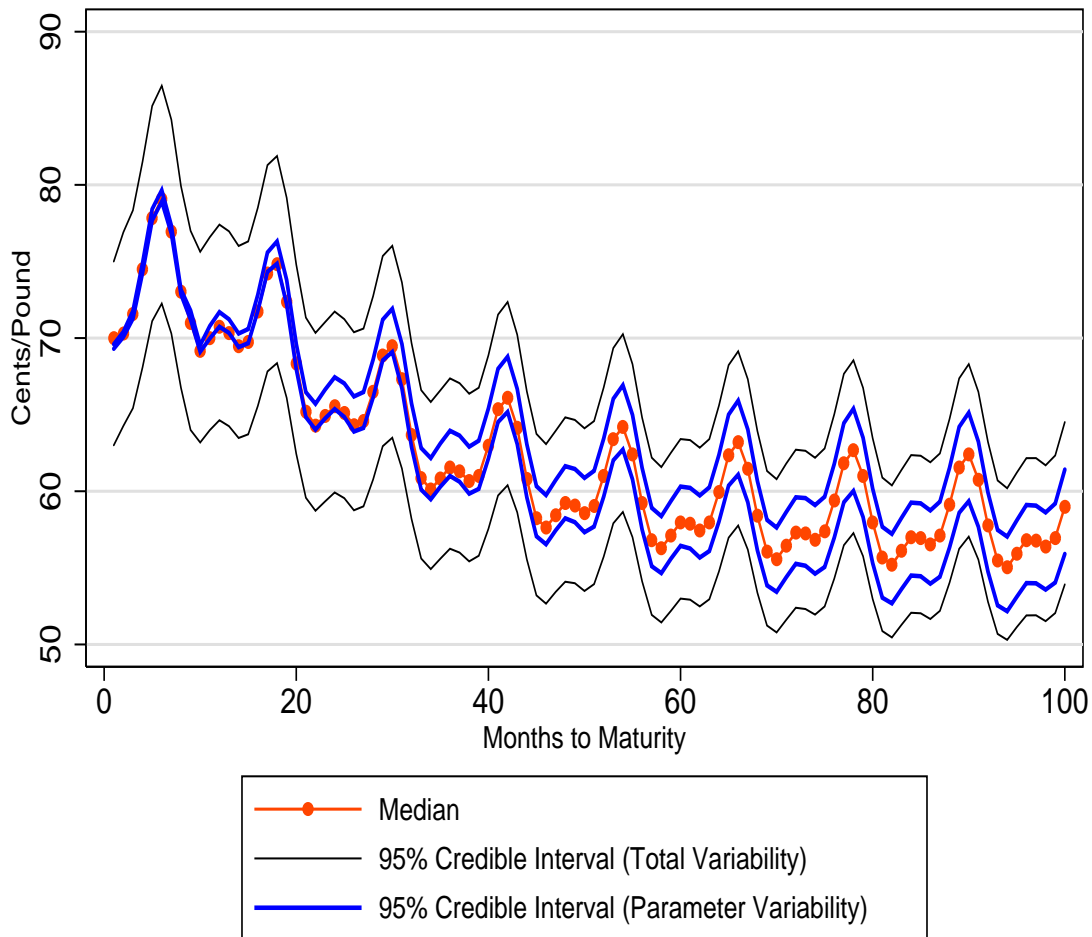


Figure 2.6: 95 percent credible band of futures prices predicted by Model 3 for lean hog market on January 15, 2010.

2.6 Conclusion

With the purpose of developing a method to estimate the long-term futures curve for agricultural futures, we generalize Schwartz's two-factor model by allowing for both mean reversion in spot prices and seasonality. These are key features of agricultural commodity markets. Closed-form futures pricing formulas are derived. We show that Schwartz's model is a special case of our model. Soybean and lean hog futures price data from the CME are employed to estimate the models by means of a Bayesian MCMC algorithm. Estimates for Schwartz's model are obtained by imposing the corresponding restrictions to our model.

We show results for the markets during two historical pricing periods as examples. The first example represents a period of relatively high prices, whereas the second corresponds to a period of low prices. In both instances the results suggest an intuitive relationship between the short-term futures we observe and the long-run expected production cost. The addition of mean reversion and seasonality is supported by the model estimates and futures price projections are improved with their incorporation. The evolution of this model and the projections of long-term futures prices from it could provide support for the continued development of agricultural swaps. The price projections could also support development of long-term price risk management tools and insurance products.

2.7 Appendix

2.7.1 Appendix A

According to equation (2.22), $\frac{\partial \beta_1(t, T)}{\partial t} = k_x \beta_1(t, T)$. Together with the boundary condition $\beta_1(T, T) = 1$, this implies that $\beta_1(t, T) = \exp(k_x(t - T))$. Also from equation (2.22),

$$\begin{aligned} \frac{\partial \beta_2(t, T)}{\partial t} &= \beta_1(t, T) + k_y \beta_2(t, T) \\ &= \exp(k_x(t - T)) + k_y \beta_2(t, T). \end{aligned}$$

Therefore, $\beta_2(t, T) = \frac{\exp(k_x(t - T)) - \exp(k_y(t - T))}{k_x - k_y}$.

Using the above expressions for $\beta_1(t, T)$ and $\beta_2(t, T)$, equation (2.23) can be written as

$$\frac{\partial \alpha(t, T)}{\partial t} = (r - \sigma_x^2/2)\beta_1(t, T) + \psi(t)\beta_2(t, T) - \frac{1}{2}\beta_1(t, T)V\beta(t, T).$$

Hence,

$$\begin{aligned} \alpha(t, T) &= \frac{r - \sigma_x^2/2}{k_x} (\exp(k_x(t - T)) - 1) + \frac{\psi_0}{k_x - k_y} \left[\frac{1}{k_x} (\exp(k_x(t - T)) - 1) - \left(\frac{1}{k_y} (\exp(k_y(t - T)) - 1) \right) \right] \\ &+ \sum_{h=1}^2 \frac{\psi_{h, \cos}}{k_x - k_y} \left(\frac{1}{k_x^2 + 4\pi^2 h^2} - \frac{1}{k_y^2 + 4\pi^2 h^2} \right) \times \\ &\{k_x [\exp(k_x(t - T)) \cos(2\pi ht) - \cos(2\pi hT)] + 2\pi h [\exp(k_x(t - T)) \sin(2\pi ht) - \sin(2\pi hT)]\} \\ &+ \sum_{h=1}^2 \frac{\psi_{h, \sin}}{k_x - k_y} \left(\frac{1}{k_x^2 + 4\pi^2 h^2} - \frac{1}{k_y^2 + 4\pi^2 h^2} \right) \times \\ &\{k_x [\exp(k_x(t - T)) \sin(2\pi ht) - \sin(2\pi hT)] + 2\pi h [\exp(k_x(t - T)) \cos(2\pi ht) - \cos(2\pi hT)]\} \\ &- \frac{1}{2} \left\{ \left[\frac{\sigma_x^2}{2k_x} + \frac{\rho_{xy} \sigma_x \sigma_y}{k_x(k_x - k_y)} + \frac{\sigma_y^2}{2k_x(k_x - k_y)^2} \right] \times [\exp(2k_x(t - T)) - 1] \right. \\ &- \left. \left[\frac{2\rho_{xy} \sigma_x \sigma_y}{k_x^2 - k_y^2} + \frac{2\sigma_y^2}{(k_x + k_y)(k_x - k_y)^2} \right] \times [\exp((k_x + k_y)(t - T)) - 1] \right. \\ &\left. + \frac{\sigma_y^2}{2k_y(k_x - k_y)^2} [\exp(2k_y(t - T)) - 1] \right\}. \end{aligned}$$

2.7.2 Appendix B

Equation (2.25) can be written as

$$\begin{aligned} x_{t+\Delta} - x_t &= (r - \sigma_x^2/2 - k_x x_t - y_t + \lambda_x(t))\Delta + \sqrt{\Delta}\varepsilon_{1,t}, \\ y_{t+\Delta} - y_t &= (\psi(t) - k_y y_t + \lambda_y(t))\Delta + \sqrt{\Delta}\varepsilon_{2,t}, \end{aligned}$$

where $t = \frac{1}{12}, \frac{2}{12}, \dots, \frac{T-1}{12}$, T is the total number of observation dates, and $cov(\varepsilon_{1,i}, \varepsilon_{2,j}) = V$ if $i = j$, and is zero otherwise. The above two equations can be rearranged to yield

$$\begin{aligned} z_{1,t} &= \lambda_{x,0} + \sum_{h=1}^2 (\lambda_{x,h,\cos} \cos(2\pi ht) + \lambda_{x,h,\sin} \sin(2\pi ht)) + \frac{1}{\sqrt{\Delta}}\varepsilon_{1,t}, \\ z_{2,t} &= \lambda_{y,0} + \sum_{h=1}^2 (\lambda_{y,h,\cos} \cos(2\pi ht) + \lambda_{y,h,\sin} \sin(2\pi ht)) + \frac{1}{\sqrt{\Delta}}\varepsilon_{2,t}, \end{aligned}$$

where $z_{1,t} \equiv \frac{x_{t+\Delta} - x_t}{\Delta} - (r - \sigma_x^2/2 - k_x x_t - y_t)$ and $z_{2,t} \equiv \frac{y_{t+\Delta} - y_t}{\Delta} - (\psi(t) - k_y y_t)$. The latter equations can be expressed as the matrix equality

$$\begin{bmatrix} Z_1 \\ Z_2 \end{bmatrix} = \begin{bmatrix} X_1 & 0 \\ 0 & X_2 \end{bmatrix} \begin{bmatrix} \gamma_1 \\ \gamma_2 \end{bmatrix} + \begin{bmatrix} \xi_1 \\ \xi_2 \end{bmatrix},$$

where $Z_i \equiv [z_{i,1/12}, z_{i,2/12}, \dots, z_{i,(T-1)/12}]'$ for $i = 1$ and 2 , $\gamma_1 \equiv [\lambda_{x,0}, \lambda_{x,1,\cos}, \lambda_{x,1,\sin}, \lambda_{x,2,\cos}, \lambda_{x,2,\sin}]'$, $\gamma_2 \equiv [\lambda_{y,0}, \lambda_{y,1,\cos}, \lambda_{y,1,\sin}, \lambda_{y,2,\cos}, \lambda_{y,2,\sin}]'$, $\xi_i \equiv [\frac{1}{\sqrt{\Delta}}\varepsilon_{i,1/12}, \frac{1}{\sqrt{\Delta}}\varepsilon_{i,2/12}, \dots, \frac{1}{\sqrt{\Delta}}\varepsilon_{i,(T-1)/12}]'$ for $i = 1$ and 2 , and

$$X_1 = X_2 \equiv \begin{bmatrix} 1, & \cos(2\pi \times \frac{1}{12}), & \sin(2\pi \times \frac{1}{12}), & \cos(4\pi \times \frac{1}{12}), & \sin(4\pi \times \frac{1}{12}) \\ 1, & \cos(2\pi \times \frac{2}{12}), & \sin(2\pi \times \frac{2}{12}), & \cos(4\pi \times \frac{2}{12}), & \sin(4\pi \times \frac{2}{12}) \\ \vdots & \vdots & \vdots & \vdots & \vdots \\ 1, & \cos(2\pi \times \frac{T-1}{12}), & \sin(2\pi \times \frac{T-1}{12}), & \cos(4\pi \times \frac{T-1}{12}), & \sin(4\pi \times \frac{T-1}{12}) \end{bmatrix}.$$

By employing obvious notation, the above matrix equation can be written more compactly as $Z = X \Gamma + \Xi$, where $cov(\Xi) = \Sigma \otimes I_{T-1}$ and $\Sigma \equiv \frac{1}{\Delta}V$. This is a standard problem of Bayesian inference on the SUR model. Giles (2001) points out that Γ satisfies a multivariate normal distribution with mean equal to $[X' (\Sigma^{-1} \otimes I_{T-1}) X]^{-1} X' (\Sigma^{-1} \otimes I_{T-1}) Z$ and variance equal to $[X' (\Sigma^{-1} \otimes I_{T-1}) X]^{-1}$.

2.7.3 Appendix C

Table 2.4: Gelman-Rubin test statistics for the lean hog and soybean futures markets.

Parameters	Lean Hogs			Soybean		
	Model 1	Model 2	Model 3	Model 1	Model 2	Model 3
k_x		1.047	1.007		1.038	1.001
k_c/k_y	1.017	1.014	1.050	1.044	1.042	1.047
$\lambda_c/\lambda_{y,0}$	1.010	1.002	1.006	1.013	1.001	1.079
$\lambda_{y,1,sin}$			1.014			1.001
$\lambda_{y,1,cos}$			1.031			1.006
$\lambda_{y,2,sin}$			1.006			1.017
$\lambda_{y,2,cos}$			1.001			1.032
$u_{x,0}$	1.010	1.001	1.001	1.003	1.002	1.029
$u_{x,1,sin}$			1.027			1.006
$u_{x,1,cos}$			1.003			1.001
$u_{x,2,sin}$			1.001			1.015
$u_{x,2,cos}$			1.001			1.001
$u_{c,0}/u_{y,0}$	1.012	1.061	1.084	1.027	1.033	1.032
$u_{y,1,sin}$			1.007			1.006
$u_{y,1,cos}$			1.001			1.007
$u_{y,2,sin}$			1.001			1.040
$u_{y,2,cos}$			1.008			1.003
σ_x	1.004	1.001	1.051	1.002	1.004	1.001
σ_y	1.009	1.007	1.011	1.068	1.064	1.079
$\rho_{x,y}$	1.003	1.045	1.011	1.013	1.004	1.013
ρ	1.007	1.004	1.001	1.026	1.039	1.007
σ_e	1.001	1.001	1.002	1.072	1.006	1.001

2.7.4 Appendix D

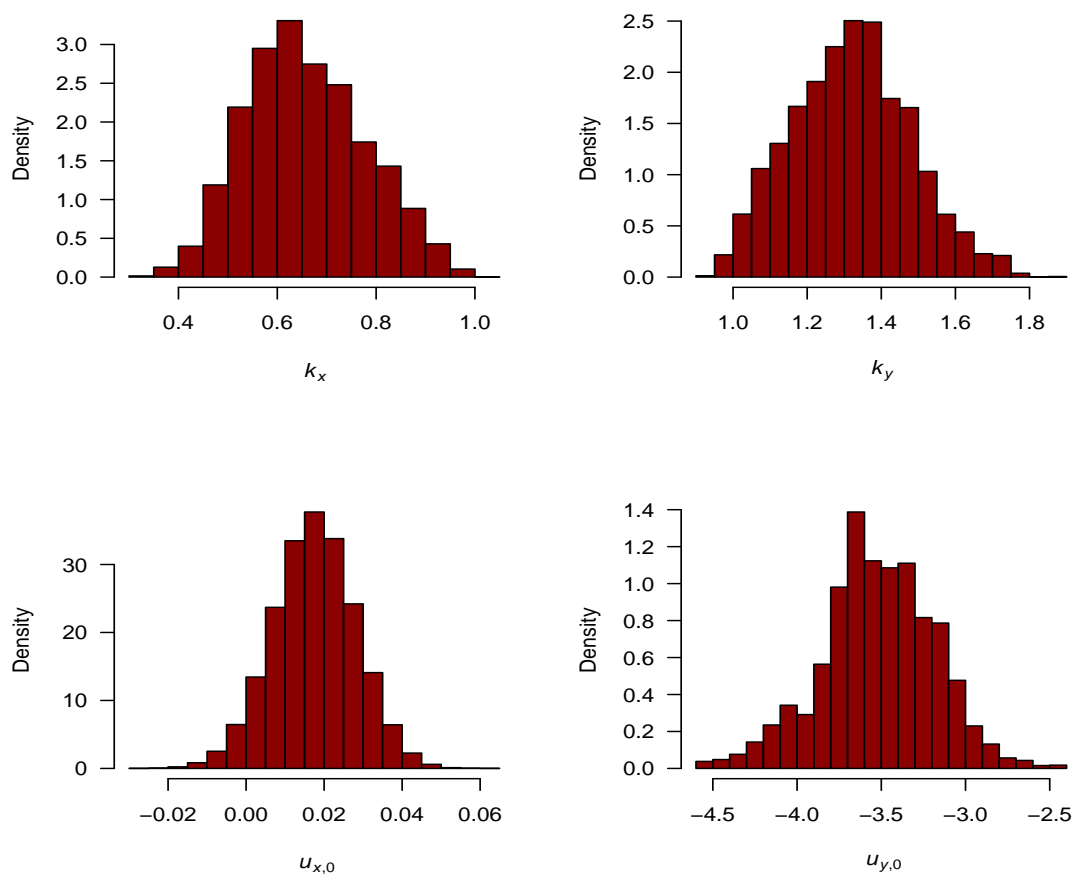


Figure 2.7: Posterior distributions of selected parameters for Model 3, corresponding to lean hog futures prices.

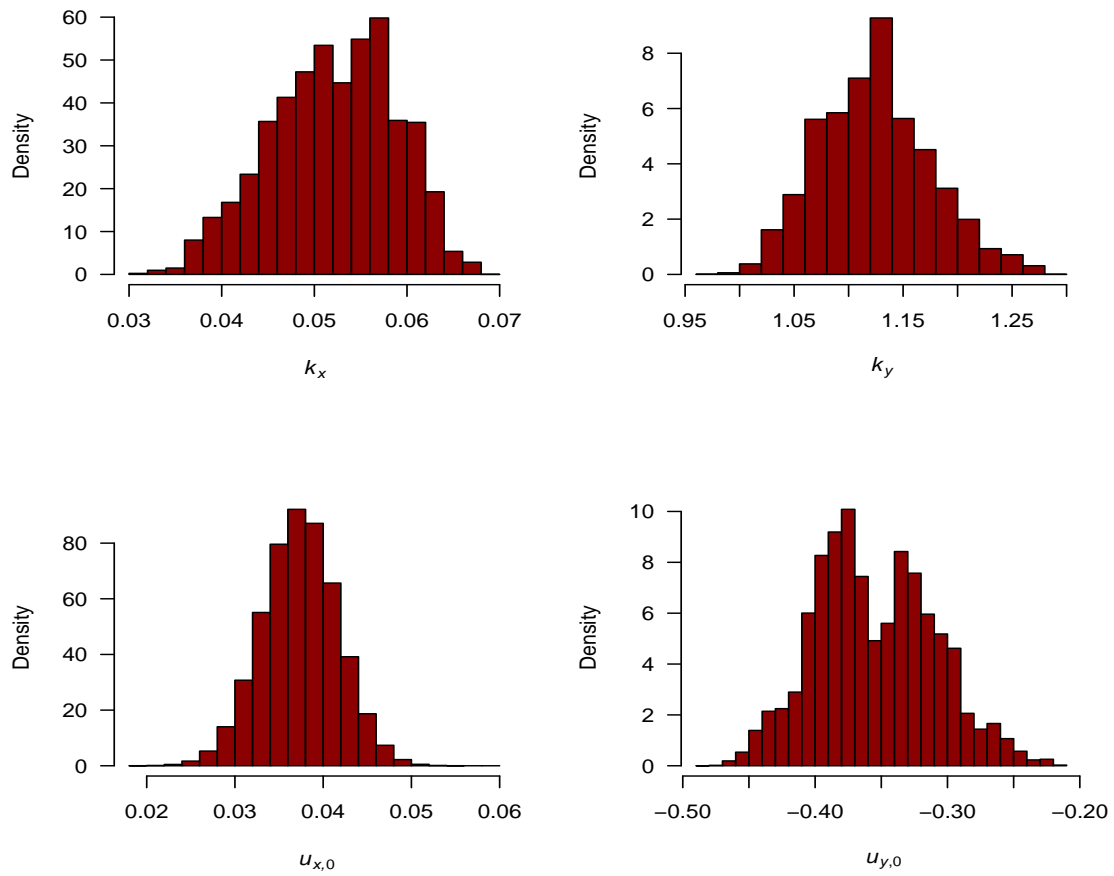


Figure 2.8: Posterior distributions of selected parameters for Model 3, corresponding to soybean futures prices.

References

- Allen, M.T., C.K. Ma, and R.D. Pace. 1994. "Over-Reactions in U.S. Agricultural Commodity Prices." *Journal of Agricultural Economics* 45: 240-51.
- Ball, C, and W. Torous. 1996 "Futures Options and the Volatility of Futures Prices." *Journal of Finance*, 41, 857-870.
- Bernard, J.T., L. Khalaf, M. Kichian, and S. McMahon. 2008. "Forecasting Commodity Prices: GARCH, Jumps, and Mean Reversion." *Journal of Forecasting* 27: 279-91.
- Chen, R., and L. Scott. 1993. "Maximum Likelihood Estimation for a Multifactor Equilibrium Model of the Term Structure of Interest Rates." *Journal of Fixed Income* 3(3): 14-31.
- Christen, A.J., and C. Fox. 2010. "A General Purpose Sampling Algorithm for Continuous Distributions (the T-Walk)." *Bayesian Analysis* 5(2): 263-82.
- Duffie, D.J., J. Pan, and K.J. Singleton. 2000. "Transform Analysis and Asset Pricing for Affine Jump-Diffusions." *Econometrica* 68: 1343-76.
- Durbin, J., and S. Koopman. 2000. "Time Series Analysis of Non-Gaussian Observations Based on State Space Models from Both Classical and Bayesian Perspectives." *Journal of the Royal Statistical Society Series B* 62: 3-56.
- Gelman, A., and D.B. Rubin. 1992. "Inference from Iterative Simulation Using Multiple Sequences." *Statistical Science* 7: 457-511.
- Giles, D.E. 2001. *Computer-Aided Econometrics*. New York: Marcel Dekker.
- Harvey, A.C., 1981. *The Econometric Analysis of Time Series*. Deddington: Philip Allan Publishers.

Harvey, A. and S. Koopman. 2009. "Unobserved Components Models in Economics and Finance." *Control Systems, IEEE* 29: 71-81.

Hore, S., M. Johannes, H. Lopes, R. McCulloch, and N. Polson. 2010. "Bayesian Computation in Finance." In *Frontiers of Statistical Decision Making and Bayesian Analysis*, eds. M. Chen, D. Dey, P. Mueller, D. Sun, and K. Ye. New York: Springer.

Just, E.R., and G.C. Rausser. 1981. "Commodity Price Forecasting with Large-Scale Econometric Models and the Futures Market." *American Journal of Agricultural Economics* 63(2): 197-208.

Kaldor, N. 1939. "Speculation and Economic Stability." *Review of Economic Studies* 7(1): 1-27.

Lence, S.H., and M.L. Hayenga. 2001. "On the Pitfalls of Multi-Year Rollover Hedges: The Case of Hedge-to-Arrive Contracts." *American Journal of Agricultural Economics* 83(1): 107-19.

Peterson, R.L., C.K. Ma, and R.J. Ritchey. 1992. "Dependence in Commodity Prices." *Journal of Futures Markets* 12: 429-46.

Richter, M.C., and C. Sørensen. 2002. "Stochastic Volatility and Seasonality in Commodity Futures and Options: The Case of Soybeans." Working Paper, Dept. of Finance, Copenhagen Business School.

Schwartz, E.S. 1997. "The Stochastic Behavior of Commodity Prices: Implications for Valuation and Hedging." *Journal of Finance* 52(3): 923-73.

Schwartz, E.S., and J.E. Smith. 2000. "Short-Term Variations and Long-Term Dynamics in Commodity Prices." *Management Science* 46(7): 893-911.

Smith, A. 2005. "Partially Overlapping Time Series: A New Model for Volatility Dynamics in Commodity Futures." *Journal of Applied Econometrics* 20: 405-22

Sørensen, C. 2002. "Modeling Seasonality in Agricultural Commodity Futures." *Journal of Futures Markets* 22(5): 393-426.

Spiegelhalter, D.J., N.G. Best, B.P. Carlin, and A. van der Linde. 2002. "Bayesian Measures of Model Complexity and Fit." *Journal of the Royal Statistical Society Series B* 64: 1-34.

Trolle, A., and E.S. Schwartz. 2009. "Unspanned Stochastic Volatility and the Pricing of Commodity Derivatives." *The Review of Financial Studies* 22: 4423-61.

Walburger, A.M., and K.A. Foster. 1995. "Mean Reversion as a Test for Inefficient Price Discovery in U.S. Regional Cattle Markets." *American Journal of Agricultural Economics* 77(5): 1358-89.

CHAPTER 3. Price Mean Reversion, Seasonality, and Options Markets

3.1 Introduction

The Black and Black-Scholes option pricing models assume that spot price volatility increases in proportion to the square root of time (Black (1976)). This assumption is reasonable for stocks and currencies but is inconsistent with mean reversion in spot commodity prices. Most agricultural commodity markets demonstrate mean reversion to production costs (Bessembinder et al. (1995)), which suggests that prices will eventually revert to this cost because of supply response. If this is true, and if price volatility is incorrectly assumed to increase in proportion to the square root of time, the fair value of long-term options will be overestimated. Without an accurate pricing formula, sellers and buyers of renewable commodity futures options may not be able to agree on a price that they can trade. In this regard, it is interesting to note that options on key agricultural commodities such as soybeans and lean hogs do not trade beyond a 12- to 14-month window.

Schwartz (1997) recognized one aspect of this problem in the context of commodity futures. He had the insight that price imbalances caused by temporary shortages and surpluses would eventually disappear without impacting the long-run volatility level. For example, an oil shortage can make the convenience yield greater than the storage cost and this can cause nearby futures prices to exceed the prices of more distant contracts. Several researchers (Miltersen and Schwartz (1998) and Hilliard and Reis (1998)) have proposed closed-form option-pricing models that incorporate reversion to the mean in the convenience yield. However, the spot price in Schwartz's (1997) two-factor model is assumed to be trending rather than mean reverting. If convenience yield is a constant, the spot price in the Schwartz model is assumed to follow a geometric Brownian motion. Therefore, such models are most likely to be relevant to exhaustible commodity markets such as gold and oil, for which Hotelling's Principle might be expected to hold.

A number of studies report evidence of mean reversion in commodity prices (e.g., Peterson, Ma, and Ritchie (1992); Allen, Ma, and Pace (1994); Walburger and Foster (1995), Casassus and Collin-Dufresne (2005)). Cassasus and Collin-Dufresne (2005) developed a three-factor futures model for non-seasonal commodities. Their model assumes convenience yield is a linear function of spot prices and interest rates, which induces mean-reversion in prices under the risk-neutral measure. Although closed-form solutions for the corresponding option valuation formulas are not available based on their model setup, the authors are able to report European option values using a Fourier inversion approach. The authors estimated the model using futures prices for silver, gold, and copper. They found empirical evidence of mean reversion in the spot prices, thereby implying lower estimates of option prices.

We argue that mean reversion in the spot price level as well as in the convenience yield is a key feature of agricultural commodity markets such as grains and livestock. For example, when prices are relatively high, supply will increase, which will in turn put downward pressure on prices. On the demand side, when prices are high, demand will decrease, which will also induce prices to decrease. A similar story can be told when prices are relatively low.

In the model outlined below, convenience yield consists of two parts. The first part satisfies an Ornstein-Uhlenbeck process. The second part captures the fact that convenience yield is usually positively correlated with the spot price. When the first component of convenience yield is stabilized, the spot price behaves as an Ornstein-Uhlenbeck process. Allowing convenience yield to be a function of the spot commodity price leads to mean reversion of spot prices under both the historical and risk-neutral measures. This model structure also incorporates the Schwartz model as a special case.

Seasonality is known to be an empirical characteristic of most commodity markets. It is especially important for agricultural commodities with seasonal production or demand patterns. Given the same data set, models that ignore seasonality will likely induce a higher estimated volatility of the factors than their counterparts augmented with seasonality. This in turn will lead to a prediction of larger option prices.

Sørensen (2002) modeled seasonality in agricultural commodity futures. He introduced seasonality by adding a deterministic seasonal component to the commodity spot price. A closed-form futures pricing formula is derived based on his one-factor model with seasonality. Richter and Sørensen (2002) proposed a three-factor model to explore seasonal patterns in both the spot price level and the volatil-

ity in commodity markets. They allow a parameter in the drift term of the convenience yield to be a trigonometric function of time. Seasonality in the volatility term is incorporated by adding a deterministic trigonometric function of time. However, closed-form solutions for futures and option pricing formulas are not available based on their model setup.

Seasonality is introduced into our model by allowing the parameters in the drift terms of the two factors (spot price and convenience yield) to be a periodic function of calendar time. The evaluation of futures and option pricing expressions can be reduced to the problem of solving ordinary differential equations (Duffie, Pan, and Singleton (2000)). Adding seasonality into the model makes the solution more complicated, since the involved stochastic differential equations are inhomogeneous in time because the drift coefficients are functions of calendar time. However, we still get closed-form expressions for both futures and option pricing formulas, which greatly facilitates the empirical work.

A negative relationship between supply/inventories and convenience yields is predicted by the theory of storage. Thus, the convenience yield from marginal storage is high when inventory is low or supply is scarce, and the opposite is true when inventory is high or supply is large. Since commodity supply exhibits seasonality, the convenience yield is also assumed to behave as a mean-reverting process with seasonality.

We apply a Bayesian Markov Chain Monte Carlo (MCMC) algorithm to estimate our model using futures prices for two agricultural commodities, soybeans and lean hogs, and for one commercial commodity, crude oil. At each sample date, we observe a panel of futures prices, which are related to the latent variables through the futures and option pricing formulas. Following the ideas in Chen and Scott (1993), we assume that all but two futures contract prices are observed with measurement error. The latent value of the state variables can be filtered out at each sample date using the futures pricing formula by inversion based on the two futures contract prices observed without error. The empirical results support the hypothesis that spot prices in commodity markets are mean reverting, and the speed of mean reversion is highest in the lean hog market and lowest in the crude oil market. The estimation shows strong seasonal patterns for agricultural commodities but not for crude oil. The empirical work suggests that while Schwartz's model is well suited to the crude oil market; it has limitations in renewable commodity markets. The impact of how the basic assumption of mean-reverting spot prices and seasonality affects the model's prediction about the price of commodity derivatives with short and long

times to maturity is shown by comparing Black's model, Schwartz's model, and our model.

The rest of this chapter is organized as follows. Section 3.2 uses graphical examples to intuitively show how the basic assumption of mean reversion will affect the fair value of option prices. In section 3.3, we generalize Schwartz's two-factor model. Seasonality is also introduced into the proposed model and four two-factor models are defined. In section 3.4, futures and option pricing formulas are derived. Section 3.5 describes the empirical model, the data set, and the estimation method. The econometric analysis and estimation results are discussed in section 3.6. The last section concludes the chapter.

3.2 Graphical examples

Figures 1, 2, and 3 are graphical representations of the three assumptions that underlie the three models (Black, Schwartz, and our model) and they show how our model differs from those of Schwartz and Black. All three figures depict the same simulated time series of (the logarithm of) prices x_t , and all contain the upper and lower confidence intervals for these prices at two points in time.

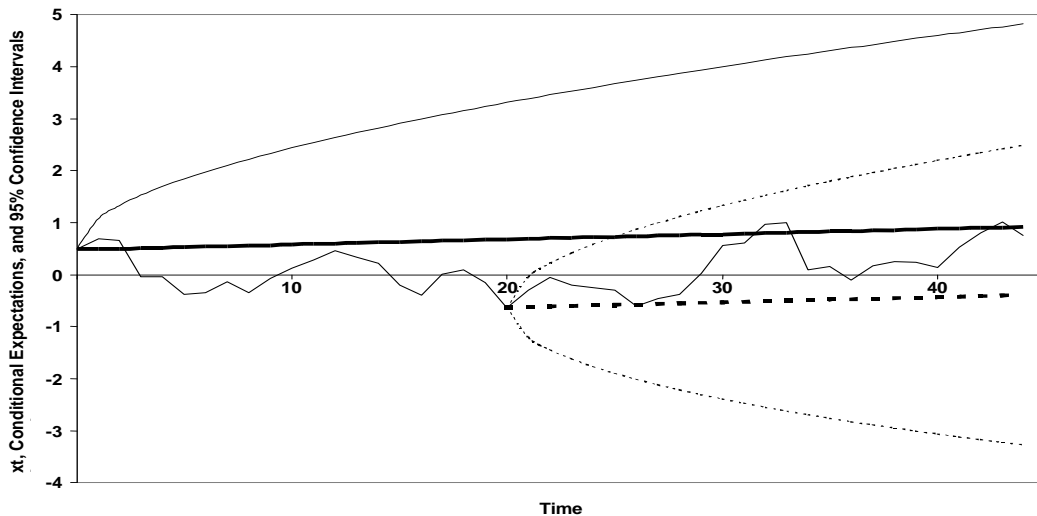


Figure 3.1: Behavior of x_t , conditional expectations, and 95% confidence intervals under Black's model

Figure 3.1 shows prices under the standard Black assumption of Brownian motion. It can be observed that the confidence interval for prices increases in proportion to the square root of time. The heavy solid line shows the expected price path as of time zero and this demonstrates a small amount of growth as might be expected for the cash prices for some commodities or stocks. If futures markets

existed for this asset, this heavy line would reflect the temporal basis. At time 20 the realized cash price is lower than was expected at time 0 and the heavy dotted line shows the expected price path from this lower point. All of the price reduction from time 0 through time 20 is viewed as permanent in this model. Therefore, the updated expected price path runs parallel to the original but at a level that reflects the underperformance of price between times 0 and 20.

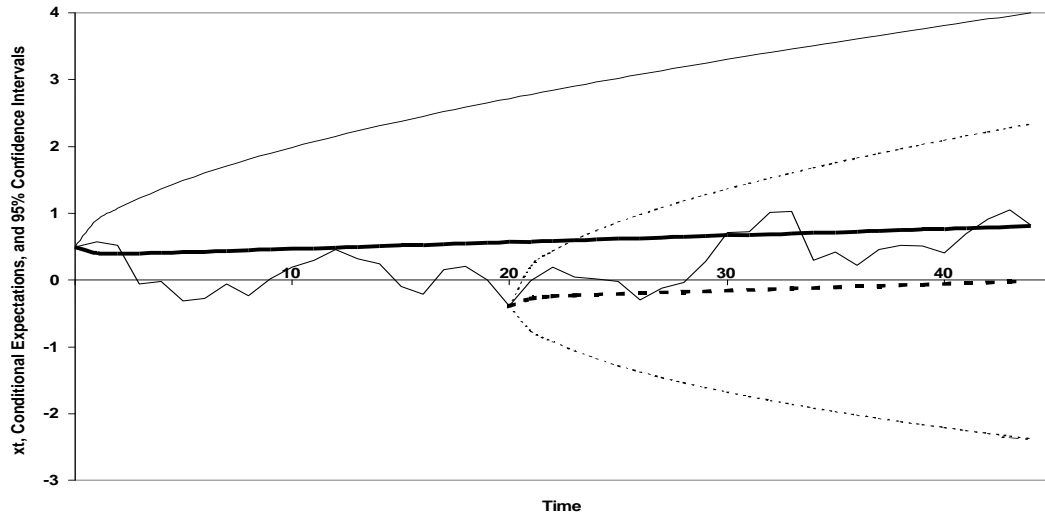


Figure 3.2: Behavior of x_t , conditional expectations, and 95% confidence intervals under Schwartz's model

Figure 3.2 shows the Schwartz model, and is otherwise identical to Figure 3.1. A key difference between Figures 3.1 and 3.2 is that when the price path is updated at time 20, the Schwartz model recognizes that the price drop that occurred just before time 20 was in part due to a temporary reduction in the convenience yield (c_t) reflecting a temporary surplus of the commodity. The model assumes that this temporary component will gradually disappear, and therefore it adjusts the expected time path of cash prices for this expected price recovery. However, once this temporary adjustment vanishes, Schwartz's model behaves very much like Black's.

Figure 3.3 illustrates the model we propose here. The price path after time 20 contains an adjustment to the temporary imbalance as in Schwartz's model. However, the model also contains one additional piece of information. It recognizes that the generally low level of prices observed at time 20 is well below the production costs for this commodity. This suggests a reduction in supply until prices recover to these expected production costs. Therefore, the heavy dotted line approaches the heavy solid line as the

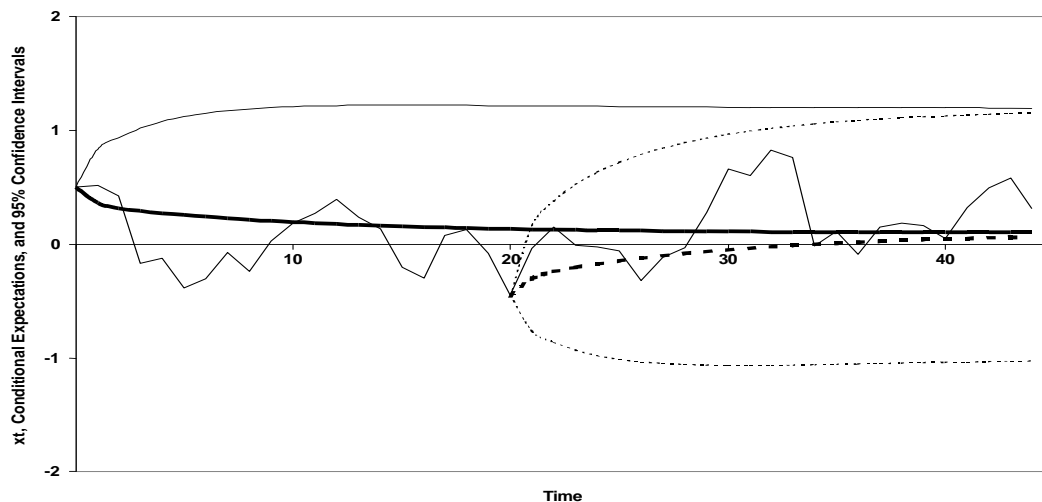


Figure 3.3: Behavior of x_t , conditional expectations, and 95% confidence intervals under our model

model implicitly adjusts supply and demand so that expected future prices lie on the path representing expected production costs. This additional piece of information has a dramatic effect on the upper and lower confidence levels, because the model recognizes that all price deviations around these expected production costs are of a temporary nature and it therefore tightens the confidence interval around this price path.

The upper and lower confidence intervals are directly related to the fair option price. Therefore, this intuitive evidence suggests that when mean reversion in the price level is added to mean reversion in the convenience yield, the fair option value will be lower. The degree to which models that neglect mean reversion in the price level overprice option premia will depend on the parameters of the models, but it is clear that the degree of overpricing will increase with the time to expiration of the option.

3.3 Schwartz's model and generalization

Schwartz advanced a path-breaking model of commodity prices. His fundamental insight is that commodity prices are characterized by convenience yields. He postulated that the convenience yield net of storage cost, c_t , follows the Ornstein-Uhlenbeck stochastic process,

$$dc_t = (u_c - k_c c_t)dt + \sigma_c dw_c(t), \quad (3.1)$$

where u_c/k_c is the long-run mean of the convenience yield, $k_c > 0$ is the convenience yield's speed of

mean reversion, and $dw_c(t)$ is a Wiener process. However, Schwartz assumes that the commodity spot price process, S_t , behaves as a geometric Brownian motion, when convenience yield c_t is a constant,

$$dS_t = (u_s - c_t)S_t dt + \sigma_s S_t dw_s(t), \quad (3.2)$$

where $dw_s(t)$ is a Wiener process and $dw_c(t)dw_s(t) = \rho_{sc}dt$. Defining $x_t \equiv \ln(S_t)$, application of Ito's Lemma yields the stochastic process for x_t ,

$$dx_t = (u_x - c_t)dt + \sigma_x dw_x(t), \quad (3.3)$$

where $u_x \equiv u_s - \sigma_s^2/2$, $\sigma_x \equiv \sigma_s$, $dw_x(t) \equiv dw_s(t)$, and $\rho_{xc} \equiv \rho_{sc}$. The expected rate of return to the commodity holder consists of the expected relative price change ($E(dS_t/S_t)$) plus the net convenience yield (c_t). In equilibrium, the expected rate of return to the commodity holder must equal the risk-free rate (r) plus the risk premium associated with the stochastic process x_t (λ_x), $u_s - c_t + c_t = r + \lambda_x$. Then, the corresponding risk-neutral processes are

$$dc_t = (u_c - k_c c_t - \lambda_c)dt + \sigma_c dw_c^Q(t) \text{ and} \quad (3.4)$$

$$dS_t = (r - c_t)S_t dt + \sigma_s S_t dw_s^Q(t), \quad (3.5)$$

where λ_c is the market price for the risk associated with stochastic process of c_t and $dw_c^Q(t)$ and $dw_s^Q(t)$ are the Wiener processes under the equivalent martingale measure. By applying Ito's lemma, the risk-neutral process of dx_t is

$$dx_t = (r - \sigma_x^2/2 - c_t)dt + \sigma_x dw_x^Q(t). \quad (3.6)$$

Note that $dw_x^Q(t) = dw_s^Q(t)$ and $dw_c^Q(t)dw_x^Q(t) = \rho_{xc}dt$. We call this Model 1 for convenience. Schwartz derived futures prices based on this model. The corresponding option prices were obtained by Miltersen and Schwartz (1998) and Hilliard and Reis (1998).

3.3.1 Price mean reversion

A stylized fact of commodity markets is that convenience yields are positively associated with spot prices. Typically, when a commodity is in relatively short supply, its price is high and its convenience yield is high as well. Hence, the convenience yield net of storage costs is postulated to consist of the following function of the logarithm of the spot price:

$$c_t = y_t + k_x x_t. \quad (3.7)$$

The first component of c_t is assumed to follow the Ornstein-Uhlenbeck stochastic process

$$dy_t = (u_y - k_y y_t)dt + \sigma_y dw_y(t), \quad (3.8)$$

where $dw_x(t)dw_y(t) = \rho_{xy}dt$.

Then, the corresponding stochastic process for the spot prices is the following:

$$dS_t = [u_s - y_t - k_x \ln(S_t)]S_t dt + \sigma_s S_t dw_s(t). \quad (3.9)$$

Ito's Lemma yields the following Ornstein-Uhlenbeck stochastic process for the logarithm of the spot prices:

$$dx_t = (u_x - y_t - k_x x_t)dt + \sigma_x dw_x(t). \quad (3.10)$$

In equilibrium, the instantaneous expected total return to commodity holders must equal the risk-free rate plus the associated market price of risk,

$$r + \lambda_x = (u_s(t) - y_t - k_x x_t) + (y_t + k_x x_t) \quad (3.11)$$

$$\Rightarrow (u_s(t) - y_t - k_x x_t) - \lambda_x = r - (y_t + k_x x_t). \quad (3.12)$$

Therefore, the risk-neutral process of dS_t may be written as

$$dS_t = [r - (y_t + k_x x_t)]S_t dt + \sigma_s S_t dw_s^Q(t). \quad (3.13)$$

Then, applying Ito's lemma yields

$$dx_t = [r - \sigma_x^2/2 - (y_t + k_x x_t)]dt + \sigma_x dw_x^Q(t). \quad (3.14)$$

Letting the market price for the y_t risk be λ_y , the risk-neutral process of dy_t is

$$dy_t = (u_y - k_y y_t - \lambda_y)dt + \sigma_y dw_y^Q(t), \quad (3.15)$$

where $dw_x^Q(t)dw_y^Q(t) = \rho_{xy}dt$.

This generalized model is referred to as Model 2. It is clear that Model 1 is a special case of Model

2. If k_x is restricted to be equal to zero and $c_t = y_t$, then these two models are identical. The key

difference between Model 1 and Model 2 is that, when c_t is constant, the log of spot prices in Model 1 exhibits geometric Brownian motion. In contrast, when y_t is constant, the log of spot prices in Model 2 satisfies an Ornstein-Uhlenbeck stochastic process. Empirically, testing whether k_x is equal to zero or not allows us to determine whether the spot prices are mean reverting or not in a given market.

3.3.2 Seasonality

So far we have assumed that all parameters are constant throughout the year. However, most commodity markets differ from the markets for stocks, bonds, and other conventional financial assets, in that they typically exhibit seasonal patterns. For example, prices for annual crops are typically high in the pre-harvest season and low at peak-harvest, and pork prices are usually high during the barbecue season. To capture this feature, the periodicity is introduced in selected parameters by a truncated Fourier series. We add seasonality into the spot price by setting u_x in equations (3.3) and (3.10) to be a periodic deterministic function of time,

$$u_x(t) = u_{x,0} + \sum_{h=1}^H [u_{x,h,\cos} \cos(2\pi ht) + u_{x,h,\sin} \sin(2\pi ht)], \quad (3.16)$$

where H determines the number of terms in the sum and $u_{x,0}$, $u_{x,h,\cos}$ and $u_{x,h,\sin}$ are constant seasonal parameters. H is selected to be equal to 2. This choice is based on the Akaike Information Criterion (AIC); see, e.g., Harvey (1981). Note that if $u_{x,h,\cos} = u_{x,h,\sin} = 0$, for $\forall h \geq 1$, then the model does not exhibit seasonality. The long-term mean parameter of the first component of convenience yield in equation (3.8), u_y , is also generalized to allow for seasonality, with a functional form for $u_y(t)$ analogous to the one for $u_x(t)$ shown above. If the convenience yield does not display seasonal behavior, then $u_{y,h,\cos} = u_{y,h,\sin} = 0$ for $\forall h \geq 1$.

Similar to the expression for u_x , the risk premiums λ_x and λ_y in the previous section are also assumed to be periodic functions of calendar time,

$$\lambda_i(t) \equiv \lambda_{i,0} + \sum_{h=1}^H [\lambda_{i,h,\cos} \cos(2\pi ht) + \lambda_{i,h,\sin} \sin(2\pi ht)], \quad (3.17)$$

where $i = x, y$. For simplicity, Model 1 and Model 2 augmented with seasonality are referred to as Model 3 and Model 4, respectively. The risk-neutral processes (3.14) and (3.15) incorporating seasonality provide us the basic foundations for pricing futures and option contracts on commodity markets, which we address in the next section.

3.4 Futures and option pricing

Commodity spot prices and convenience yields are modeled in continuous time as a system of stochastic differential equations in an affine term structure class. The key advantage of affine models is that they are tractable for asset pricing purposes. We rely on the traditional no-arbitrage approach to price commodity derivatives. The seasonality part makes the derivation more complicated. However, we still get closed-form solutions for the pricing formulas. The following two subsections show how to price commodity futures and options written on commodity futures.

3.4.1 Futures pricing

The risk-neutral process of the two latent variables defined in Section 3 for the advocated model can be written as

$$\begin{bmatrix} dx_t \\ dy_t \end{bmatrix} \sim N \left(\begin{bmatrix} r - \sigma_x^2/2 - k_x x_t - y_t \\ u_y(t) - \lambda_y(t) - k_y y_t \end{bmatrix} dt, \begin{bmatrix} \sigma_x^2 & \rho_{xy} \sigma_x \sigma_y \\ \rho_{xy} \sigma_x \sigma_y & \sigma_y^2 \end{bmatrix} dt^Q \right). \quad (3.18)$$

Define

$$\theta(t) \equiv u_y(t) - \lambda_y(t) \equiv \theta_0 + \sum_{h=1}^H [\theta_{h,\cos} \cos(2\pi ht) + \theta_{h,\sin} \sin(2\pi ht)], \quad (3.19)$$

where $\theta_0 \equiv u_{y,0} - \lambda_{y,0}$, $\theta_{h,\cos} \equiv u_{y,h,\cos} - \lambda_{y,h,\cos}$, and $\theta_{h,\sin} \equiv u_{y,h,\sin} - \lambda_{y,h,\sin}$. Define $\kappa_0(t) \equiv [r - \sigma_x^2/2, \theta(t)]^T$, $\kappa_1 \equiv \begin{bmatrix} k_x & 1 \\ 0 & k_y \end{bmatrix}$, $V \equiv \begin{bmatrix} \sigma_x^2 & \rho_{xy} \sigma_x \sigma_y \\ \rho_{xy} \sigma_x \sigma_y & \sigma_y^2 \end{bmatrix}$, and $\mu_t \equiv [x_t, y_t]^T$. Then,

$$d\mu_t = (\kappa_0(t) - \kappa_1 \mu_t) dt + V dw^Q(t). \quad (3.20)$$

Given that $\mu(t)$ follows an affine diffusion under the martingale measure, it is convenient to apply the method proposed by Duffie, Pan, and Singleton (DPS) (2000)¹ to get a closed-form solution for the futures price at date t maturing at time T as follows:

$$\begin{aligned} F(t, T) &= E_t^Q[S(T)] \\ &= E_t^Q\{\exp[\phi_0 + \phi^T \mu(T)]\} \\ &= \exp[\alpha(t, T) + \beta(t, T) \mu(t)] \\ &\Rightarrow X_{t,T} \equiv \ln(F(t, T)) = \alpha(t, T) + \beta(t, T) \mu(t), \end{aligned} \quad (3.21)$$

¹In their Appendix B, the authors also allow for a time-dependent coefficient, and the method is still valid.

where $E_t^Q[\cdot]$ is the expectation operation under the risk-neutral probability measure. Since the first factor is the log of the spot price, $\phi_0 = 0$ and $\phi^T = [1, 0]$. Equations $\alpha(t, T)$ and $\beta(t, T)$ need to satisfy the following ordinary differential equations (ODEs)

$$\beta'(t, T) = \kappa_1^T \beta(t, T) \quad (3.22)$$

$$\alpha'(t, T) = -\kappa_0(t) \cdot \beta(t, T) - \frac{1}{2} \beta^T(t, T) V \beta(t, T) \quad (3.23)$$

with boundary conditions $\beta(T, T) = \phi$ and $\alpha(T, T) = \phi_0$, where $\alpha'(t, T) \equiv \frac{\partial \alpha(t, T)}{\partial t}$ and $\beta'(t, T) \equiv \frac{\partial \beta(t, T)}{\partial t}$. The solution for $\alpha(t, T)$ and $\beta(t, T)$ is outlined in Appendix A.

3.4.2 Option pricing

The process to solve for the European option pricing expression is very similar to the one we propose for deriving the futures price formula. Let $C[F(t, T), K, t, T_1]$ denote the price at time t of a European call option with a strike price of K expiring at T_1 on a futures contract that expires at time $T \geq T_1$. The payoff of such an option at the expiration date is $\max[F(T_1, T) - K, 0]$. Standard arguments can be applied to show that its price at time t is given by

$$C[F(t, T), K, t, T_1] = \exp[r(t - T_1)] E_t^Q \{ \max[F(T_1, T) - K, 0] \}. \quad (3.24)$$

The moment-generating function of the logarithm of futures prices at time T_1 under the equivalent martingale measure is defined by

$$M_{\ln[F(T_1, T)]} \equiv E_t^Q \{ \exp[z \ln(F(T_1, T))] \}. \quad (3.25)$$

Using the futures price formula derived in the previous section to substitute for $\ln(F(T_1, T))$, we obtain

$$M_{\ln[F(T_1, T)]}(z) \equiv E_t^Q \{ \exp[z \ln(F(T_1, T))] \} \quad (3.26)$$

$$= E_t^Q \{ \exp[z \alpha(T_1, T) + z \beta(T_1, T) \mu(T_1)] \} \quad (3.27)$$

$$= \exp\{z \alpha(T_1, T)\} E_t^Q \{ \exp\{z \beta_1(T_1, T) x_{T_1} + z \beta_2(T_1, T) y_{T_1}\} \}. \quad (3.28)$$

The expectation term on the right-hand side is of the same form as equation (2.3) in DPS, so their method can be applied again. The underlying risk-neutral process does not change so the ODEs do not change. However, the boundary conditions are different. Let the solution to the expectation term be

$$E_t^Q \{ \exp\{z \beta_1(T_1, T) x_{T_1} + z \beta_2(T_1, T) y_{T_1}\} \} = \exp[A(t, T_1) + B(t, T_1) \mu(t)]. \quad (3.29)$$

Then $A(t, T_1)$ and $B(t, T_1)$ satisfy the following ODEs:

$$B'(t, T_1) = \kappa_1^\top B(t, T_1) \quad (3.30)$$

$$A'(t, T_1) = -\kappa_0(t) \cdot B(t, T_1) - \frac{1}{2} B^\top(t, T_1) V B(t, T_1), \quad (3.31)$$

where $A'(t, T_1) \equiv \frac{\partial A(t, T_1)}{\partial t}$, $B'(t, T_1) \equiv \frac{\partial B(t, T_1)}{\partial t}$, and the following boundary conditions are satisfied:

$$B_1(T_1, T_1) = z\beta_1(T_1, T), \quad (3.32)$$

$$B_2(T_1, T_1) = z\beta_2(T_1, T), \text{ and} \quad (3.33)$$

$$A(T_1, T_1) = 0. \quad (3.34)$$

Solving this system of ODEs using the same strategy as employed to solve for the futures price, we get

$$B_1(t, T_1) = z\beta_1(t, T) \text{ and } B_2(t, T_1) = z\beta_2(t, T).$$

By definition of $\eta_1(t, T)$ and $\eta_2(t, T)$ from Appendix A,

$$A(t, T_1) = (\eta_1(t, T) - \eta_1(T_1, T))z + (\eta_2(t, T) - \eta_2(T_1, T))z^2.$$

Therefore, the following expression for the moment-generating function can be obtained:

$$M_{\ln[F(T_1, T)]}(z) = \exp[\varpi(t, T_1, T)z + \frac{1}{2}\sigma(t, T_1, T)^2z^2],$$

where

$$\varpi(t, T_1, T) = \eta_1(T_1, T) + \eta_2(T_1, T) + \eta_1(t, T) - \eta_1(T_1, T) + \beta_1(t, T)x_t + \beta_2(t, T)y_t \quad (3.35)$$

$$= \eta_2(T_1, T) + \eta_1(t, T) + \beta_1(t, T)x_t + \beta_2(t, T)y_t \text{ and} \quad (3.36)$$

$$\sigma(t, T_1, T)^2 = 2[\eta_2(t, T) - \eta_2(T_1, T)]. \quad (3.37)$$

The specific form of the moment-generating function reminds us that $\ln[F(T_1, T)]$ is distributed as a normal random variable with mean $\varpi(t, T_1, T)$ and variance $\sigma(t, T_1, T)^2$. In addition,

$$\begin{aligned} \exp[\varpi + \frac{1}{2}\sigma^2] &= \exp[\eta_1(t, T) + \eta_2(t, T) + \beta_1(t, T)x_t + \beta_2(t, T)y_t] \\ &= \exp[\alpha(t, T) + \beta(t, T)\mu(t)] = F(t, T). \end{aligned} \quad (3.38)$$

Using the probability density function of $\ln[F(T_1, T)]$, it is straightforward to derive the option price from equation (16) (see Appendix B). For notational simplicity, we define $F_{T_1} \equiv F(T_1, T)$. Then

$$E_t^Q\{\max[F_{T_1} - K, 0]\} = \int_{\ln(K)}^{\infty} (F_{T_1} - K) \frac{1}{\sqrt{2\pi\sigma^2}} \exp\left\{-\frac{1}{2} \left[\frac{\ln(F_{T_1}) - \varpi}{\sigma}\right]^2\right\} d\ln(F_{T_1})$$

and the analytical solution for the price of the call option is

$$C[F(t, T), K, t, T_1] = \exp[r(t - T_1)][F(t, T)\mathcal{N}(d_1) - K\mathcal{N}(d_2)], \quad (3.39)$$

where $\mathcal{N}(\cdot)$ is the standard normal cumulative distribution function, $d_1 \equiv \frac{\ln[F(t, T)/K] + 0.5\sigma(t, T_1, T)^2}{\sigma(t, T_1, T)}$, and $d_2 \equiv \frac{\ln[F(t, T)/K] - 0.5\sigma(t, T_1, T)^2}{\sigma(t, T_1, T)}$.

Given a strike price, the underlining futures price and the time to maturity, the option price depends on $\sigma(t, T_1, T)$, which is a function of $\eta_2(\cdot, \cdot)$. See the definition of $\eta_2(\cdot, \cdot)$ in appendix A, seasonal parameters are not included. Lo and Wang (1995) also recognize that the parameters in the drift do not enter the option pricing formula. They generalize the Black-Scholes model to include a trending Ornstein-Uhlenbeck process in stock prices. They show that, in the end, the option formula based on their model is identical to the Black-Scholes formula. They also show that because their model provides a higher estimated volatility, it results in predicting a higher option value than Black-Scholes. In contrast, in our model, which is developed with commodities, and not stocks in mind, introduces a mean reversion parameter into the drift term and k_x does enter into the option pricing formula. Our option pricing formula is identical to the option formula based on Schwartz's two factor model, only if we take the limit of option pricing formula, as k_x approaches zero. Though seasonal parameters do not affect the formula, we will show in Section 6 that they do affect the estimates of the other parameters.

Put-call parity can be used to get the analogous European put option price as follows:

$$\begin{aligned} P[F(t, T), K, t, T_1] &= \exp[r(t - T_1)]E_t^Q\{\max[K - F(T_1, T), 0]\} \\ &= \exp[r(t - T_1)]E_t^Q\{\max[F(T_1, T) - K, 0] + K - F(T_1, T)\} \\ &= \exp[r(t - T_1)]\{E_t^Q[\max(F(T_1, T) - K, 0)] + K - E_t^Q[F(T_1, T)]\}. \end{aligned}$$

By definition, $\exp[r(t - T_1)]E_t^Q[\max(F(T_1, T) - K, 0)] = C[F(t, T), K, t, T_1]$. Since the futures price $F(T_1, T)$ itself is a martingale under the risk-neutral measure, $E_t^Q[F(T_1, T)] = F(t, T)$. So, the put option formula can be written as

$$P[F(t, T), K, t, T_1] = C[F(t, T), K, t, T_1] + \exp[r(t - T_1)][K - F(t, T)]. \quad (3.40)$$

3.5 Empirical analysis

3.5.1 Empirical model

In our model, we employ the log of the spot price and the convenience yield as the two latent state variables. Recall equation (3.20) and define

$$\Lambda(t) \equiv \begin{bmatrix} \lambda_x(t) \\ \lambda_y(t) \end{bmatrix}. \quad (3.41)$$

Then, the historical process of the two latent variables can be written in matrix form as

$$d\mu_t \sim N((\kappa_0(t) - \kappa_1\mu_t + \Lambda(t))dt, Vdt). \quad (3.42)$$

We apply the first-order Euler discretized version of the continuous time model (3.42) with the discretization interval $\Delta = \frac{1}{12}$ to reflect monthly data. The discretized empirical model is

$$\mu_{t+\Delta} = \mu_t + (\kappa_0(t) - \kappa_1\mu_t + \Lambda(t))\Delta + \sqrt{\Delta}\varepsilon_t, \quad \varepsilon_t \sim N(\mathbf{0}_{(2 \times 1)}, V). \quad (3.43)$$

Equation (3.43) can be estimated from the two observed futures prices assumed to be perfectly correlated with the factors. But additional futures and option prices are observed from the markets, and the likelihood of observing them can be inferred from the following empirical futures and option models.

According to the futures pricing formula outlined in Section 4, $X_{t,T} \equiv \ln(F(t, T)) = \alpha(t, T) + \beta(t, T)\mu(t)$. Suppose we have a historical data set consisting of $M > 2$ series of (logarithms of) futures prices with M different times to maturity. Among the M futures contracts with distinct maturity dates, two of the prices are assumed to be perfectly correlated with the state variables μ_t , and the remaining $M - 2$ are assumed to be observed with normally distributed errors e_t . Denote the vector with the two perfectly correlated futures prices with $X_t^\circ \equiv [X_{t,T_1^\circ}, X_{t,T_2^\circ}]^T$ and their maturity dates $[T_1^\circ, T_2^\circ]^T$, and the $(M - 2)$ imperfectly correlated futures with $X_t^\bullet \equiv [X_{t,T_1^\bullet}, X_{t,T_2^\bullet}, \dots, X_{t,T_{M-2}^\bullet}]^T$ and their maturity dates $[T_1^\bullet, \dots, T_{M-2}^\bullet]^T$. So,

$$\begin{bmatrix} X_{t,T_1^\circ} \\ X_{t,T_2^\circ} \end{bmatrix} = \begin{bmatrix} \alpha(t, T_1^\circ) \\ \alpha(t, T_2^\circ) \end{bmatrix} + \begin{bmatrix} \beta_1(t, T_1^\circ) & \beta_2(t, T_1^\circ) \\ \beta_1(t, T_2^\circ) & \beta_2(t, T_2^\circ) \end{bmatrix} \begin{bmatrix} x_t \\ y_t \end{bmatrix},$$

$$\begin{bmatrix} X_{t,T_1}^\bullet \\ \vdots \\ X_{t,T_{M-2}}^\bullet \end{bmatrix} = \begin{bmatrix} \alpha(t, T_1^\bullet) \\ \vdots \\ \alpha(t, T_{M-2}^\bullet) \end{bmatrix} + \begin{bmatrix} \beta_1(t, T_1^\bullet) & \beta_2(t, T_1^\bullet) \\ \vdots & \vdots \\ \beta_1(t, T_{M-2}^\bullet) & \beta_2(t, T_{M-2}^\bullet) \end{bmatrix} \begin{bmatrix} x_t \\ y_t \end{bmatrix} + \begin{bmatrix} e_{t,1} \\ \vdots \\ e_{t,M-2} \end{bmatrix},$$

$$\begin{bmatrix} e_{t,1} \\ \vdots \\ e_{t,M-2} \end{bmatrix} \sim N(\underline{0}_{((M-2) \times 1)}, \sigma_e^2 \Omega).$$

Putting them into matrix form, we get

$$X_t^\circ = \alpha^\circ + \beta^\circ \mu_t \text{ and} \quad (3.44)$$

$$X_t^\bullet = \alpha^\bullet + \beta^\bullet \mu_t + e_t, \quad (3.45)$$

where $\underline{0}_{((M-2) \times 1)}$ is an $(M-2)$ vector of zeros, $\sigma_e^2 > 0$ is a scalar, Ω is an $(M-2) \times (M-2)$ matrix, with the i, j th element equal to $\rho^{|i-j|}$, for $\rho \in (-1, 1)$, and $\alpha(t, T)$ and $\beta(t, T)$ as defined in Section 4. Since the two latent factors are not observed, direct estimation of the historical evolution equation (3.43) is not feasible. However, given equation (3.44), if the 2×2 matrix β° is invertible, the factors can be solved for as $\mu_t = (\beta^\circ)^{-1}(X_t^\circ - \alpha^\circ)$. In this way, the value of the state variables can be exactly filtered out at each sample date by inversion based on the two futures prices observed without error.

Our estimation strategy is capable of using both options and futures. As with the imperfectly correlated futures prices, option prices are also assumed to be observed with errors. According to equations (3.39) and (3.40), the empirical model is specified as

$$\begin{aligned} \ln(C[F(t, T), K, t, T_1]) &= \ln(\exp[r(t - T_1)][F(t, T)N(d_1) - KN(d_2)]) + \varepsilon_{t,c} \text{ and} \\ \ln(P[F(t, T), K, t, T_1]) &= \ln(\exp[r(t - T_1)][F(t, T)N(d_1) - KN(d_2)] \\ &\quad + \exp[r(t - T_1)][K - F(t, T)]) + \varepsilon_{t,p}, \end{aligned}$$

where $\varepsilon_{t,c} \sim N(0, \sigma_c^2)$ and $\varepsilon_{t,p} \sim N(0, \sigma_p^2)$. We add a serially and cross-sectionally uncorrelated mean-zero disturbance into the put and call option formulas to take into account nonsimultaneity of the observations, errors in the data, and other potential sources of errors. The set of model parameters to be estimated is $V, \lambda_y, \lambda_x, u_x, u_y, k_x,$ and k_y . In addition, estimation yields parameter values associated with the model's goodness of fit (i.e., σ_e and ρ for the estimation using futures data only, and $\sigma_e, \rho, \sigma_c,$ and σ_p for the estimation relying on both futures and options data).

3.5.2 Description of the data

The futures data employed to estimate the models consist of monthly observations of futures prices for one commercial commodity, crude oil, and two agricultural commodities, soybeans and lean hogs. Panel data of soybean and lean hog futures prices are obtained from the Chicago Mercantile Exchange (CME). Both futures markets are observed monthly from January 1978 through January 2010, for a total of 385 observation dates. The futures prices involved are the settlement prices for the 15th calendar day of the month. If the 15th of the month falls on a weekend or a holiday, the nearest trading day's settlement price is used. The settlement prices observed with zero trading volume are discarded, because it is set by the administration of CME for the purpose of calculating margins. In other words, these prices are not actual trading prices. The price units are cents/bushel and cents/pound, for soybean futures, and lean hogs futures, respectively.

Since the longest maturity in the soybean (lean hogs) futures sample is 34 (19) months, the ideal data set would consist of a panel of $385 \times 34 = 13,090$ ($385 \times 19 = 7,315$) observations. However, futures for some maturities are not traded. Soybean futures currently have only seven maturity months: January, March, May, July, August, September, and November. Lean hog futures have eight maturity months: February, April, May, June, July, August, October, and December. In addition, data with far-away maturities are often missing because they are not traded. For example, on January 1980 only seven prices are observed for soybean futures, corresponding to the expiration dates of March, May, July, August, September, and November of 1980 and January of 1981. Letting the i, j th element of our data set be the price of the futures contract that expires j months after date i , this means that all elements of the 25th row of our soybean data set are missing except 2nd, 4th, 6th, 7th, 8th, 10th, and 12th column. As a result, the total number of observations available on soybean (lean hog) futures prices are 3,157 (3,032). Similarly, crude oil futures prices are observed from NYMEX during the period December 1983 to December 2009. Crude oil futures are listed in dollars per barrel and are available in every month. The longest time to maturity in the sample period is 84 months. In total, 5,528 crude oil futures prices are observed. There are missing observations from the ideal data set for the same reason as for the soybean and lean hogs futures markets.

For soybeans, we also estimated the model using data on option prices written on futures. Soybean

futures options are observed from 1988 until 2010, with 265 observation dates. Futures option contracts expire around three-quarters of a month prior to the expiration of the underlying futures contracts.

At any particular date, a variety of option contracts with different underlying futures contracts and/or strike prices are traded. The longest maturity date for the option's underlying futures contract is 13 months in our sample. No option contracts are written on futures with more than 13 months until maturity.

Our model applies only to European options, while the options data correspond to American options. American options are more valuable than their European counterparts, because of the existence of early exercise opportunity for the former. However, after calculating values for both American- and European-type options, Plato (1985) concluded that the difference between the two for near-the-money option values is negligible. Hence, we estimate the model using only premiums for options with strike prices immediately above and immediately below the corresponding observed futures price. Our ideal option premium data set consists of 6,890 observations for call and put options. However, only 3,676 (3,413) call (put) option prices are observed during the sample period because of limited trading.

3.5.3 Empirical method

Bayesian MCMC methods are employed to estimate the parameters associated with the advocated model. The risk-free interest rate (r) is a constant in our two-factor model and is fixed at 5%.² Define $\vec{\lambda}_i \equiv [\lambda_{i,0}, \lambda_{i,1,cos}, \lambda_{i,1,sin}, \lambda_{i,2,cos}, \lambda_{i,2,sin}]$, $\vec{u}_i \equiv [u_{i,0}, u_{i,1,cos}, u_{i,1,sin}, u_{i,2,cos}, u_{i,2,sin}]$ for $i = x, y$, and $\vec{\theta} \equiv [\theta_0, \theta_{1,cos}, \theta_{1,sin}, \theta_{2,cos}, \theta_{2,sin}]$. We use non-informative priors for $\vec{\theta}$, $k_x, k_y, V, \rho, \vec{\lambda}_y$, and $\vec{\lambda}_x$. The prior information for $\sigma_e^2, \sigma_c^2, \sigma_p^2$ is proposed as follows:

$$\sigma_e^2 \sim Inv-\chi^2(v_e^0, \sigma_e^0),$$

$$\sigma_c^2 \sim Inv-\chi^2(v_c^0, \sigma_c^0), \text{ and}$$

$$\sigma_p^2 \sim Inv-\chi^2(v_p^0, \sigma_p^0).$$

The parameters for the lean hog and crude oil markets are estimated using futures data only. We estimate the parameters for the soybean market using two different data sets. First, we use futures data

²This model can be extended by explicitly modeling the stochastic interest rate. However, the pricing error for commodity futures that arises from ignoring the stochastic nature of interest rate is negligible; see, e.g., the discussion in Schwartz (1997) and Trolle and Schwartz (2009).

only to estimate the parameter set $\{V, \vec{\lambda}_y, \vec{\lambda}_x, \vec{\theta}, k_x, k_y, \rho, \sigma_e\}^A$.³ Then the whole panel data comprising both futures and option prices across different maturities and exercise prices are employed to estimate $\{V, \vec{\lambda}_y, \vec{\lambda}_x, \vec{\theta}, k_x, k_y, \rho, \sigma_e\}^B$, along with σ_c and σ_p . By comparing $\{V, \vec{\lambda}_y, \vec{\lambda}_x, \vec{\theta}, k_x, k_y, \rho, \sigma_e\}^A$ and $\{V, \vec{\lambda}_y, \vec{\lambda}_x, \vec{\theta}, k_x, k_y, \rho, \sigma_e\}^B$, we can assess whether option prices are driven by the same set of underlying parameters as futures.

The MCMC empirical method described here is designed to estimate Model 4 using both futures and options data. Models 1, 2, and 3, and/or estimation using futures data only can be easily retrieved by imposing the corresponding restrictions into the procedure. The MCMC iteration steps are as follows.

Step 1. Initialization: Specify starting values for parameter and missing observations

$$\Theta^{(0)} \equiv \{V^{(0)}, \vec{\lambda}_y^{(0)}, \vec{\lambda}_x^{(0)}, \vec{\theta}^{(0)}, k_x^{(0)}, k_y^{(0)}, \rho^{(0)}, \sigma_e^{(0)}, \sigma_c^{(0)}, \sigma_p^{(0)}\}.$$

Let $\Theta_{-v}^{(j)}$ represent all the components of $\Theta^{(j)}$, except v , at their current values.

Step 2. Compute the unobserved factors $\mu_t^{(j)}$ by solving equation (3.44).⁴

Step 3. Given $[\mu_t^{(j)}, V^{(j)}, \vec{\lambda}_y^{(j)}, \vec{\lambda}_x^{(j)}, \sigma_e^{(j)}, \sigma_c^{(j)}, \sigma_p^{(j)}]$, estimate $[\vec{\theta}^{(j+1)}, k_x^{(j+1)}, k_y^{(j+1)}, \rho^{(j+1)}]$ by an effective adaptive, general purpose MCMC algorithm called t-walk developed by Christen and Fox (2010). The t-walk compares the likelihood of observing futures and option prices and state variables given (i.1) - (i.4) (the likelihood given existing parameter values) with (ii.1) - (ii.4) (the likelihood given proposal parameter values). We use C_t and P_t to represent $C[F(t, T), K, t, T_1]$, and $P[F(t, T), K, t, T_1]$ respectively,

where (i.1) $[X_t^\bullet - \alpha^\bullet(j) - \beta^\bullet(j)\mu_t^{(j)}] \sim N(\mathbf{0}_{((M-2) \times 1)}, \sigma_e^{2(j)}\Omega^{(j)})$,

$$(i.2) \left[\mu_{t+\Delta}^{(j)} - \mu_t^{(j)} - (\kappa_0^{(j)}(t) - \kappa_1^{(j)}\mu_t^{(j)} + \Lambda(t)^{(j)})/\Delta \right] / \sqrt{\Delta} \sim N(\mathbf{0}_{(2 \times 1)}, V^{(j)}),$$

$$(i.3) \ln(C_t) - \ln(\exp[r(t - T_1)][F(t, T)N(d_1^{(j)}) - KN(d_2^{(j)})]) \sim N(0, \sigma_c^{2(j)}),$$

$$(i.4) \ln(P_t) - \ln(\exp[r(t - T_1)][F(t, T)N(d_1^{(j)}) - KN(d_2^{(j)})]) \\ - \exp[r(t - T_1)][K - F(t, T)] \sim N(0, \sigma_p^{2(j)}),$$

$$(ii.1) [X_t^{\bullet(prop)} - \alpha^{\bullet(prop)} - \beta^{\bullet(prop)}\mu_t^{(prop)}] \sim N(\mathbf{0}_{((M-2) \times 1)}, \sigma_e^{2(j)}\Omega^{(prop)}),$$

$$(ii.2) \left[\mu_{t+\Delta}^{(prop)} - \mu_t^{(prop)} - (\kappa_0^{(prop)}(t) - \kappa_1^{(prop)}\mu_t^{(prop)} + \Lambda(t)^{(j)})/\Delta \right] / \sqrt{\Delta} \sim N(\mathbf{0}_{(2 \times 1)}, V^{(j)}),$$

$$(ii.3) \ln(C_t) - \ln(\exp[r(t - T_1)][F(t, T)N(d_1^{(prop)}) - KN(d_2^{(prop)})]) \sim N(0, \sigma_c^{2(j)}),$$

$$(ii.4) \ln(P_t) - \ln(\exp[r(t - T_1)][F(t, T)N(d_1^{(prop)}) - KN(d_2^{(prop)})]) - \exp[r(t - T_1)][K -$$

³Parameter \vec{u}_x can be recovered by using equation (3.12) after we estimate $\vec{\lambda}_x$; \vec{u}_y can be recovered by equation (3.19) after we estimate $\vec{\theta}$ and $\vec{\lambda}_y$.

⁴The perfectly correlated futures prices are selected to be among the observed data.

$$F(t, T)] \sim N(0, \sigma_p^{2(j)}),$$

where $\mu_t^{(prop)}$ is computed from equation (3.44) using $\vec{\theta}^{(prop)}$, $k_x^{(prop)}$, and $k_y^{(prop)}$. The unobserved prices in $X_t^{(j)}$, $C_t^{(j)}$, $P_t^{(j)}$, and $\mu_t^{(j)}$ are then updated after obtaining $[\theta^{(j+1)}, k_x^{(j+1)}, k_y^{(j+1)}, \rho^{(j+1)}]$, using equations (3.21), (3.39), (3.40), and (3.44).

Step 4. Given $[\mu_t^{(j)}, \vec{\theta}^{(j+1)}, k_x^{(j+1)}, k_y^{(j+1)}, \rho^{(j+1)}, \vec{\lambda}_y^{(j)}, \vec{\lambda}_x^{(j)}, \sigma_e^{(j)}, \sigma_c^{(j)}, \sigma_p^{(j)}]$, use the Metropolis-Hastings algorithm to generate $V^{(j+1)}$, as follows.

Generate $V^{(prop)} \sim Inv\text{-Wishart}_{Nobs-3}((Nobs-3)V^{(j)})$.

$$\text{Calculate the acceptance ratio, } R = \frac{Pr(V^{(prop)} | \Theta_{-V}^j, X_t^{(j)}, C_t^{(j)}, P_t^{(j)}, \mu_t^{(j)}) Pr(V^{(prop)} | V^{(j)})}{Pr(V^{(j)} | \Theta_{-V}^j, X_t^{(j)}, C_t^{(j)}, P_t^{(j)}, \mu_t^{(j)}) Pr(V^{(j)} | V^{(prop)})}$$

Generate a random variable γ from a standard uniform distribution.

If $\gamma < R$, $V^{(j+1)} = V^{(prop)}$. Otherwise $V^{(j+1)} = V^{(j)}$.

Step 5. Update the unobserved futures and option prices to get $X_t^{(j+1)}$, $C_t^{(j+1)}$, $P_t^{(j+1)}$ and $\mu_t^{(j+1)}$ given $[V^{(j+1)}, \vec{\theta}^{(j+1)}, k_x^{(j+1)}, k_y^{(j+1)}]$, using equations (3.21), (3.39), (3.40), and (3.44).

Step 6. Given $[V^{(j+1)}, \mu_t^{(j+1)}, \vec{\theta}^{(j+1)}, k_x^{(j+1)}, k_y^{(j+1)}, \rho^{(j+1)}, \sigma_e^{(j)}, \sigma_c^{(j)}, \sigma_p^{(j)}]$, draw $\vec{\lambda}_y^{(j+1)}$ and $\vec{\lambda}_x^{(j+1)}$. Recall from equation (3.43) that $\vec{\lambda}_x^{(j+1)}$ and $\vec{\lambda}_y^{(j+1)}$ can be drawn from a multivariate normal distribution.

Step 7. Given $[\vec{\lambda}_y^{(j+1)}, \vec{\lambda}_x^{(j+1)}, V^{(j+1)}, \mu_t^{(j+1)}, \vec{\theta}^{(j+1)}, k_x^{(j+1)}, k_y^{(j+1)}, \rho^{(j+1)}, \sigma_c^{(j)}, \sigma_p^{(j)}]$, compute $\sigma_e^{2(j+1)}$:

$\sigma_e^{2(j+1)} | X_t, \Theta_{-\sigma_e}^j \sim Inv\text{-}\chi^2(v_e^0 + n_f, \frac{v_e^0 \sigma_e^0 + n_f v_e}{v_e^0 + n_f})$, where n_f is the total number of observed futures prices, and v_e is the mean squared error of observed futures prices.

Step 8. Given $[\vec{\lambda}_y^{(j+1)}, \vec{\lambda}_x^{(j+1)}, V^{(j+1)}, \mu_t^{(j+1)}, \vec{\theta}^{(j+1)}, k_x^{(j+1)}, k_y^{(j+1)}, \rho^{(j+1)}, \sigma_e^{2(j+1)}, \sigma_p^{(j)}]$, generate $\sigma_c^{2(j+1)}$:

$\sigma_c^{2(j+1)} | C_t, \Theta_{-\sigma_c}^j \sim Inv\text{-}\chi^2(v_c^0 + n_c, \frac{v_c^0 \sigma_c^0 + n_c v_c}{v_c^0 + n_c})$, where n_c is the total number of observed call option prices, and v_c is the mean squared error of observed call option prices.

Step 9. Given $[\vec{\lambda}_y^{(j+1)}, \vec{\lambda}_x^{(j+1)}, V^{(j+1)}, \mu_t^{(j+1)}, \vec{\theta}^{(j+1)}, k_x^{(j+1)}, k_y^{(j+1)}, \rho^{(j+1)}, \sigma_e^{(j+1)}, \sigma_c^{(j+1)}]$, generate $\sigma_p^{2(j+1)}$:

$\sigma_p^{2(j+1)} | P_t, \Theta_{-\sigma_p}^j \sim Inv\text{-}\chi^2(v_p^0 + n_p, \frac{v_p^0 \sigma_p^0 + n_p v_p}{v_p^0 + n_p})$, where n_p is the total number of observed put option prices, and v_p is the mean squared error of observed put option prices.

⁵ Calculating $Pr(V^{(prop)} | \Theta_{-V}^j, X_t^{(j)}, C_t^{(j)}, P_t^{(j)}, \mu_t^{(j)})$ and $Pr(V^{(j)} | \Theta_{-V}^j, X_t^{(j)}, C_t^{(j)}, P_t^{(j)}, \mu_t^{(j)})$ will again resort to the empirical equations (i.1) to (i.4).

Step 10. Set $j = j + 1$.

Step 11. If the maximum iteration is reached, stop. Otherwise, go to Step 2.

Note that Steps 8 and 9 are necessary only if the option data set is also used in estimating the model.

3.6 Estimation results

The Bayesian MCMC procedure is performed using four different initial values of the parameters for two million iterations on the four models in each market. The first one million iterations are discarded. We perform Gelman and Rubin tests on the remaining one million iterations for the four chains. All of the chains converge adequately for the four models in all markets. All of the tables reporting results show the 2.5, 50, and 97.5 percentiles of the posterior probability band for the corresponding parameter.

3.6.1 *Lean hog market*

Parameter estimates for the lean hog market are shown in Table 3.1. It is observed that seasonality plays a significant role in the lean hog market. In Model 4, all of the seasonal parameters are significantly different from zero. In Model 3, there is only one seasonal parameter that is not significantly different from zero ($u_{y,1,sin}$). The estimates of σ_e describe the inferred standard deviation on the noise terms that allow for deviations between theoretical and observed (log) futures prices.

Table 3.1: Parameter Estimates: Lean Hogs

Parameters	Model 1	Model 2	Model 3	Model 4
k_x	0	(0.4141, 0.6569, 1.0145)	0	(0.4468, 0.6468, 0.9020)
k_y/k_c	(2.3296, 2.6083, 2.8871)	(1.4606, 1.9354, 2.3553)	(1.8066, 1.9871, 2.1833)	(1.0272, 1.3120, 1.6479)
$\lambda_c/\lambda_{y,0}$	(-0.4488, -0.2871, -0.1255)	(-0.3687, -0.2248, -0.0993)	(-0.2842, -0.2110, -0.1379)	(-0.2082, -0.1512, 0.0998)
$\lambda_{y,1,\sin}$	0	0	(0.7604, 0.8347, 0.9090)	(0.6367, 0.6987, 0.7675)
$\lambda_{y,1,\cos}$	0	0	(-0.2230, -0.1489, -0.0749)	(-0.4849, -0.3914, -0.3010)
$\lambda_{y,2,\sin}$	0	0	(-2.0026, -1.8629, -0.1723)	(-1.8984, -1.7575, -1.6120)
$\lambda_{y,2,\cos}$	0	0	(1.2967, 1.4288, 1.5609)	(1.4608, 1.6025, 1.7441)
$u_{x,0}$	(-0.0612, -0.0202, 0.0208)	(-0.0489, -0.0057, 0.0356)	(-0.0208, 0.0009, 0.0228)	(-0.0035, 0.0175, 0.0379)
$u_{x,1,\sin}$	0	0	(0.0887, 0.1137, 0.1386)	(0.0200, 0.0514, 0.0825)
$u_{x,1,\cos}$	0	0	(0.0787, 0.1051, 0.1315)	(0.0681, 0.0926, 0.1172)
$u_{x,2,\sin}$	0	0	(-0.1301, -0.1108, -0.0915)	(-0.1276, -0.1084, -0.0891)
$u_{x,2,\cos}$	0	0	(-0.2677, -0.2466, -0.2255)	(-0.2673, -0.2465, -0.2256)
$u_{c,0}/u_{y,0}$	(-0.1975, -0.0853, 0.0267)	(-6.5972, -5.2543, -3.8173)	(-0.0709, -0.0249, 0.0210)	(-4.2302, -3.5271, -2.8872)
$u_{y,1,\sin}$	0	0	(-0.1873, -0.0415, 0.1043)	(-0.4569, -0.3072, -0.1549)
$u_{y,1,\cos}$	0	0	(-1.9026, -1.7543, -1.6058)	(-2.2774, -2.1141, -1.9454)
$u_{y,2,\sin}$	0	0	(2.3449, 2.6826, 3.0204)	(2.3754, 2.7163, 3.0571)
$u_{y,2,\cos}$	0	0	(2.8090, 3.1591, 3.5092)	(2.9081, 3.2607, 3.6132)
σ_x	(0.4247, 0.4487, 0.4729)	(0.4093, 0.4304, 0.4543)	(0.3380, 0.3538, 0.3696)	(0.3268, 0.3417, 0.3564)
σ_y	(1.2820, 1.4471, 1.6122)	(0.9306, 1.1067, 1.3042)	(0.7876, 0.8562, 0.9349)	(0.5317, 0.6168, 0.7019)
$\rho_{x,y}$	(0.8676, 0.8836, 0.8981)	(0.6079, 0.7283, 0.8029)	(0.8388, 0.8555, 0.8721)	(0.5081, 0.6276, 0.7256)
ρ	(0.1562, 0.1904, 0.2246)	(0.1608, 0.1962, 0.2308)	(0.0753, 0.1112, 0.1471)	(0.0612, 0.0991, 0.1370)
σ_e^2	(0.0060, 0.0065, 0.0070)	(0.0059, 0.0064, 0.0069)	(0.0019, 0.0021, 0.0022)	(0.0019, 0.0021, 0.0022)

Note: The three quantities within parentheses denote respectively the 2.5, 50, and 97.5 percentiles of the posterior probability band.

Seasonality has a very large impact on the model's ability to fit the historical futures data. As we can see from Table 3.1, models with seasonality estimates have a significantly lower value of σ_e^2 than their counterparts without seasonality, which is a signal of better fitting the observed data set. The significance of the seasonality parameters suggests that the lean hog market exhibits a strong seasonal pattern. If prices are characterized by seasonal fluctuations and the model fails to incorporate them, the movement of the factors caused by the seasonal pattern will be unnecessarily included in the instantaneous volatility term. In other words, fitting models without seasonality to seasonal data yields significantly higher estimates of σ_x and σ_y than the models augmented with seasonality, which is confirmed by the empirical results in Table 3.1. One can easily check that, given all other variables equal, higher values of σ_x and σ_y will induce higher option premiums.

A significantly positive k_x is estimated in both Models 2 and 4, which supports the hypothesis that convenience yield is a function of the spot price. This also implies that the spot price in the lean hog market is mean reverting. Comparing Model 1 and Model 3 with Model 2 and Model 4 respectively, we can see that the correlation coefficient between the two factors is significantly smaller in Model 2 and Model 4, after we set the convenience yield to be a function of the log of the spot price. The highest speed of adjustment in the spot price and the highest speed of mean reversion in convenience yield is observed in this market (compared to the soybean and the crude oil markets). One possible reason for this fact is that the lean hog market has the shortest production cycle, which allows producers to adjust the supply faster. The total expected return on the spot price (u_x) is not significantly different from zero in all four models. The nonseasonal part of market price of convenience yield risk ($\lambda_{y,0}$) are all significantly negative except in Model 4.

Figures 3.4 and 3.5 show the term structure of futures prices implied by the four models on January 15, 2010, and December 16, 2002, respectively.

On January 15, 2010, the spot price on the lean hog market was high relative to production costs. For contracts with a short time to maturity, the curvature of the futures curve implied by the Schwartz model depends on the relative value of convenience yield. However, in the long run, the futures curve implied by the Schwartz model (Model 1) depends on the risk-neutral drift of the spot price process. If we evaluate the drift at the risk-neutral long-run mean of convenience yield, it is negative. Consequently, the futures curve has a constant negative slope in the long run. Model 2 incorporates mean reversion

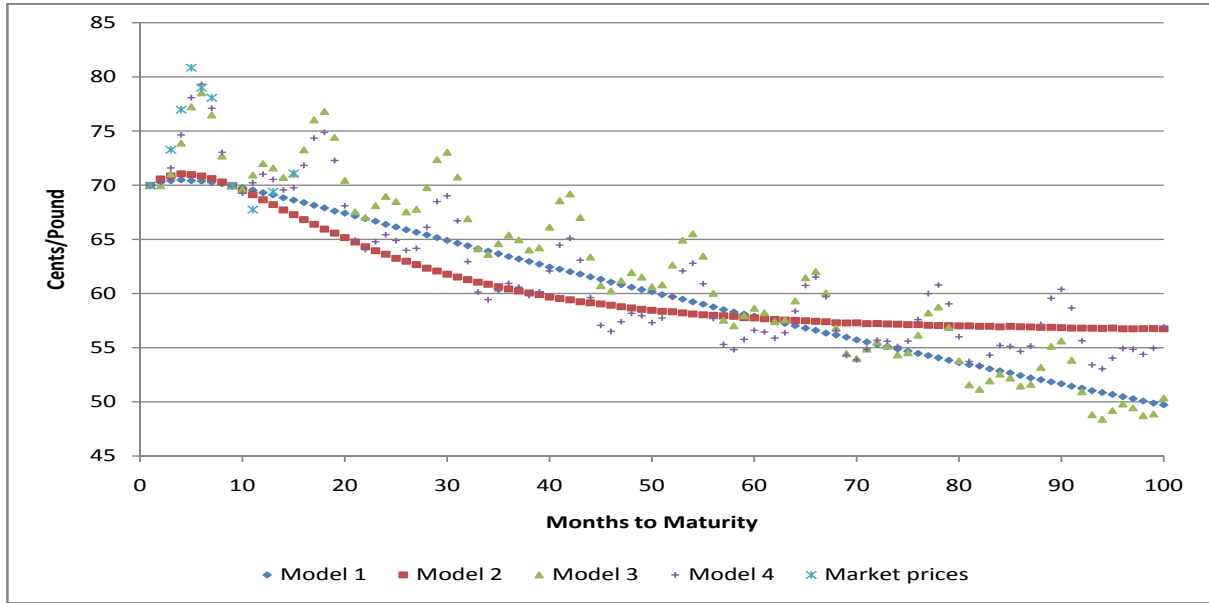


Figure 3.4: Projection of lean hog futures prices on Jan. 15, 2010

in the spot price. So when the spot price is relatively high, the futures curve implied by Model 2 is expected to decrease at a faster rate initially than the futures curve implied by the Schwartz model and then to flatten out as prices approach the market's estimate of production costs. This long-run futures price ($F(t, \infty)$) is independent of the current spot price and convenience yield. The futures curve implied by Model 4 (Model 3) follows the trend of Model 2 (Model 1), but with seasonality.

It is clear that futures prices implied by Model 4 fit the observed prices more precisely compared to those models that ignore seasonality. A local maximum is observed when the time to maturity is six months corresponding to a July maturity date. July is the traditional barbecue season in the U.S., when demand for pork is relatively high, and this is consistent with our observation of historical futures prices.

In contrast to January 15, 2010, the spot price for lean hogs was relatively low on December 16, 2002. With mean reversion imbedded, Model 2 predicts that the futures curve will increase at a decreasing rate and converge to the long-run futures price $F(t, \infty)$. On the other hand, while the curvature of the futures curve implied by the Schwartz model with a short time to maturity depends on the relative level of spot price and convenience yield on that date, with longer-term maturity futures the futures curve is predicted to be decreasing regardless of the fact that the spot price today may have already been well below production costs.

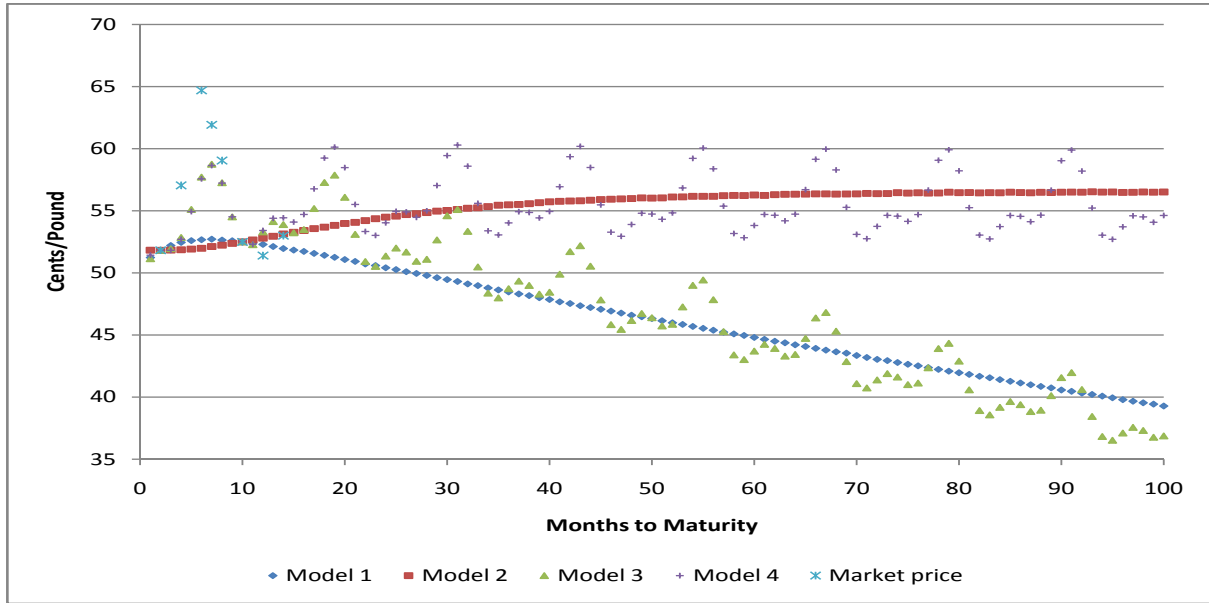


Figure 3.5: Projection of lean hog futures prices on Dec. 16, 2002

Of particular interest are the prices of options on futures. Equation (3.39) shows that at-the-money call option prices are an increasing function of the underlying futures prices. To compute option prices, we use the observed futures prices. When they are not available, we use model-implied futures prices to calculate the corresponding model's implied option price. However, different models predict different futures prices. For example, in Figure 5, Models 2 and 4 predict much higher futures price than Models 1 and 3, respectively. So, in order to reasonably compare the four models' predictions of call option premia given the seasonality and mean reversion assumptions, it is best to look at the normalized at-the-money call options (option premium/underlying futures price), which are shown in Figure 6. Black's model is also employed to predict the normalized at-the-money call option premiums. We did not estimate Black's model using the futures data set; instead, we observed all the option contracts on January 15, 2010, then calculated the implied volatility and took the average to calculate Black's implied normalized option curve.

Figure 3.6 shows the term structure of normalized at-the-money call option premiums on January 15, 2010. The horizontal axis denotes time to maturity of the call option, whereas the vertical axis is the value of the normalized call premium. It is clear that the one-factor model (Black's model) predicts the highest option value among the five models. When we compare Model 1 (Model 3) with Model 2 (Model 4), we observe that the predictions from the two models are very close when the time to maturity

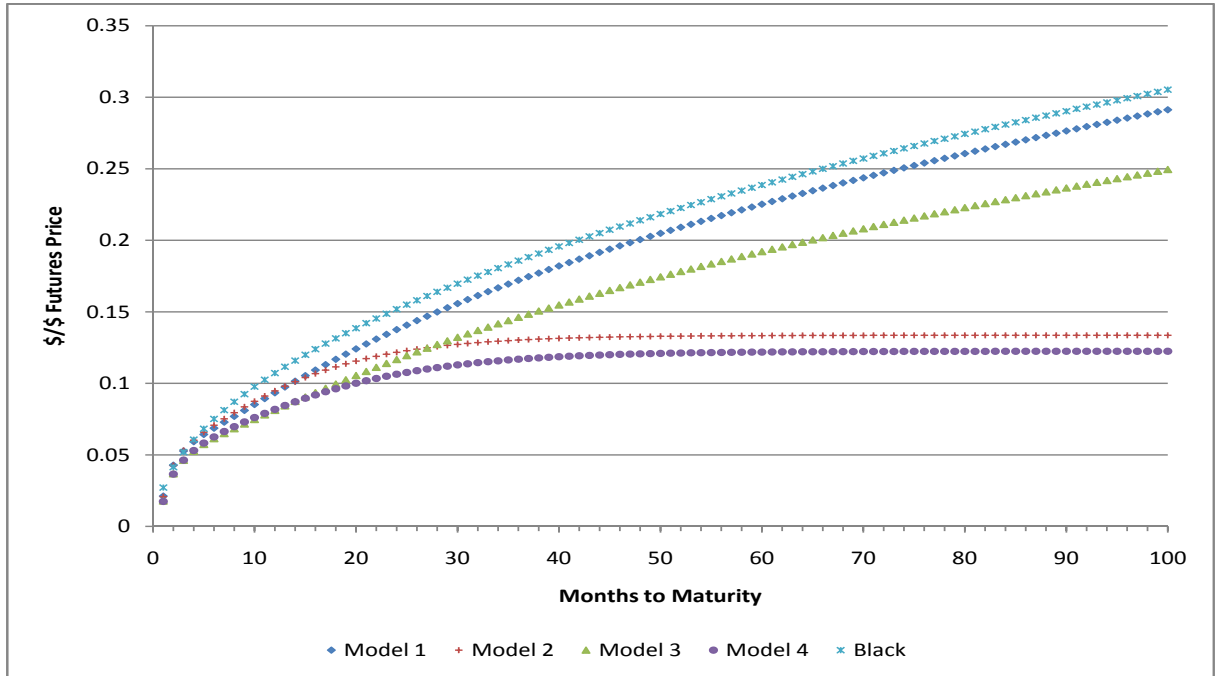


Figure 3.6: Projection of normalized at-the-money call option prices: lean hogs

of the underlying future contracts is less than 18 months. However, as time to maturity increases, the difference becomes economically significant. This discrepancy is consistent with the key assumption of mean-reversion in the spot price in Models 2 and 4. When time to maturity is over 50 months, the option premium predicted by Models 2 and 4 approach a constant. The difference between Model 1 (Model 2) and Model 3 (Model 4) is seasonality. As we observed from Table 3.1, models augmented with seasonality estimate a significantly smaller σ_x and σ_y , which will in turn reduce the option premium. This is consistent with Figure 3.6, which shows that the option curve implied by Model 1 (Model 2) lies on top of the curve for Model 3 (Model 4).

3.6.2 Soybean market

Results for the soybean data estimated using futures prices only and both futures prices and options prices are listed in Tables 3.2 and 3.3 respectively. Comparing Table 3.2 with Table 3.3, we can see that the estimated parameters from the two data sets are very similar. There is a large overlap between the 95% estimated posterior intervals. We cannot reject the hypothesis that $\{V, \vec{\lambda}_y, \vec{\lambda}_x, \vec{\theta}, k_x, k_y, \rho, \sigma_e\}^A$ is equal to $\{V, \vec{\lambda}_y, \vec{\lambda}_x, \vec{\theta}, k_x, k_y, \rho, \sigma_e\}^B$.

Table 3.2: Parameter Estimates: Soybeans (Futures data Only)

Parameters	Model 1	Model 2	Model 3	Model 4
k_x	0	(0.0047, 0.0220, 0.0381)	0	(0.0382, 0.0523, 0.0634)
k_y/k_c	(0.9508, 1.0614, 1.1697)	(0.9778, 1.0752, 1.1721)	(1.0206, 1.1008, 1.1880)	(1.0313, 1.1239, 1.2311)
$\lambda_c/\lambda_{y,0}$	(-0.0607, -0.0462, -0.0326)	(-0.0538, -0.0397, -0.0254)	(-0.0547, -0.0424, -0.0305)	(-0.0379, -0.0246, -0.0127)
$\lambda_{y,1,\sin}$	0	0	(0.1852, 0.2018, 0.2195)	(0.1829, 0.2003, 0.2183)
$\lambda_{y,1,\cos}$	0	0	(-0.0199, -0.0020, 0.0162)	(-0.0263, -0.0076, 0.0100)
$\lambda_{y,2,\sin}$	0	0	(-0.3696, -0.2667, -0.177)	(-0.3386, -0.2454, -0.1591)
$\lambda_{y,2,\cos}$	0	0	(0.1984, 0.2887, 0.3733)	(0.2311, 0.3146, 0.3951)
$u_x/0$	(0.0208, 0.0295, 0.0383)	(0.0235, 0.0324, 0.0413)	(0.0217, 0.0299, 0.0381)	(0.0289, 0.0374, 0.0456)
$u_{x,1,\sin}$	0	0	(0.0807, 0.0926, 0.1046)	(0.0790, 0.0908, 0.1028)
$u_{x,1,\cos}$	0	0	(0.0545, 0.0664, 0.0781)	(0.0518, 0.0638, 0.0757)
$u_{x,2,\sin}$	0	0	(-0.1113, -0.0990, -0.0866)	(-0.1077, -0.0955, -0.0832)
$u_{x,2,\cos}$	0	0	(-0.1125, -0.1010, -0.0894)	(-0.1134, -0.1020, -0.0906)
$u_c/u_{y,0}$	(0.0052, 0.0141, 0.0228)	(-0.2486, -0.1379, -0.0178)	(0.0065, 0.0150, 0.0236)	(-0.4381, -0.3607, -0.2624)
$u_{y,1,\sin}$	0	0	(0.2071, 0.2510, 0.2954)	(0.2032, 0.2490, 0.2892)
$u_{y,1,\cos}$	0	0	(-0.6265, -0.5803, -0.5379)	(-0.6512, -0.6043, -0.5592)
$u_{y,2,\sin}$	0	0	(0.4466, 0.5862, 0.7238)	(0.5077, 0.6360, 0.7681)
$u_{y,2,\cos}$	0	0	(0.2297, 0.3645, 0.5273)	(0.223, 0.3558, 0.5010)
σ_x	(0.2472, 0.2574, 0.2684)	(0.2474, 0.2576, 0.2686)	(0.2408, 0.2509, 0.2615)	(0.2414, 0.2513, 0.2621)
σ_y	(0.2451, 0.2626, 0.2808)	(0.2455, 0.2615, 0.2786)	(0.2451, 0.2596, 0.2755)	(0.2407, 0.2563, 0.2749)
$\rho_{x,y}$	(0.6691, 0.7000, 0.7286)	(0.6469, 0.6827, 0.7155)	(0.6749, 0.7053, 0.7334)	(0.6254, 0.6618, 0.6956)
ρ	(0.0764, 0.1074, 0.1383)	(0.0796, 0.1086, 0.1403)	(0.0829, 0.1140, 0.1456)	(0.0837, 0.1150, 0.1476)
σ_e^2	(0.00093, 0.00099, 0.0011)	(0.00093, 0.00098, 0.0010)	(0.00063, 0.00067, 0.00071)	(0.00061, 0.00065, 0.00069)

Note: The three quantities within parentheses denote respectively the 2.5, 50, and 97.5 percentiles of the posterior probability band.

Table 3.3: Parameter Estimates: Soybeans (Futures and Options)

Parameters	Model 1	Model 2	Model 3	Model 4
k_x	0	(0.0017, 0.0260, 0.0547)	0	(0.0338, 0.0618, 0.0909)
k_y/k_c	(0.8175, 0.9344, 1.0696)	(0.8154, 0.9516, 1.0953)	(0.9379, 1.0403, 1.1586)	(0.9348, 1.0664, 1.1655)
$\lambda_c/\lambda_{y,0}$	(-0.0520, -0.0343, -0.0190)	(-0.0522, -0.0292, -0.0076)	(-0.0520, -0.0353, -0.0201)	(-0.0359, -0.0146, 0.0073)
$\lambda_{y,1,\sin}$	0	0	(0.1824, 0.2013, 0.2205)	(0.1789, 0.1991, 0.2191)
$\lambda_{y,1,\cos}$	0	0	(-0.0201, 0.0001, 0.0202)	(-0.0299, -0.0059, 0.0169)
$\lambda_{y,2,\sin}$	0	0	(-0.3846, -0.2786, -0.1690)	(-0.3627, -0.2451, -0.1119)
$\lambda_{y,2,\cos}$	0	0	(0.1774, 0.2878, 0.3894)	(0.2140, 0.3232, 0.4268)
$u_{x,0}$	(0.0158, 0.0257, 0.0352)	(0.0163, 0.0283, 0.04)	(0.015, 0.0245, 0.0336)	(0.0225, 0.0338, 0.0453)
$u_{x,1,\sin}$	0	0	(0.0802, 0.0927, 0.1050)	(0.0780, 0.0909, 0.1041)
$u_{x,1,\cos}$	0	0	(0.0543, 0.0665, 0.0787)	(0.0514, 0.0637, 0.0762)
$u_{x,2,\sin}$	0	0	(-0.1128, -0.0997, -0.0868)	(-0.1083, -0.0951, -0.0822)
$u_{x,2,\cos}$	0	0	(-0.1121, -0.1003, -0.0884)	(-0.1137, -0.1018, -0.0898)
$u_{c,0}/u_{y,0}$	(-0.0007, 0.0088, 0.0177)	(-0.3181, -0.1502, -0.0027)	(-0.0012, 0.0085, 0.0178)	(-0.6052, -0.4042, -0.2279)
$u_{y,1,\sin}$	0	0	(0.2048, 0.2549, 0.3073)	(0.1933, 0.2530, 0.3086)
$u_{y,1,\cos}$	0	0	(-0.6325, -0.5790, -0.5270)	(-0.6605, -0.6041, -0.5469)
$u_{y,2,\sin}$	0	0	(0.4073, 0.5781, 0.7413)	(0.4791, 0.6451, 0.8080)
$u_{y,2,\cos}$	0	0	(0.2143, 0.3891, 0.5607)	(0.1622, 0.3638, 0.5518)
σ_x	(0.2367, 0.2506, 0.2634)	(0.2369, 0.2512, 0.2641)	(0.2316, 0.2454, 0.2585)	(0.2319, 0.2460, 0.2588)
σ_y	(0.2236, 0.2447, 0.2695)	(0.2205, 0.2437, 0.2697)	(0.2298, 0.2503, 0.2741)	(0.2253, 0.2469, 0.2698)
$\rho_{x,y}$	(0.6357, 0.6902, 0.7360)	(0.6041, 0.6677, 0.7219)	(0.6448, 0.6976, 0.7427)	(0.5789, 0.6451, 0.7025)
ρ	(0.0681, 0.1066, 0.1432)	(0.0655, 0.1078, 0.1495)	(0.0771, 0.1125, 0.1491)	(0.0775, 0.1149, 0.1513)
σ_e^2	(0.0009, 0.0010, 0.0011)	(0.0009, 0.0010, 0.0011)	(0.0006, 0.0007, 0.0007)	(0.0006, 0.0007, 0.0007)
σ_p^2	(0.1277, 0.1416, 0.1575)	(0.1293, 0.1434, 0.1593)	(0.1194, 0.1315, 0.1455)	(0.1209, 0.1332, 0.1473)
σ_c^2	(0.0994, 0.1092, 0.1209)	(0.0999, 0.1107, 0.1216)	(0.0946, 0.1030, 0.1128)	(0.0955, 0.1039, 0.1141)

Note: The three quantities within parentheses denote respectively the 2.5, 50, and 97.5 percentiles of the posterior probability band.

Parameter k_x is significantly positive, which provides empirical support for the postulation that the process of spot prices in the soybean market is mean reverting. Parameter u_x in Schwartz's model describes the expected appreciation rate of the non-stationary state variable (log of the spot price), and is significantly positive. The estimates in Table 3.2 indicate that the mean-reversion parameters k_c and k_y are positive in Model 1 and Model 2, respectively; hence that the state variable c_t in the Schwartz model and y_t in Model 2 are stationary in the soybean market. The median of the estimated k_c and k_y is about 1.06, corresponding to half-lives of 7.7 months.⁶ Parameter u_c is significantly positive in Model 1 and Model 3, which implies that the long-run mean of the convenience yield in the soybean market is positive. Parameter u_y is significantly negative in Model 2 and Model 4. However, convenience yield in Model 2 and 4 is defined as $c_t = y_t + k_x x_t$. If we take the long-run mean of y_t , and x_t to evaluate c_t it is also positive.

All of the models yield a similar instantaneous volatility and instantaneous correlation coefficient for the two Gaussian factors. Although k_x is statistically positive, its magnitude is small and it has little impact on the model's ability to fit the historical data. Comparing Model 1 (Model 3) with Model 2 (Model 4), there is no significant difference between the estimated σ_e^2 . Seasonality is also important and significant in this market. There is only one seasonality parameter ($\lambda_{y,1,cos}$) that is not significantly different from zero in Models 3 and 4. Furthermore, the models with seasonality (Model 4 and Model 3) yield a significantly smaller σ_e^2 than their counterparts without seasonality (Model 2 and Model 1). The non-seasonal part of the risk premia associated with the convenience yield process is significantly negative in all of the models.

The estimates of σ_e , σ_c , and σ_p describe the inferred standard deviation of the noise terms that allow for some deviation between theoretical and observed (log) futures prices, call option prices, and put option prices, respectively. In Table 3.3, σ_e^2 is significantly smaller in the models augmented with seasonality; it is about 2.6% of the soybean futures prices. The median estimates of σ_c and σ_p are also smaller in Model 3 and Model 4; however, they are not significantly lower.

Figure 3.7 shows the projection of normalized at-the-money call option prices for the soybean market on January 15, 2010, corresponding to Models 1 through 4 and Black's model. It is observed that

⁶ The half-life expresses the time it takes before a given shock to this process is expected to have leveled off by half of the shock; the half-life in the Ornstein-Uhlenbeck process is calculated as $\ln(2)/k$. In our case $\ln(2)/1.07 = 0.65$ years, which is about 7.7 months.

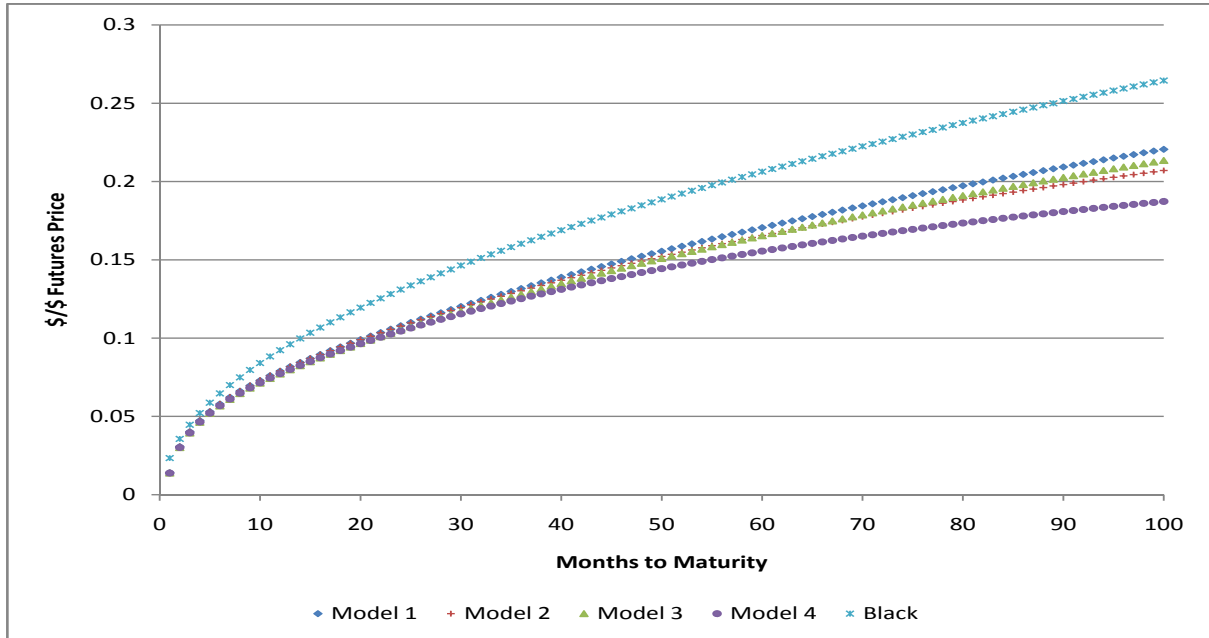


Figure 3.7: Projection of normalized at-the-money call option prices: soybeans

the one-factor model predicts higher option values than all of the two-factor models, especially for options with longer times to maturity. Unlike Figure 3.6, the option premiums predicted by Models 2 and 4 are still growing in the time period investigated (up to 100 months). This is because compared to the lean hog market, the parameter of speed adjustment in the spot price is much smaller for soybeans (0.0523 in Model 4 and 0.0220 in Model 2) than for lean hogs (0.6468 in Model 4 and 0.6569 in Model 2). Though it is not as clear as in Figure 3.6, we still can observe that models generalized with mean reversion (Models 2 and 4) predict lower option value than their nonstationary counterparts (Models 1 and 3). And models that are augmented with seasonality (Models 3 and 4) predict a smaller option price than those that are not (Models 1 and 2).

3.6.3 Crude oil market

The estimates reported in Table 3.4 show that, unlike agricultural commodities, the long-run mean of the first component (y_t) of the convenience yield in the crude oil market is positive and significant at the 95 percent level.

Table 3.4: Parameter Estimates: Crude Oil

Parameters	Model 1	Model 2	Model 3	Model 4
k_x	0	(0.0049, 0.0131, 0.0220)	0	(0.0070, 0.0136, 0.0207)
k_y/k_c	(1.1475, 1.2352, 1.3389)	(1.0784, 1.1743, 1.2802)	(1.1581, 1.2316, 1.3202)	(1.0877, 1.1644, 1.2584)
$\lambda_c/\lambda_{y,0}$	(0.0568, 0.0760, 0.0970)	(0.0631, 0.0819, 0.1023)	(0.0573, 0.0756, 0.0949)	(0.0633, 0.0810, 0.0999)
$\lambda_{y,1,\sin}$	0	0	(-0.1110, -0.0907, -0.0710)	(-0.1068, -0.0875, -0.0686)
$\lambda_{y,1,\cos}$	0	0	(-0.0957, -0.0759, -0.0563)	(-0.0870, -0.0673, -0.0482)
$\lambda_{y,2,\sin}$	0	0	(-0.0109, 0.0264, 0.0639)	(-0.0059, 0.0306, 0.0678)
$\lambda_{y,2,\cos}$	0	0	(-0.1748, -0.1363, -0.0977)	(-0.1833, -0.1466, -0.1096)
$u_{x,0}$	(0.1326, 0.1461, 0.1597)	(0.1363, 0.1501, 0.1638)	(0.1329, 0.1461, 0.1594)	(0.1367, 0.1500, 0.1633)
$u_{x,1,\sin}$	0	0	(0.0223, 0.0404, 0.0586)	(0.0235, 0.0414, 0.0594)
$u_{x,1,\cos}$	0	0	(-0.2762, -0.2581, -0.2401)	(-0.2762, -0.2581, -0.2402)
$u_{x,2,\sin}$	0	0	(-0.0158, 0.0021, 0.0200)	(-0.0177, 0.0002, 0.0180)
$u_{x,2,\cos}$	0	0	(-0.2025, -0.1845, -0.1666)	(-0.2010, -0.1830, -0.1652)
$u_{c,0}/u_{y,0}$	(0.1013, 0.1202, 0.1415)	(0.0355, 0.0735, 0.1134)	(0.1023, 0.1200, 0.1402)	(0.0396, 0.0709, 0.1034)
$u_{y,1,\sin}$	0	0	(-0.0999, -0.0603, -0.0209)	(-0.0936, -0.0576, -0.0196)
$u_{y,1,\cos}$	0	0	(-0.1291, -0.0886, -0.0489)	(-0.1187, -0.0803, -0.0419)
$u_{y,2,\sin}$	0	0	(-0.0169, 0.1027, 0.2079)	(-0.0270, 0.0640, 0.1550)
$u_{y,2,\cos}$	0	0	(-0.2015, -0.0905, 0.0217)	(-0.2178, 0.1088, 0.0405)
σ_x	(0.3717, 0.3888, 0.4074)	(0.3713, 0.3881, 0.4069)	(0.3667, 0.3834, 0.4016)	(0.3659, 0.3828, 0.4009)
σ_y	(0.3936, 0.4195, 0.4493)	(0.3765, 0.4035, 0.4337)	(0.3929, 0.4171, 0.4443)	(0.3756, 0.3998, 0.4273)
$\rho_{x,y}$	(0.8173, 0.8379, 0.8564)	(0.8075, 0.8297, 0.8496)	(0.8218, 0.8417, 0.8596)	(0.8120, 0.8334, 0.8528)
ρ	(0.8216, 0.8434, 0.8670)	(0.8391, 0.8602, 0.8827)	(0.8207, 0.8425, 0.8674)	(0.8376, 0.8590, 0.8790)
σ_e^2	(0.0004, 0.0005, 0.0007)	(0.0004, 0.0005, 0.0007)	(0.0004, 0.0005, 0.0007)	(0.0004, 0.0005, 0.0007)

Note: The three quantities within parentheses denote respectively the 2.5, 50, and 97.5 percentiles of the posterior probability band.

The correlation coefficient between the two factors is large and highly significant. The speed of mean reversion in spot price in the crude oil market is much lower than in renewable commodity markets. Compared to the two agricultural commodity markets, seasonality is weak in the nonrenewable crude oil market. There are four seasonality parameters that are not significantly different from zero ($\lambda_{y,2,sin}$, $u_{x,2,sin}$, $u_{y,2,sin}$, and $u_{y,2,cos}$), and the magnitude of the significant seasonality parameters is small compared to the seasonality parameters in the lean hog and soybean markets. The median of total expected return on the spot commodity (u_x) is 0.1461, which is much higher than the total expected return on the soybean (0.0295) and lean hogs markets (-0.0202).

Although Model 4's speed of adjustment coefficient in the spot price (k_x) is significantly positive, its median value is small (0.0136) compared to those of the lean hog market (0.6468) and the soybean market (0.0523). Since seasonality is not strong and the speed of adjustment (k_x) in the spot price is low, it has little impact on the models' prediction on futures and option prices. It is not surprising to see that none of the common parameters in the four models is significantly different in Table 3.4. We would also expect a similar term structure of the call option curves implied by the four models, which is confirmed in Figure 3.8.

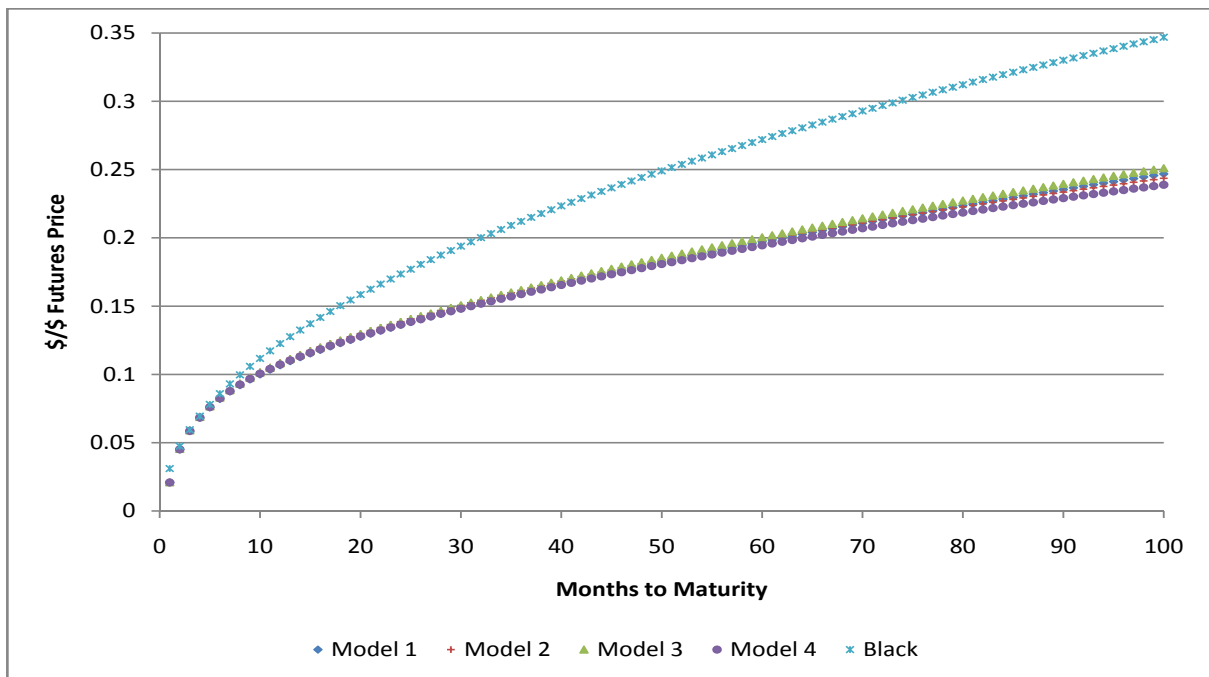


Figure 3.8: Projection of normalized at-the-money call option prices: crude oil

These results suggest that the Schwartz model works quite well for crude oil. It is clear from Figure 3.8 that all the two-factor models predict similar normalized at-the-money call option premiums. The one-factor Black's model predicts a premium similar to the two-factor models when the time to maturity of the call option is less than eight months.

3.7 Conclusion

We generalize Schwartz's two-factor model by allowing mean reversion in spot prices, which is a key feature of agricultural commodity markets. Agricultural commodity markets also exhibit clear seasonal patterns. We introduce seasonality into our model by adding periodic functions to the parameters associated with commodity prices. Closed-form futures and option pricing formulas are derived. We show that Schwartz's model is a special case of our model.

Soybean and lean hog futures price data from the CME and crude oil futures data from NYMEX are employed to estimate the models by means of a Bayesian MCMC algorithm. Estimates for the Schwartz model are obtained by imposing the corresponding restrictions on our model.

In January 2010, the spot prices of lean hogs were historically high. Our futures curve shows a market expectation of a reduction in price levels to the market's estimate of production costs. On the other hand, when the lean hog spot price was relatively low, as on December 16th, 2002, the term structure of futures price implied by our model indicates that futures price will increase to the state independent long-term futures price. The results for soybeans were equally intuitive.

Our option pricing model incorporates mean reversion to long-run production costs that was found in lean hog and soybean markets, and as a result it provides option premia that are significantly lower than in the Black or Schwartz models. This is the key finding of our work and it suggests that the inappropriate use of these other models will result in overpricing of long-term options. And, in fact, these markets suffer from a lack of liquidity for long-term options.

The Schwartz model was originally applied to the specific circumstances of crude oil futures, and our results suggest that it is well suited to this market. Clear seasonal patterns were found in agricultural commodity markets. A version of our option pricing model that incorporates seasonality also shows a

decrease in the size of options premia.

3.8 Appendix

3.8.1 Appendix A

$$\begin{aligned}\beta'(t, T) &= \kappa_1^T \beta(t, T), \text{ and} \\ \alpha'(t, T) &= -\kappa_0(t) \cdot \beta(t, T) - \frac{1}{2} \beta^T(t, T) V \beta(t, T)\end{aligned}$$

with boundary conditions $\beta(T, T) = \phi$, and $\alpha(T, T) = 0$.

$$\beta'_1(t, T) = k_x \beta_1(t, T), \text{ together with boundary conditions } \Rightarrow \beta_1(t, T) = \exp(k_x(t - T))$$

$$\beta'_2(t, T) = \beta_1(t, T) + k_y \beta_2(t, T)$$

$$\Rightarrow \beta'_2(t, T) = \exp(k_x(t - T)) + k_y \beta_2(t, T)$$

$$\Rightarrow \beta_2(t, T) = \frac{\exp(k_x(t - T)) - \exp(k_y(t - T))}{k_x - k_y}$$

$$\begin{aligned}\alpha'(t, T) &= -\kappa_0(t) \cdot \beta(t, T) - \frac{1}{2} \beta^T(t, T) V \beta(t, T) \\ &= (r - \sigma_x^2/2) \beta_1(t, T) + \theta(t) \beta_2(t, T) - \frac{1}{2} \beta^T(t, T) V \beta(t, T)\end{aligned}$$

\Rightarrow

$$\begin{aligned}\alpha(t, T) &= \frac{r - \sigma_x^2/2}{k_x} (\exp(k_x(t - T)) - 1) + \frac{\theta_0}{k_x - k_y} \left[\left(\frac{1}{k_x} (\exp(k_x(t - T)) - 1) - \left(\frac{1}{k_y} (\exp(k_y(t - T)) - 1) \right) \right) \right. \\ &+ \sum_{h=1}^2 \frac{\theta_{h, \cos}}{k_x - k_y} \left(\frac{1}{k_x^2 + 4\pi^2 h^2} - \frac{1}{k_y^2 + 4\pi^2 h^2} \right) \times \\ &\left. \{ k_x [\exp(k_x(t - T)) \cos(2\pi h t) - \cos(2\pi h T)] + 2\pi h [\exp(k_x(t - T)) \sin(2\pi h t) - \sin(2\pi h T)] \} \right. \\ &+ \sum_{h=1}^2 \frac{\theta_{h, \sin}}{k_x - k_y} \left(\frac{1}{k_x^2 + 4\pi^2 h^2} - \frac{1}{k_y^2 + 4\pi^2 h^2} \right) \times \\ &\left. \{ k_x [\exp(k_x(t - T)) \sin(2\pi h t) - \sin(2\pi h T)] + 2\pi h [\exp(k_x(t - T)) \cos(2\pi h t) - \cos(2\pi h T)] \} \right. \\ &- \frac{1}{2} \left[\frac{\sigma_x^2}{2k_x} + \frac{\rho_{xy} \sigma_x \sigma_y}{k_x(k_x - k_y)} + \frac{\sigma_y^2}{2k_x(k_x - k_y)^2} \right] \times [\exp(2k_x(t - T)) - 1] \\ &- \left[\frac{2\rho_{xy} \sigma_x \sigma_y}{k_x^2 - k_y^2} + \frac{2\sigma_y^2}{(k_x + k_y)(k_x - k_y)^2} \right] \times [\exp((k_x + k_y)(t - T)) - 1] \\ &+ \frac{\sigma_y^2}{2k_y(k_x - k_y)^2} [\exp(2k_y(t - T)) - 1] \end{aligned}$$

Define

$$\begin{aligned}
 \eta_1(t, T) &\equiv \frac{r - \sigma_x^2/2}{k_x} (\exp(k_x(t - T)) - 1) + \frac{\theta_0}{k_x - k_y} \left[\left(\frac{1}{k_x} (\exp(k_x(t - T)) - 1) - \left(\frac{1}{k_y} (\exp(k_y(t - T)) - 1) \right) \right) \right. \\
 &\quad + \sum_{h=1}^2 \frac{\theta_{h,\cos}}{k_x - k_y} \left(\frac{1}{k_x^2 + 4\pi^2 h^2} - \frac{1}{k_y^2 + 4\pi^2 h^2} \right) \times \\
 &\quad \left. \{ k_x [\exp(k_x(t - T)) \cos(2\pi h t) - \cos(2\pi h T)] + 2\pi h [\exp(k_x(t - T)) \sin(2\pi h t) - \sin(2\pi h T)] \} \right. \\
 &\quad + \sum_{h=1}^2 \frac{\theta_{h,\sin}}{k_x - k_y} \left(\frac{1}{k_x^2 + 4\pi^2 h^2} - \frac{1}{k_y^2 + 4\pi^2 h^2} \right) \times \\
 &\quad \left. \{ k_x [\exp(k_x(t - T)) \sin(2\pi h t) - \sin(2\pi h T)] + 2\pi h [\exp(k_x(t - T)) \cos(2\pi h t) - \cos(2\pi h T)] \} \right]; \\
 \eta_2(t, T) &\equiv -\frac{1}{2} \left\{ \left[\frac{\sigma_x^2}{2k_x} + \frac{\rho_{xy} \sigma_x \sigma_y}{k_x(k_x - k_y)} + \frac{\sigma_y^2}{2k_x(k_x - k_y)^2} \right] \times [\exp(2k_x(t - T)) - 1] \right. \\
 &\quad - \left[\frac{2\rho_{xy} \sigma_x \sigma_y}{k_x^2 - k_y^2} + \frac{2\sigma_y^2}{(k_x + k_y)(k_x - k_y)^2} \right] \times [\exp((k_x + k_y)(t - T)) - 1] \\
 &\quad \left. + \frac{\sigma_y^2}{2k_y(k_x - k_y)^2} [\exp(2k_y(t - T)) - 1] \right\}.
 \end{aligned}$$

Then $\alpha(t, T) = \eta_1(t, T) + \eta_2(t, T)$.

3.8.2 Appendix B

The call option formula can be obtained by noting that if $\ln[F(T_1, T)]$ is distributed as a normal random variable with mean $\varpi(t, T_1, T)$ and variance $\sigma(t, T_1, T)^2$ (use ϖ and σ^2 for short in this section), then

$$\begin{aligned} E_t^Q\{\max[F_{T_1} - K, 0]\} &= \int_{\ln(K)}^{\infty} (F_{T_1} - K) \frac{1}{\sqrt{2\pi\sigma^2}} \exp\left\{-\frac{1}{2} \left[\frac{\ln(F_{T_1}) - \varpi}{\sigma}\right]^2\right\} d\ln(F_{T_1}) \\ &= \int_{\ln(K)}^{\infty} F_{T_1} \frac{1}{\sqrt{2\pi\sigma^2}} \exp\left\{-\frac{1}{2} \left[\frac{\ln(F_{T_1}) - \varpi}{\sigma}\right]^2\right\} d\ln(F_{T_1}) \\ &\quad - K \int_{\ln(K)}^{\infty} \frac{1}{\sqrt{2\pi\sigma^2}} \exp\left\{-\frac{1}{2} \left[\frac{\ln(F_{T_1}) - \varpi}{\sigma}\right]^2\right\} d\ln(F_{T_1}) \end{aligned}$$

because $F_{T_1} > K \Rightarrow \ln(F_{T_1}) > \ln(K)$. But $\ln(F_{T_1}) > \ln(K) \Rightarrow [\ln(F_{T_1}) - \varpi]/\sigma > [\ln(K) - \varpi]/\sigma = [\ln(K) - \varpi - \sigma^2/2 + \sigma^2/2]/\sigma$. By equation (3.38), $[\ln(K) - \varpi - \sigma^2/2 + \sigma^2/2]/\sigma = [\ln(K) - \ln(F_t) + \sigma^2/2]/\sigma$, so that

$$\begin{aligned} \int_{\ln(K)}^{\infty} \frac{1}{\sqrt{2\pi\sigma^2}} \exp\left\{-\frac{1}{2} \left[\frac{\ln(F_{T_1}) - \varpi}{\sigma}\right]^2\right\} d\ln(F_{T_1}) &= 1 - N[(\ln(K/F_t) + \sigma^2/2)/\sigma] \\ &= N[(\ln(F_t/K) - \sigma^2/2)/\sigma]. \end{aligned} \quad (3.46)$$

In addition,

$$\begin{aligned} &\int_{\ln(K)}^{\infty} F_{T_1} \frac{1}{\sqrt{2\pi\sigma^2}} \exp\left\{-\frac{1}{2} \left[\frac{\ln(F_{T_1}) - \varpi}{\sigma}\right]^2\right\} d\ln(F_{T_1}) \\ &= \int_{\ln(K)}^{\infty} \frac{1}{\sqrt{2\pi\sigma^2}} \exp\left\{\ln(F_{T_1}) - \frac{1}{2} \left[\frac{\ln(F_{T_1}) - \varpi}{\sigma}\right]^2\right\} d\ln(F_{T_1}) \\ &= \int_{\ln(K)}^{\infty} \frac{1}{\sqrt{2\pi\sigma^2}} \exp\left\{\varpi + \frac{\sigma^2}{2} - \frac{1}{2} \left[\frac{\ln(F_{T_1}) - (\varpi + \sigma^2)}{\sigma}\right]^2\right\} d\ln(F_{T_1}) \\ &= \exp\left(\varpi + \frac{\sigma^2}{2}\right) \int_{\ln(K)}^{\infty} \frac{1}{\sqrt{2\pi\sigma^2}} \exp\left\{-\frac{1}{2} \left[\frac{\ln(F_{T_1}) - (\varpi + \sigma^2/2) - \sigma^2/2}{\sigma}\right]^2\right\} d\ln(F_{T_1}) \\ &= F_t \int_{\ln(K)}^{\infty} \frac{1}{\sqrt{2\pi\sigma^2}} \exp\left\{-\frac{1}{2} \left[\frac{\ln(F_{T_1}) - \ln(F_t) - \sigma^2/2}{\sigma}\right]^2\right\} d\ln(F_{T_1}) \\ &= F_t \{1 - N[(\ln(K/F_t) - \sigma^2/2)/\sigma]\} \\ &= F_t N[(\ln(F_t/K) + \sigma^2/2)/\sigma]. \end{aligned} \quad (3.47)$$

So, combining equation (3.46) and equation (3.47), we get

$$E_t^Q\{\max[F_{T_1} - K, 0]\} = F_t N[(\ln(F_t/K) + \sigma^2/2)/\sigma] - KN[(\ln(F_t/K) - \sigma^2/2)/\sigma].$$

References

- Allen, M., Ma, C., Pace, D., 1994. Over-reactions in U.S. agricultural commodity prices, *Journal of Agricultural Economics* 45, 240-251.
- Bessembinder, H., Jay C., Seguin, P., Smoller, M., 1995. Mean reversion in equilibrium asset prices: Evidence from the futures term structure, *Journal of Finance*, 50(1), 361-375.
- Black, F., 1976, The pricing of commodity contracts, *Journal of Financial Economics* 3, 167-179.
- Casassus, J., and P. Collin-Dufresne. 2005. Stochastic Convenience Yield Implied from Commodity Futures and Interest Rates. *Journal of Finance* 60, 2283-2331.
- Chen, R., Scott, L., 1993. Maximum likelihood estimation for a multifactor equilibrium model of the term structure of interest rates, *Journal of Fixed Income* 3(3), 14-31.
- Christen, A., and Fox, C. 2010. A General Purpose Sampling Algorithm for Continuous Distributions (the t-walk), *Bayesian Analysis* 5(2), 263-282.
- Duffie, D., Pan, J., Singleton, K., 2000. Transform analysis and asset pricing for affine jump-diffusions, *Econometrica* 68, 1343-1376.
- Giles, D., 2001. *Computer-Aided Econometrics*. (Marcel Dekker, New York US).
- Harvey, A., 1981. *The Econometric Analysis of Time Series* (Philip Allan Publishers, Deddington, UK).
- Hilliard, J., and Reis, J., 1998. Valuation of commodity futures and options under stochastic convenience yields, interest rates, and jump diffusions in the spot, *Journal of Financial and Quantitative Analysis* 33(1), 61-86.
- Lo, A., Wang, J., 1995. Implementing option pricing models when asset returns are predictable. *Journal of Finance* 50, 87-129.
- Miltersen, K., and Schwartz, E., 1998. Pricing of options on commodity futures with stochastic term structure of convenience yields and interest rates, *Journal of Financial and Quantitative Analysis* 33, 33-59.
- Plato, G., 1985. Valuing American options on commodity futures contracts, *Agricultural Economics Research* 37, 1-14.

Peterson, R., Ma, C., Ritchey R., 1992. Dependence in commodity prices, *Journal of Futures Markets* 12, 429-46.

Richter, M., Sørensen, C., 2002. Stochastic volatility and seasonality in commodity futures and options: The case of soybeans, Unpublished working paper, Copenhagen Business School.

Schwartz, E., 1997. The stochastic behavior of commodity prices: Implications for valuation and hedging, *Journal of Finance* 52(3), 923-973.

Sørensen, C., 2002. Modeling seasonality in agricultural commodity futures, *Journal of Futures Markets* 22(5), 393-426.

Trolle, A., Schwartz, E., 2009. Unspanned stochastic volatility and the pricing of commodity derivatives, *Review of Financial Studies* 22, 4423-4461.

Walburger, A., and Foster, K., 1995. Mean reversion as a test for inefficient price discovery in U.S. regional cattle markets, *American Journal of Agricultural Economics* 77(5), 1358-1389.

CHAPTER 4. Test of Samuelson Hypothesis in Commodity Futures Market: An Analysis Using Term Structure Models

4.1 Introduction

In an important paper Samuelson (1965) proposes that futures price return volatility will increase as the contract approaches maturity. Since Samuelson first introduced this hypothesis, many studies have investigated it from both theoretical and empirical perspectives.

Anderson and Danthine (1983) propose that the pattern will emerge if additional information about supply and demand flows into the market near maturity. Bessembinder et al. (1996) show that a necessary condition for the hypothesis to exist is the negative co-variation between the underlying asset's spot price and net cost of carry. They predict that markets for real assets, rather than financial assets, are more likely to have spot prices exhibiting mean reversion and are consequently more likely to be consistent with the Samuelson hypothesis. Their empirical results support such a prediction by finding strong evidence in agricultural and oil markets and weaker evidence in metals markets. No evidence of maturity effect is found in financial markets, this is also consistent with their model. Khoury and Yourougou (1993) investigated six agricultural commodities and found evidence of maturity effect in all the commodities that they examined. Dusak-Miller (1979) found evidence in support of the hypothesis in live cattle futures and Castelino and Francis (1982) also found support for the hypothesis in four commodity markets. Duong and Kalev (2008) find that Samuelson effect is absent in gold market. Galloway and Kolb (1996) also provide evidence for the Samuelson hypothesis in agricultural futures, but not in precious metals futures. Fama and French (1988) also find that spot prices for gold, platinum, and silver are not consistently more variable than futures (or forward) prices.

In this chapter we employ the futures pricing model that we derived in Chapter 1 to investigate the maturity effect in commodity markets. This model starts with the process generating the commodity's

spot price and convenience yield. The model predicts that when the Samuelsson hypothesis holds, there will be a non-linear relationship between volatility and maturity.

The maturity structure of futures return volatility has important implication for option pricing. Black's (1976) option model on futures implies that the volatility of the underlying return series is constant across the time to maturity of the option. If the maturity effect exists, and a trader uses constant volatility to price options, the calculated options prices will be lower than the fair value for short term options. If traders are aware of the pattern, then the implied volatility will increase as maturity approaches. Ball and Torous (1986) test this hypothesis and find that for Deutsche mark and sugar futures the implied volatility increases as time to maturity decreases. However, the evidence from gold market is mixed. In our study, three different maturity patterns are found which are shown in Figure 4.1.

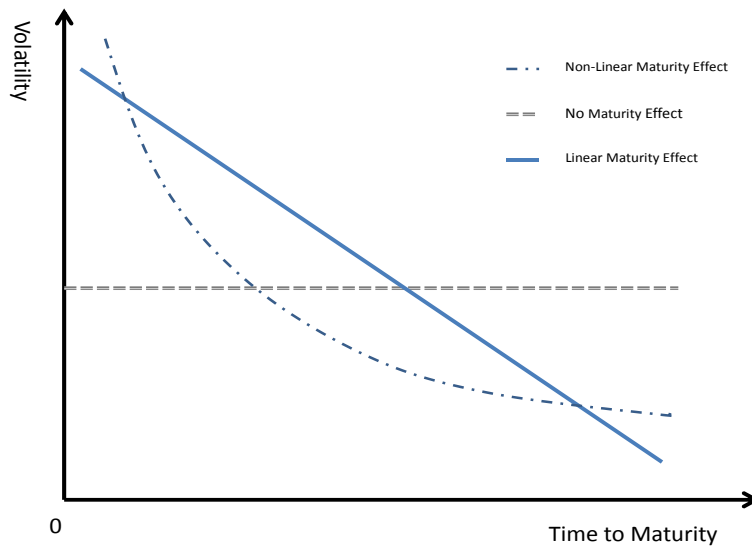


Figure 4.1: Three different patterns on futures return volatility

The horizontal line reflects the constant volatility assumed in Black's model. The straight line with the negative slope is the one found in the previous literature and the curved line emerges from our theoretical model. It is clear that when the non-linear form exists, the potential for mispricing of near to maturity options will be greatest.

The rest of the chapter is organized as follows. We derive the term structure of futures return

volatility based on the futures pricing model in section 2. Our empirical model is also proposed in this Section. Section 3 describes the data set that we employ to fit our model. Regression results are discussed in Section 4. An empirical model incorporating seasonality is proposed and estimated in section 5. The last section concludes our chapter.

4.2 Term Structure of Futures Return Volatility and Empirical Model

In this section, we use the term structure model of futures prices derived in Chapter 1 to investigate the Samuelson hypothesis. Unlike the empirical linear regression tests of Samuelson hypothesis in the literature, our analysis is based on the evolving behavior of the underlying commodity's spot price and convenience yield. Given our futures pricing formula, it is straightforward to derive the theoretical term structure of futures price return volatility using Ito's Lemma. From Chapter 1, we know the futures pricing formula can be written as:

$$\ln(F(t, T)) = \alpha(t, T) + \beta_1(t, T)x(t) + \beta_2(t, T)y(t), \quad (4.1)$$

where $dx_t = (r - \sigma_x^2/2 - c_t)dt + \sigma_x dw_x^Q(t)$, $dy_t = (u_y - k_y y_t - \lambda_y)dt + \sigma_y dw_y^Q(t)$, $\beta_1(t, T) = \exp(k_x(t - T))$, and $\beta_2(t, T) = \frac{\exp(k_x(t - T)) - \exp(k_y(t - T))}{k_x - k_y}$. Now, let us define time to maturity $\tau \equiv T - t$, then $\beta_1(\tau) = \exp(-k_x \tau)$, and $\beta_2(\tau) = \frac{\exp(-k_x \tau) - \exp(-k_y \tau)}{k_x - k_y}$.

Applying Ito's Lemma to equation (4.1), we obtain the term structure of futures return volatility implied by Model 4¹ as follows

$$\sigma_F^2(\tau) = \beta_1^2(\tau)\sigma_x^2 + \beta_2^2(\tau)\sigma_y^2 + 2\rho\beta_1(\tau)\beta_2(\tau)\sigma_x\sigma_y. \quad (4.2)$$

One interesting property of equation (4.2) is that volatility is independent of the state variables (x_t , y_t) and depends only on time to maturity of the futures contract. It implies that the return volatility is τ dependent but not t dependent. In equation (4.2) the seasonal parameters that we used to model the spot price trend, do not enter into the term structure of the futures return volatility. So, Model 1 (Model 2) will imply the same term structure of futures return volatility formula as Model 3 (Model 4). As time to maturity goes to infinity, if k_x and k_y are not equal to zero, $\lim_{\tau \rightarrow \infty} \beta_1(\tau) = 0$, and $\lim_{\tau \rightarrow \infty} \beta_2(\tau)$ is equal to zero as well. Consequently, the volatility of futures return converges to zero ($\lim_{\tau \rightarrow \infty} \sigma_F^2(\tau) = 0$

¹Model 4 is defined in Chapter 3.

). However, if we set the speed of price mean reversion parameter k_x equal to zero (as the model set up in model 3), when time to maturity approaches infinity, the volatility of futures return in this model converges to:

$$\sigma_F^2(\infty) = \sigma_x^2 + \frac{\sigma_y^2}{k_y^2} - \frac{2\rho\sigma_x\sigma_y}{k_y}. \quad (4.3)$$

The model implied volatility of return is then compared to the historical return volatility calculated from the historical cross-sectional futures prices data set. As shown in Chapter 1, models ignoring seasonality overestimate the instantaneous volatility of spot price and convenience yield, which will in turn overestimate the volatility of futures return. So, only model 3 and 4 are selected to report the model implied volatility.

Figures 4.2A, 4.2B, and 4.2C demonstrate the volatility of futures return implied by these two models for the crude oil, lean hog and soybean market, respectively. The model implied volatility is calculated by evaluating equation (4.2) at the median estimated parameter values shown in Table 3.1, 3.2, and 3.4 in Chapter 3 for lean hog, soybean and crude oil market respectively. The figures also present the historical volatility of futures return of the contracts used in the estimation of the parameters of the models. The description of the monthly data set for lean hog, soybean and crude oil market can be found in the data description section of Chapter 2 and Chapter 3.

It is surprising to see how well Models 3 and 4 fit the historical return volatility calculated from the crude oil market data from figure 4.2A, especially given the fact that only futures prices were employed in the Bayesian estimation process, and the volatility of futures return is not an input in the estimation. The only volatility that enters into the estimation procedure is the volatility of the unobserved state variables. Model 3 and Model 4 reports almost identical term structure of volatility for the crude oil market. This is not surprising, because the speed of mean reversion in spot price is found to be very low ($k_x = 0.0136$) in the crude oil market. Figure 4.2B represents the term structure of volatility on the lean hog market. The curve implied by Model 4 is close to the historical volatility. However, model 3 predicts a curve that is inconsistent with Samuelson hypothesis and also matches the historical volatility data poorly.

The lean hog market exhibits the strongest mean reversion in spot price among the markets that we have investigated. Model 3 ignores this feature and consequently predicts an inaccurate term structure

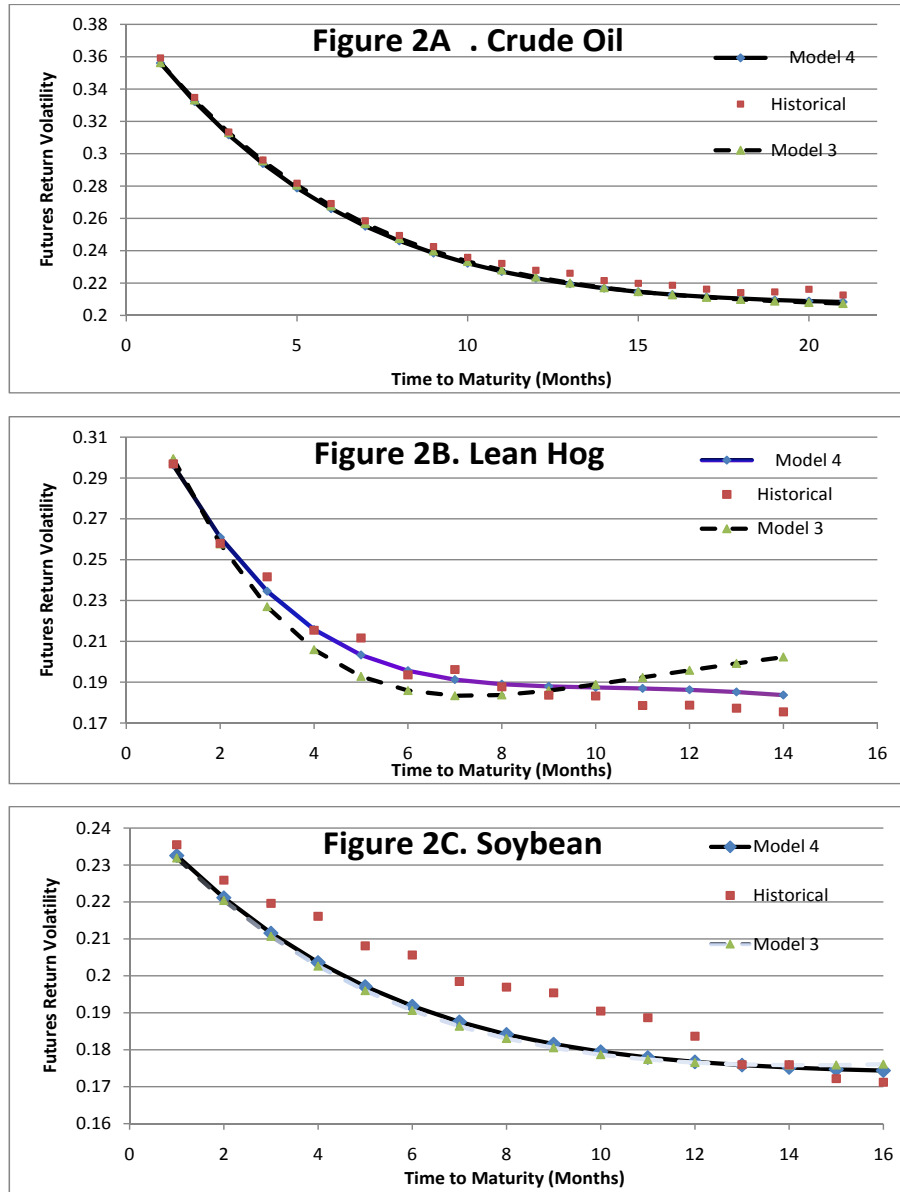


Figure 4.2: Model implied and historical volatility of futures return

of futures return volatility. If we use Schwartz’s model to estimate the futures market where mean reversion in spot price exists, the implied term structure of price return volatility can be inconsistent

with Samuelson effect.

For lean hog and crude oil market, both the historical data and the model 4 implied curve are consistent with Samuelson hypothesis. More specifically, they tend to agree that the futures return volatility decrease at a decreasing rate with respect to time to maturity. However, there is significant discrepancy between the model implied volatility and the historical volatility on the soybean market, as we can see from figure 4.2C. In this market, the historical relation between time to maturity and volatility is more linear than the model predicts, although both of them agree with Samuelson hypothesis.

In the rest of this study, we plan to empirically investigate the Samuelson effect using daily futures prices observed from ten markets. Ideally, our empirical model should be specified as

$$\sigma_F(\tau) = \sqrt{\beta_1^2(\tau)\sigma_x^2 + \beta_2^2(\tau)\sigma_y^2 + 2\rho\beta_1(\tau)\beta_2(\tau)\sigma_x\sigma_y} + \varepsilon. \quad (4.4)$$

However, this empirical model is not identifiable given futures return volatility and time to maturity data only. In other words, futures return volatility and time to maturity data are not sufficient to reveal all the information about speed of mean reversion and instantaneous volatility parameters of the underlying spot price and convenience yield processes. It is observed that τ only exists in the exponential term of the above equation. It is convenient for us to apply Taylor expansion to the right hand side of equation (4.4). Then, our empirical model can be written as follows

$$\sigma_F(\tau) = \alpha + \beta_1\tau + \beta_2\tau^2 + \beta_3\tau^3 + \beta_4\tau^4 + \dots + \varepsilon, \quad (4.5)$$

where ε is the disturbance term. β s are deterministic functions of k_x, k_y, ρ, σ_x and σ_y .

When we implement this model with the actual data set, we need to determine the number of Taylor polynomial terms that need to be included in the empirical analysis. The above regression equation is run up to 6 Taylor polynomial terms. The one reporting the smallest BIC is selected and reported in this study. The empirical results are then compared to the most popular single regressor model in literature that is used to investigate the Samuelson effect listed as follows,

$$\sigma_F(\tau) = \alpha + \beta\tau + \varepsilon, \quad (4.6)$$

where ε is the disturbance term. This is a simple linear regression of the annualized daily futures return volatility on the number of years until the contract expires. If the maturity effect does present, we expect

the coefficient β to be significantly negative. The BIC criterion is selected to compare the performance of our model with the single regressor model. If our model is more suitable to explain the maturity effect, we expect that our model will report a substantially lower BIC number.

4.3 Description of the Data

The data set utilized in this study consists of daily futures prices for 4 futures markets (energy, meats, metals and grains) from four different futures exchanges, including the New York Mercantile Exchange (NYMEX), the Chicago Mercantile Exchange (CME), the Chicago Board of Trade (CBOT) and Commodity Exchange, Inc. (COMEX). The data are recorded by and downloaded from Barchart.com, which is a leading provider of price quotes on futures and options markets.

Ten commodities are selected from these four futures markets. Crude oil and natural gas is chosen from energy market. From the meat market, we select lean hog and live cattle. Silver, gold and high grade copper are obtained from the metal market and soybean, corn and wheat are picked from the grain market.

For each of the 10 commodities, we pick 100 futures contracts most recently expired prior to August 2011.² The futures prices that are long before maturity usually have low open interest and thin trading volume. Sometimes, settlement committee, rather than market participants, determines the settlement price. Therefore, these prices are not used for analysis in our study. Suppose the maximum time to maturity with positive trading volume for commodity “ c ” is M_c days. Then the futures prices that have time to maturity more than M_c days are discarded. The resulting data set for this commodity is a $M_c \times 100$ matrix, with the i, j th element representing the futures price with $M_c + 1 - i$ days to maturity in the j th most recently expired futures contract before August 2011.

The first step of the analysis is to create a measure of volatility to represent the daily return volatility of contract prices. Many empirical works use single price series of one futures contract and follow the procedure of Bessembinder et al. (1996) to calculate the futures price return volatility. The daily futures return volatility is measured by the absolute value of the continuously compounded rate of return

²For silver market, the futures contracts that mature in February, April, June, August, October and November are traded for only about 3 months, while for futures contracts expire in the other months can be traded for more than a year. Similarly, in the gold market, contracts that expire in January, March, May, July, September and November has maximum time to maturity around 3 months. These short life span contracts are not included in our data set.

multiplied by 100. That is,

$$\sigma_{F_{t,T}} = \left| \log\left(\frac{F_{t,T}}{F_{t-1,T}}\right) \right| \times 100 \quad (4.7)$$

where $F_{t,T}$ is the settlement price on day t of a contract expiring at time T . Since our model suggests that the volatility is τ dependent and not t dependent, we can calculate $\log\left(\frac{F_{t,\tau}}{F_{t-1,\tau}}\right)$ for each of the 100 contracts that we observed. The daily realized volatility is then calculated as the standard deviation of the 100 daily returns with the same time to maturity (τ). Finally, the daily return volatility is annualized by multiplying the daily volatility by $\sqrt{252}$.³

4.4 Empirical Results

Table 4.1 and 4.2 present the results of the regression analysis for each of the 10 commodities for the one regressor OLS model and our model respectively. The table reports the coefficient estimates and the associated standard error, as well as the number of observations. Bayesian information criteria (BIC) is also reported for both empirical models for the model comparison purpose. The ten commodities that we are interested in are divided into four markets for discussion in the following subsections.

³252 is the number of trading days in a calendar year.

Table 4.1: One Regressor OLS Regression Results

	Crude Oil	Natural Gas	Lean Hog	Cattle	Silver	Gold	Copper	Soybean	Corn	Wheat
α	0.2980** (0.0029)	0.4331** (0.0048)	0.2839** (0.0030)	0.1520** (0.0016)	0.2694** (0.0050)	0.1887** (0.0027)	0.1612** (0.0026)	0.2383** (0.0031)	0.2561** (0.0031)	0.2922** (0.0033)
β	-0.0567** (0.0027)	-0.1491** (0.0044)	-0.1721** (0.0047)	-0.0750** (0.0025)	0.0068 (0.0059)	-0.0039 (0.0026)	-0.0222** (0.0035)	-0.0638** (0.0045)	-0.0563** (0.0042)	-0.0815** (0.0052)
Nobs	467	479	273	274	368	447	328	297	323	273
BIC	-1908.81	-1451.05	-1245.97	-1607.10	-1181.92	-1905.55	-1523.39	-1316.44	-1389.57	-1193.12

Note: Standard errors in parentheses. * indicates significance at 5% level. ** indicates significance at 1% level.

Table 4.2: Regression Results of Our Model

	Crude Oil	Natural Gas	Lean Hog	Cattle	Silver	Gold	Copper	Soybean	Corn	Wheat
α	0.3453** (0.0051)	0.5697** (0.0075)	0.3501** (0.0054)	0.1635** (0.0022)	0.2712** (0.0076)	0.1904** (0.0041)	0.1726** (0.0039)	0.2215** (0.0044)	0.2511** (0.0047)	0.2921** (0.0049)
β_1	-0.2591** (0.0237)	-0.7750** (0.0544)	-0.7863** (0.0686)	-0.1376** (0.0091)	-0.0008 (0.0238)	-0.0096 (0.0105)	-0.0744** (0.0135)	0.0206 (0.0172)	-0.0330* (0.0168)	-0.0807** (0.0209)
β_2	0.1899** (0.0295)	0.7276** (0.1155)	1.5075** (0.2541)	0.0570** (0.0080)	0.0052 (0.0156)	0.0032 (0.0057)	0.0397** (0.0099)	-0.0708** (0.0139)	0.0180 (0.0125)	-0.0007 (0.0185)
β_3	-0.0485** (0.0104)	-0.3459** (0.0907)	-1.4746** (0.3482)
β_4	.	0.0607** (0.0235)	0.5276** (0.1577)
Nobs	467	479	273	274	368	447	328	297	323	273
BIC	-2023.06	-1902.53	-1416.57	-1648.37	-1176.11	-1899.75	-1559.49	-1325.72	-1385.85	-1187.50

Note: Standard errors in parentheses. * indicates significance at 5% level. ** indicates significance at 1% level.

4.4.1 *Energy Market*

Crude oil and natural gas are selected from energy market to investigate the maturity effect and to compare two empirical models. It is shown in table 4.1 that one regressor OLS regression reports a significantly negative β for both commodities in the energy market. In table 4.1, the model with 3 (4) regressors reports the minimum BIC for the crude oil (natural gas) market. All the β s are significantly different from zero at the 1% significance level. Both one regressor OLS model and our model are consistent with existing literature that energy market exhibits strong Samuelson effect. However, our model is more supported by the historical data set by comparing the BIC statistics reported by two empirical models. The BIC reported by one (multiple) regressor OLS model is -1908.81 (-2023.06) and -1451.05 (-1902.53) for crude oil and natural gas market respectively. The smaller the BIC number indicates the better fitting of the model. It is considered as strong empirical evidence that model A is preferred to model B, if model A reports a BIC number that is 10 or more units smaller than the corresponding BIC reported by model B (Kass and Raftery, 1995). In our case, the difference is more than one hundred. So, we have the conclusive evidence that maturity effect exist in the energy market, and the futures return volatility decreases at a nonconstant rate as time to maturity increases.

Figure 4.3 demonstrates the historical futures return volatility data and the lines fitted by one regressor OLS model and our model. It is clear that volatility declines with contract horizon, resulting in the Samuelson effect for both commodities. Our model fits the historical data precisely. However, the one regressor OLS model underestimates the volatility with short and long time to maturity and overestimates the volatility with medium time to maturity.

4.4.2 *Livestock Market*

For the livestock market, the story is very similar to the energy market. The one regressor OLS model also reports significantly negative β , indicating the existence of maturity effect. Our model with 4 (2) regressors yields the smallest BIC in the lean hog market (cattle market). BIC statistics also suggest that our model outperforms the one regressor linear model in terms of fitting historical volatility data.

Similar to figure 4.3, figure 4.4 shows the historical and model fitted futures return volatility on

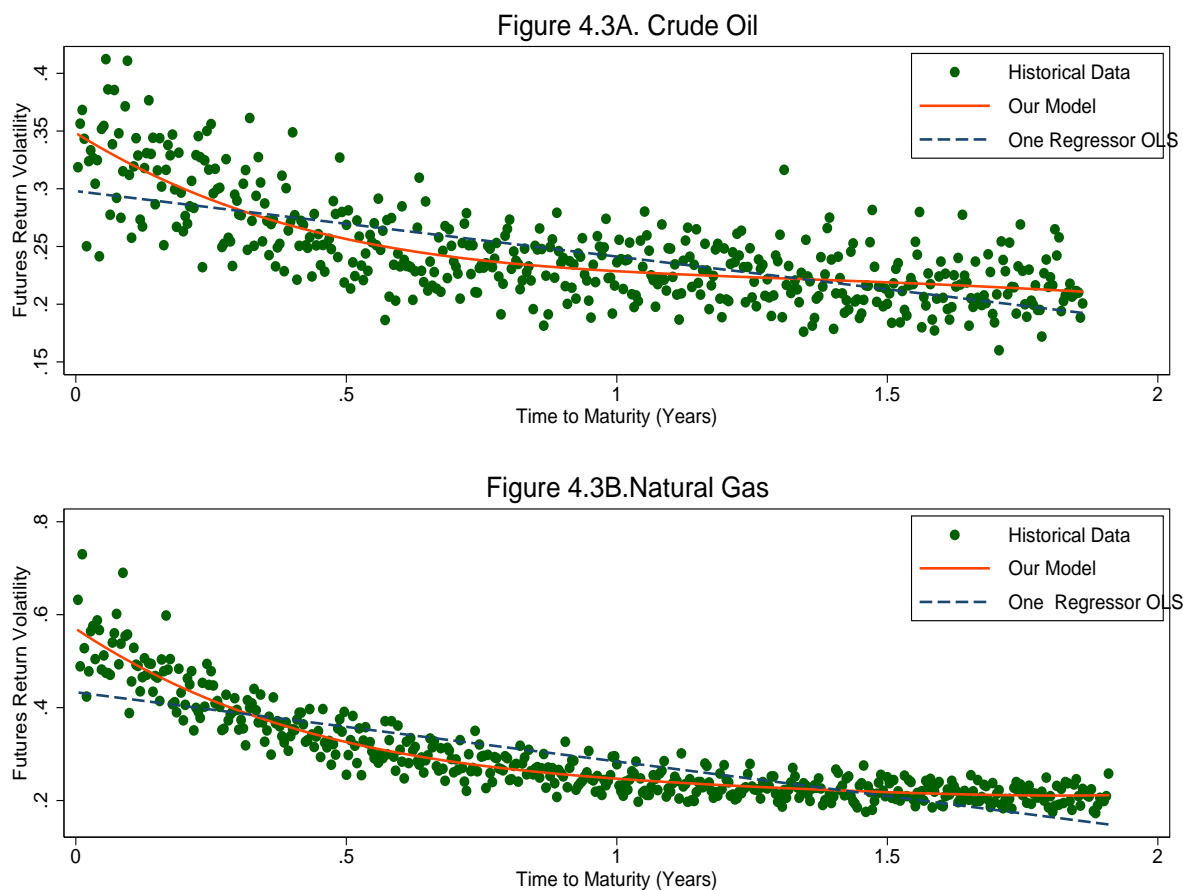


Figure 4.3: Model fitted and historical volatility of futures return on energy market

the livestock market. It provides direct evidence of Samuelson hypothesis that the closer-to-maturity contract is more volatile than those farther to maturity on the livestock market, and our model is more suitable to capture the curvature of the historical futures return volatility on the livestock market.

4.4.3 Metal Market

Most empirical studies find little or no support for Samuelson hypothesis on the metal market, especially for precious metals (Duong and Kalev, 2008; Galloway and Kolb, 1996). However, most of these studies cannot offer an explanation why Samuelson effect does not exist in the precious metal market.

From the regression results, we can see that both one regressor OLS model and our model confirm that maturity effect exists in the high grade copper market. We also get strong empirical evidence that our model is preferred to the one regressor linear model. However, the maturity effect is absent from

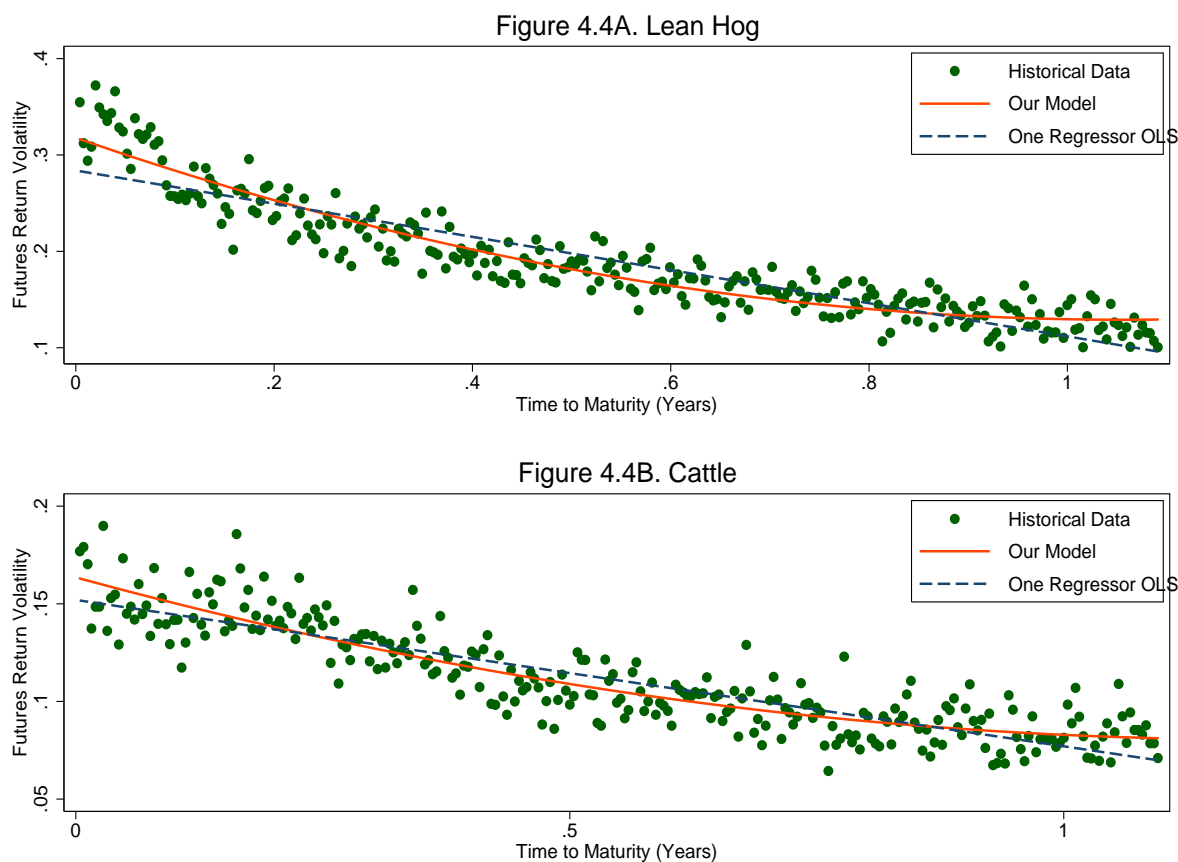


Figure 4.4: Model fitted and historical volatility of futures return on livestock market

the precious metals like gold and silver, because the parameter β (β_1, β_2) is not significantly different from zero in the one regressor (our) model. Consequently, both models yield roughly the same number of BIC, which indicates that both models have the same explanation power to the data set. Figure 4.5A and 4.5B show that the fitted line by the one regressor model overlaps with the line fitted by our model.

The empirical results for silver and gold market at the first glance do seem to be in line with our theoretical model. Cassasus and Collin-Dufresne (2005) developed a three-factor futures model for precious metals. Their model assumes convenience yield is a linear function of spot prices and interest rates. This induces mean-reversion in prices under the risk-neutral measure. These authors find that for precious metal convenience yield is small and stable. If this is true, then σ_y in our model is close to zero. These authors also find that convenience yield dependence on spot price on gold and silver market is negligible (k_x is close to zero). If we insert $\sigma_y = 0$, and $k_x = 0$ into our theoretical model (equation 4.2), it ends up with $\sigma_{F(\tau)}$ being a constant. If the commodity spot price does not exhibit mean reversion

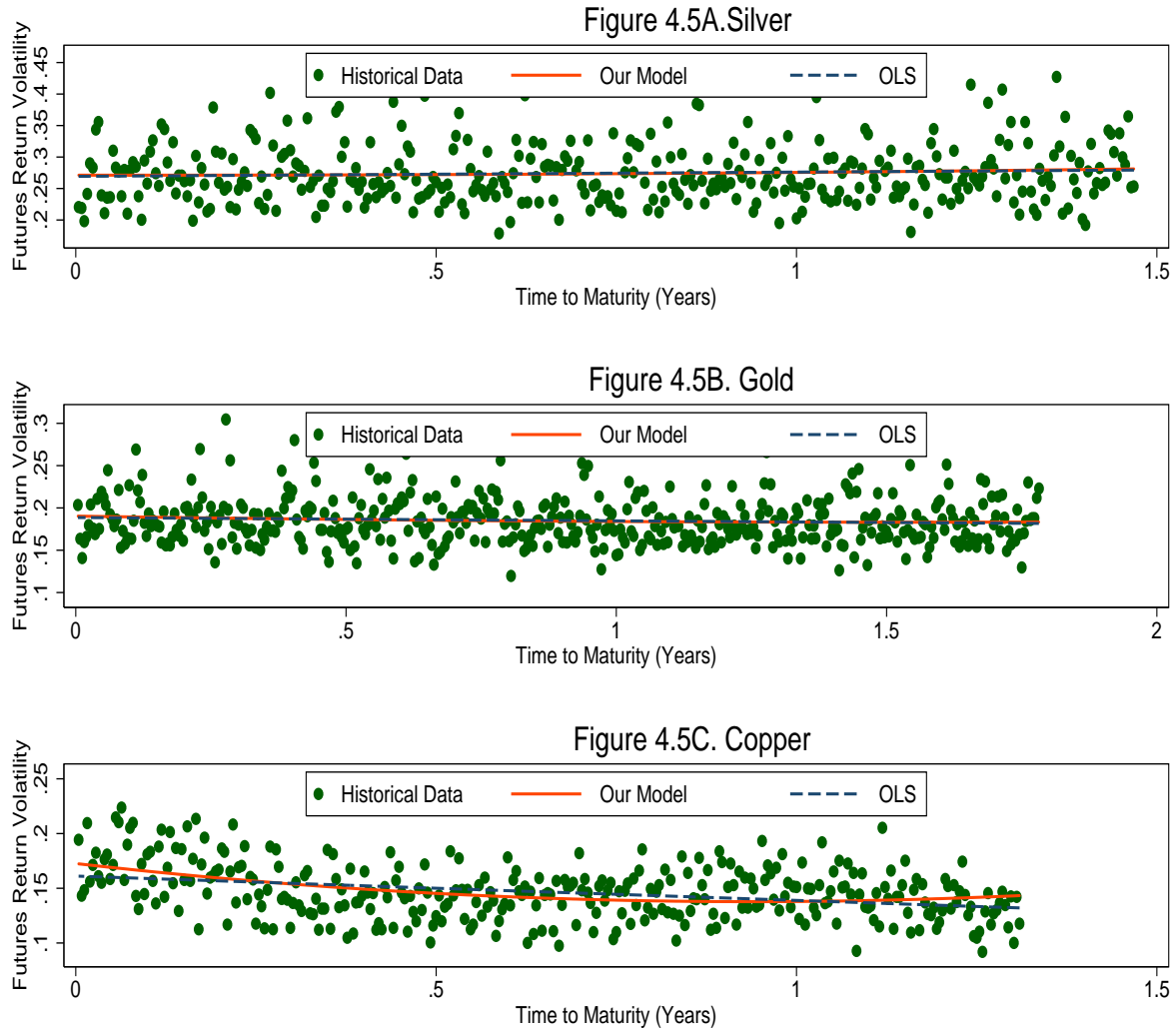


Figure 4.5: Model fitted and historical volatility of futures return on metal market

and its convenience yield is stable, the futures prices return volatility will be the same as the spot price return volatility. In this case, Samuelson effect will not be observed from the underlying market.

4.4.4 Grain Market

Most empirical studies agree that maturity effect exists on the grain markets. This effect is also significant in our analysis, since β is significantly negative in the one regressor OLS model. However, our model almost has the same explanation power as the one regressor OLS model, since the difference of BIC between the two models is small (less than 10). It is also shown in figure 4.5 that the line fitted by our model almost overlaps with line fitted by the one regressor OLS model in all three commodities.

This is inconsistent with our theoretical model, because our theoretical model suggests that if maturity effect exists, this effect is generally nonlinear.

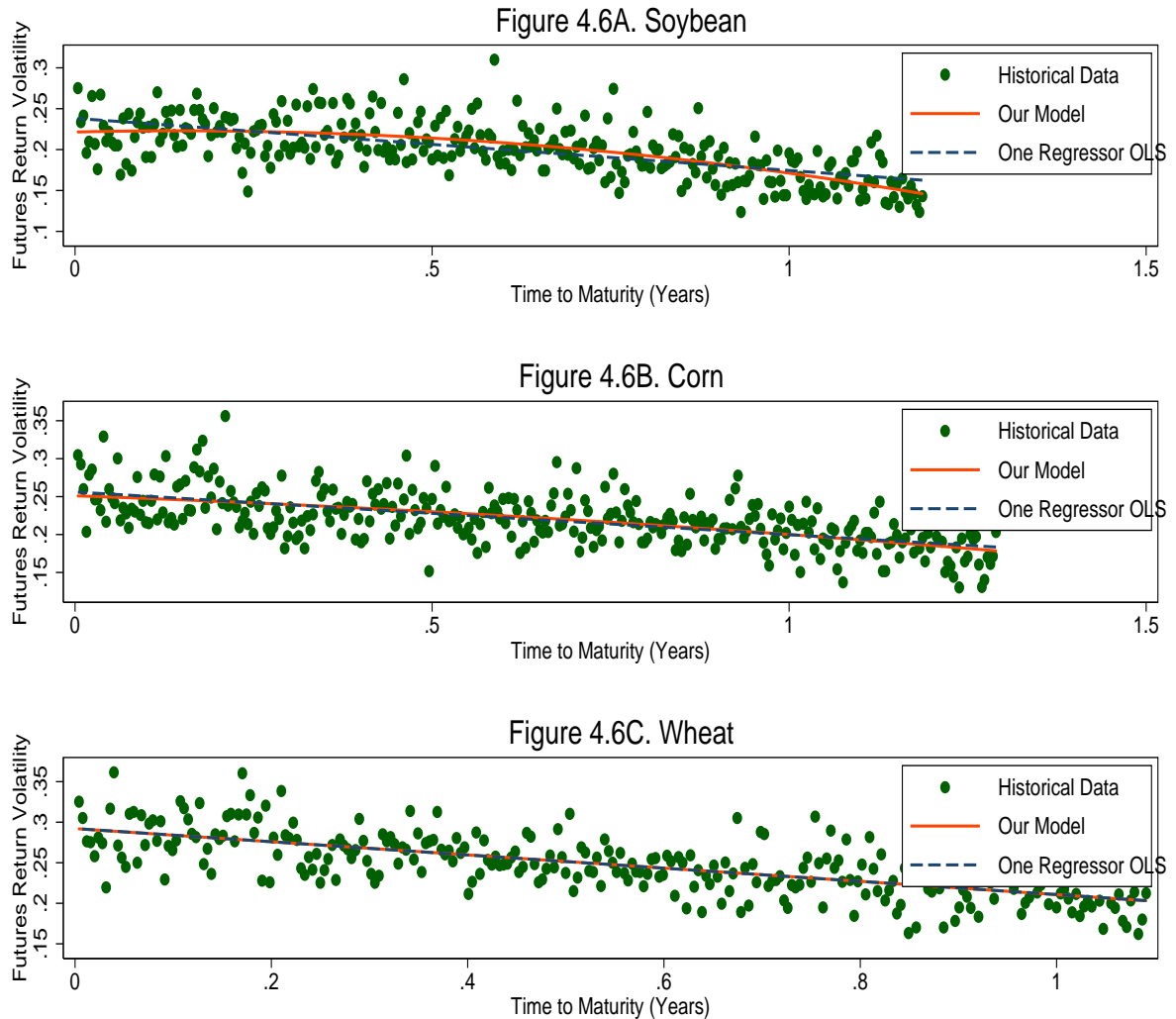


Figure 4.6: Model fitted and historical volatility of futures return on grain market

Anderson (1985) studied nine agricultural commodities and found support for the maturity effect, but concluded it is secondary to the effect of seasonality. We also explicitly model the seasonality feature of the commodity spot price, by allowing the drift term of the spot price process to be a periodic function of time. In terms of modeling futures price, our model predicts satisfactory results as we can see from Chapter 1. However, these seasonal parameters do not enter into the term structure of futures return volatility. Hence, our theoretical model cannot capture the seasonality effect in the futures return

volatility. The seasonality effect on the futures return volatility is examined in details in the next section.

4.5 *Seasonality Effect on the Futures Return Volatility*

More recently, Smith (2005) studies simultaneously traded corn futures contracts using a partially overlapping time series (POTS) model and finds support for the Samuelson effect. Smith also finds that futures return volatility exhibits strong seasonality and nonlinearity in the corn market. Karali and Thurman (2010) also find strong evidence of Samuelson effects and systematic seasonal components with volatility increasing prior to harvest times. In this section, we propose a new empirical model to answer the following questions. Does seasonality effect exist on the markets that we investigate? How the seasonality effects affect the term structure of futures return volatility? What causes the seasonality effect in the underlying market?

In order to investigate the seasonality effect, we recalculate historical volatility by grouping the contracts with same maturity month together in the way that described in the data description section. By doing so, the futures prices with same time to maturity will also be associated with the same calendar month in one subgroup. Grouping the contracts by their maturity months yields much lesser number of observations in the subgroup. So, we use the absolute value of the continuously compounded rate of return multiplied by 100 as our volatility measure. This calculation is applied to all the contracts in our sample. Then, we take the average of the volatility in the same subgroup (contracts that matured in the same month) to get the volatility measure that we use for the following analysis.

Due to seasonality, the futures return volatility is not only time to maturity τ dependent but also calendar time t dependent. So, to investigate the maturity effect and seasonality effect in the futures return volatility, the following empirical model is proposed,

$$\sigma_F(t, \tau) = \alpha + \left[\sum_{h=1}^2 [u_{h,\cos} \text{Cos}(2\pi ht/252) + u_{h,\sin} \text{Sin}(2\pi ht/252)] \right] \exp(\theta \tau) + \beta_1 \tau + \beta_2 \tau^2 + \dots + \varepsilon \quad (4.8)$$

where t is defined as the number of trading days since January 1st in one calendar year. 252 is the number of trading days in one calendar year. The sine and cosine functions are employed to capture the seasonality effect. The seasonality effect is multiplied by $\exp(\theta \tau)$ to allow for the magnitude of seasonality effect to be dependent on the time to maturity. If θ is estimated to be negative, seasonality

effect is weaker for the contracts with longer time to maturity, and vice versa. Again the number of polynomial terms and seasonality terms to be included in the analysis is determined by BIC criteria. The one that yields minimum BIC is selected and reported in the paper.

This model is implemented for all the ten markets using the data set separated by maturity month. Parameter estimates are reported in Table 4.3.

Table 4.3: Seasonality Effect on Futures Return Volatility

	Soybean	Corn	Wheat	Crude Oil	Natural Gas	Lean Hog	Cattle	Silver	Gold	Copper
α	1.1491** (0.0110)	1.2437** (0.0117)	1.4615** (0.0153)	1.7855** (0.0200)	2.7837** (0.0208)	1.0854** (0.0191)	0.7477** (0.0118)	1.2603** (0.0132)	0.7226** (0.0085)	1.2514** (0.0159)
$u_{1,cos}$	-0.1747** (0.0137)	-0.2944** (0.0170)	-0.0881** (0.0180)	0.1533** (0.0119)	0.4003** (0.0238)	-0.0602** (0.0117)	.	.	0.0359** (0.0129)	.
$u_{1,sin}$	-0.0446** (0.0081)	-0.0381** (0.0095)	0.0453** (0.0133)	0.0416** (0.0076)	-0.2958** (0.0220)	-0.0591** (0.0117)	.	0.0380* (0.0165)	.	.
$u_{2,cos}$	0.0453** (0.0080)	0.0631** (0.0099)	-0.0716** (0.0161)	.	0.2728** (0.0216)
$u_{2,sin}$	0.0467** (0.0082)	.	.	-0.0563** (0.0080)	.	.	-0.0271** (0.0075)	.	.	-0.0297* (0.0160)
θ	0.0345 (0.1102)	-0.2092* (0.0835)	-0.1295 (0.3109)	-0.3001** (0.0819)	-2.910** (0.1994)	-0.2901 (0.2965)	0.3517 (0.3989)	0.3479 (0.4652)	-0.1054 (0.2996)	0.3314 (0.3245)
β_1	-0.2200** (0.1630)	-0.3174** (0.0160)	-0.4217** (0.0247)	-2.1921** (0.1481)	-4.4620** (0.1509)	-0.5033** (0.1517)	-0.3711** (0.0933)	-0.0455 (0.0160)	-0.0170 (0.0104)	-0.0351** (0.0101)
β_2	.	.	.	2.8556** (0.3225)	4.4986** (0.3217)	-2.6347** (0.3227)	-0.3909* (0.1986)	.	.	.
β_3	.	.	.	-1.8068** (0.2597)	-2.2061** (0.2536)	1.5899** (0.1944)	0.3872** (0.1196)	.	.	.
β_4	.	.	.	0.4241** (0.691)	0.4214** (0.0660)
<i>Nobs</i>	2072	1610	1360	5592	5736	1904	1638	2202	2676	3924
<i>BIC</i>	113.82	-88.29	401.30	2338.23	2963.50	-662.62	-2327.47	1041.28	-1079.03	608.16

Note: Standard errors in parentheses. * indicates significance at 5% level. ** indicates significance at 1% level.

Table 4.3 shows that seasonality effect is significant in all the gain markets. Three (four) significant seasonal parameters are selected by the data set in the soybean market (corn and wheat market).

In the grain market, the information about the production of grain arrives at a nonconstant rate throughout a year. Consequently, the futures return volatility driven by information exhibits seasonality. The parameter θ is found to be significantly negative on the corn market and insignificant on the soybean and wheat market, which indicates that the magnitude of seasonality effect decreases with time to maturity on the corn market but remains about the same in the other two markets. Maturity effect still exists on the grain market, even if we separate the seasonality effect from the futures return volatility, since β_1 is significantly negative on all the grain markets investigated. However, excluding

the seasonality effect, the maturity effect is still linearly decreasing with time to maturity.

The seasonality effect in the grain market is plotted in figure 4.7.

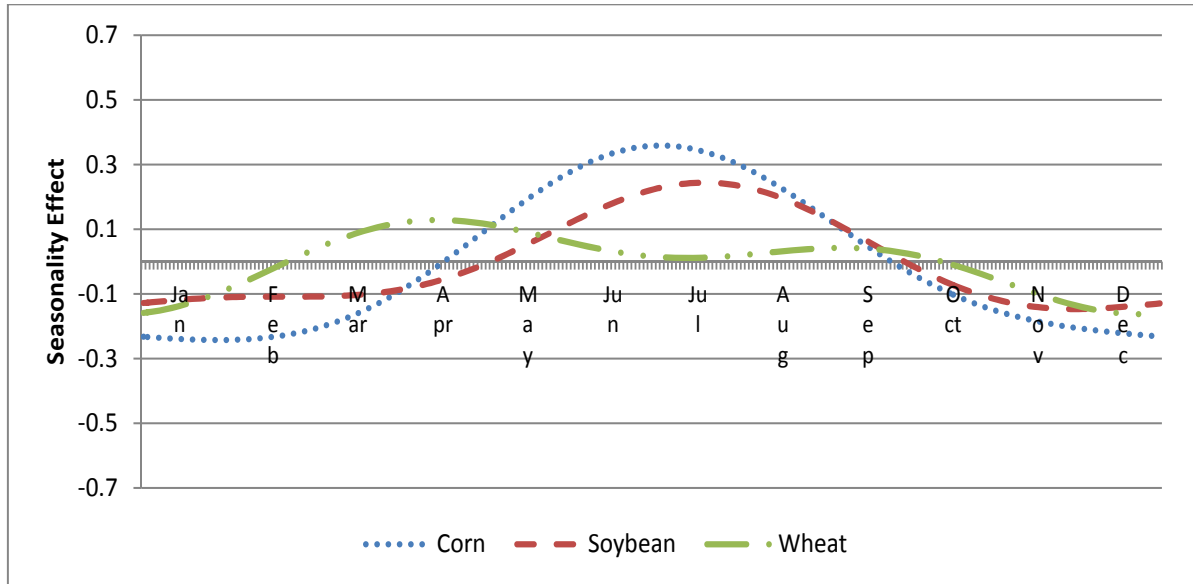


Figure 4.7: Seasonality effect in the grain market

Figure 4.7 plots the seasonal cycles implied by the estimated periodic coefficients. It reveals substantial seasonality in futures return volatility in grain market. Corn and soybean market have similar seasonal pattern on their futures return volatility. It is because these two crops have similar planting and harvesting period. Their seasonal effect is quite different from that revealed in the wheat market. This is true because wheat has a different planting and harvesting period. In the corn and soybean market, volatility peaks during the summer season, when information on changing weather conditions has the most direct impact on grain supply. The harvest resolves much of the uncertainty about the supply of soybean and corn, so volatility decreases after the harvest season.

The seasonality of futures return volatility is also significant in the energy market. As we can see from Table 4.3, three seasonal parameters are included in the empirical analysis that yields minimum BIC. The seasonal effect decreases with time to maturity in the energy market, since θ is found to be significantly negative in the both markets. The speed of decreasing is especially fast in the natural gas market due to the large negative value of θ . The seasonality effect is expected to be leveled off by half within 2.9 months.

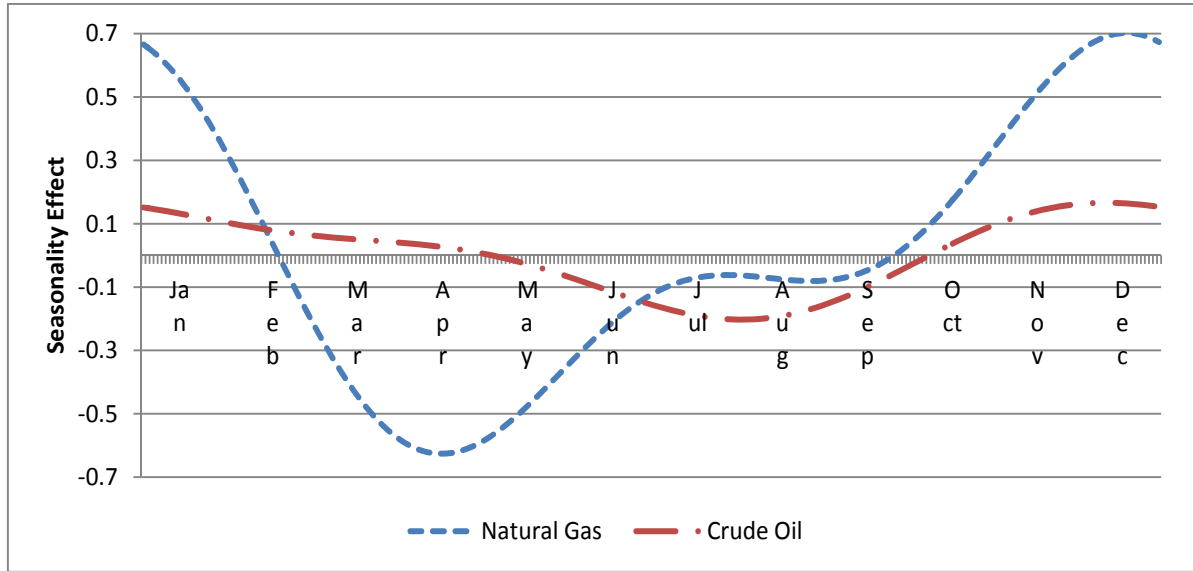


Figure 4.8: Seasonality effect in the energy market

The seasonality effect on the natural gas market is mainly from the demand side. As we can see from figure 4.8 the effect peaks during the winter season, when the weather condition reveals the most information about the demand of natural gas. A colder than normal Winter results in much higher natural gas demand, higher gas prices, while a warmer than normal winter induces lesser demand, lower gas price. This results in additional price volatility for the winter season contingent on warmer or cooler weather. However, weather does not have the long-term impact on natural gas' futures price return volatility, due to the large and significantly negative θ . This is because the demand revealed in the current winter has little impact on the demand surprise for the following months or the next winter.

As can be seen in Figure 4.8 crude oil futures return volatility also peaks in the winter season. Compared to the natural gas market, the magnitude of the seasonal effect in the crude oil market is small. While there are reasons to expect higher natural gas volatility in the winter season, it is less obvious on crude oil market. According to Fleming, Kirby and Ostdiek (2006), crude oil prices are not typically weather sensitive because over 90% of U.S. oil consumption is for transportation and industrial uses which are not sensitive to the weather. Therefore, the issue concerning a seasonal pattern in crude oil futures return volatility is subject to empirical evidence.

Figure 4.9 and 4.10 show seasonality effect on the futures return volatility in meat and metal markets. While there is only one seasonal term that is selected by the criteria of minimum BIC, the magnitude

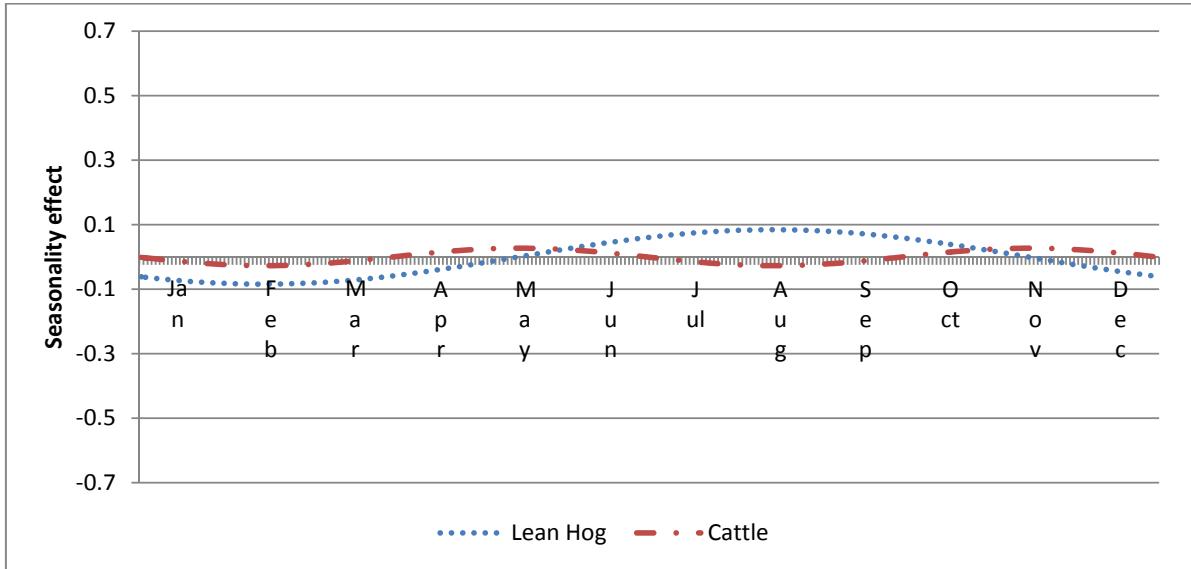


Figure 4.9: Seasonality effect in the meat market

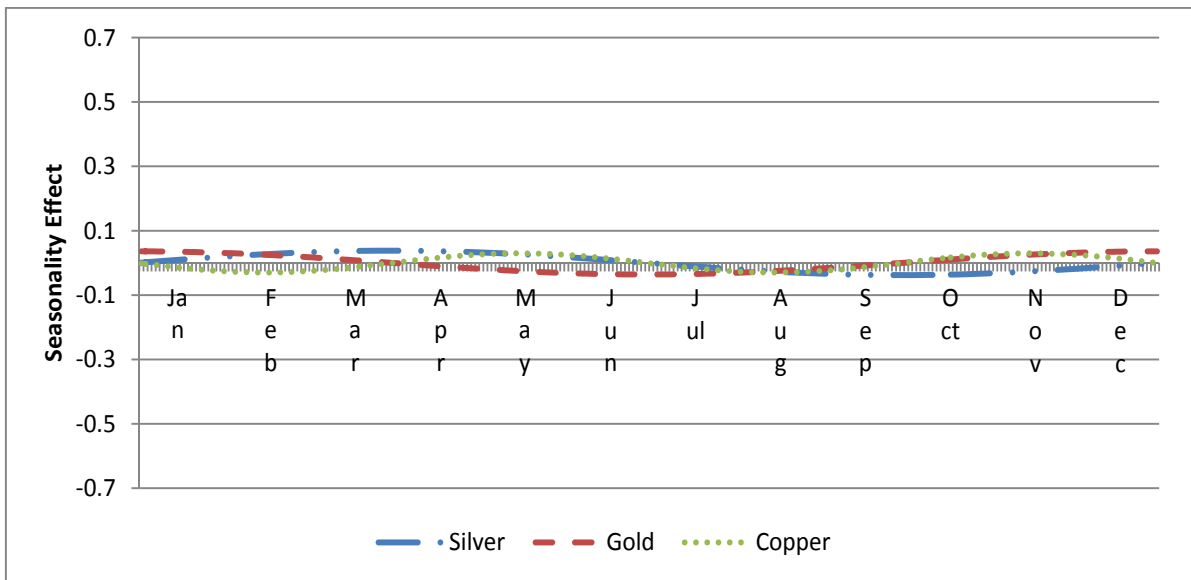


Figure 4.10: Seasonality effect in the metal market

of seasonality effect is also relatively small compared to the energy and grain market. The seasonal effect is statistically significant suggested by the data. However, due to its small magnitude it has little economic importance. After we incorporate the seasonality effect into analysis, the maturity effect is still absent from the gold and silver market.

4.6 Conclusion

In this chapter, we derive a term structure model of futures return volatility based on the futures pricing model that we proposed in Chapter 1. This model is then used to test the Samuelson hypothesis in the commodity futures market. The data set that we employed to test the hypothesis is organized in a different way from other researchers do in exploring the maturity effect. Our model suggests that for a given commodity market the volatility depends only on time to maturity. Therefore, we group 100 most recently expired contracts and calculate the return volatility on the futures prices with same time to maturity, instead of using single contract price to measure the return volatility. Compared to the existing models in the literature, our model has the following improvements. First, our model suggests that if the maturity effect exists, this effect is generally nonlinear. This is confirmed by the data set that we observed from energy and livestock market. Second, our model can also be utilized to explain why the maturity effect does not exist in the precious metal market. However, there is no significant improvement on our model in explaining structure of futures return volatility in the grain market, where the maturity effect is linear even if we control for seasonal effects.

We propose another empirical model to separate the seasonal and maturity effects. We find strong empirical evidence to support the seasonal pattern in the futures return volatility on the grain market and energy market. The seasonality effect in grain markets (energy markets) is mainly caused by the uncertainty revealed from the production side (demand side). According to our data set, a seasonal effect also exists in the metal and meat market. However, its magnitude is much smaller compared to the energy and grain market. The maturity effect still exists when we include the seasonal effect, in all the markets except precious metals.

References

- Anderson, R.W., Danthine, J., 1983. The time pattern of hedging and the volatility of futures prices. *Review of Economic Studies*, 50: 249–266.
- Anderson, R.W. 1985. Some Determinants of the Volatility of Futures Prices, *The Journal of Futures Markets*, 5: 331–348.
- Ball, C., Torous, W., 1986. Futures options and the Volatility of Futures Prices. *Journal of Finance*, 41: 857-870.
- Bessembinder, H., Coughenour, J.F., Seguin, P.J., Smoller, M.M., 1996. Is there a term structure of futures volatilities? Re-evaluating the Samuelson hypothesis. *Journal of Derivatives* 4: 45–58.
- Black, F., 1976, The pricing of commodity contracts, *Journal of Financial Economics* 3, 167-79.
- Casassus, J., and P. Collin-Dufresne. 2005. Stochastic Convenience Yield Implied from Commodity Futures and Interest Rates. *Journal of Finance* 60: 2283–2331.
- Castelino, M.G., and Francis, J.C. 1982: Basis Speculation in Commodity Futures: The Maturity Effect, *The Journal of Futures Markets*, 2: 195–206.
- Duong, H. N., Kalev, P. S. 2008. The Samuelson hypothesis in futures markets: An analysis using intraday data. *The Journal of Banking and Finance*, 32: 489–500.
- Dusak-Miller, K. 1979. The Relation Between Volatility and Maturity in Futures Contracts, Leuthold, R.M. (ed.), *Commodity Markets and Futures Prices*, Chicago Mercantile Exchange, 25–36.

Fama, E., and French, K. 1988. Business cycles and the behavior of metals prices. *Journal of Finance* 43: 1075–93.

Fleming, J., Kirby, C. and B.Ostdiek, 2006, Information, Trading and Volatility: Evidence from Weather-Sensitive Markets, *Journal of Finance* 61, 2899-2930.

Galloway, T.M., Kolb, R.W., 1996. Futures prices and the maturity effect. *Journal of Futures Markets* 16: 809–828.

Karali, B. and W. N. Thurman. 2010. Components of grain futures price volatility. *Journal of Agricultural and Resource Economics*, 35: 167–182.

Kass, R. and Raftery, A., 1995. Bayes Factors. *Journal of the American Statistical Association* 90: 773–795.

Khoury, N. and Yourougou, P., 1993. Determinants of agricultural futures prices volatilities: Evidence from Winnipeg Commodity Exchange, *Journal of Futures Markets*, 13(4): 345-56.

Samuelson, P.A., 1965. Proof that properly anticipated prices fluctuate randomly. *Industrial Management Review* 6: 41–49.

Smith, A., 2005. Partially Overlapping Time Series: A New Model for Volatility Dynamics in Commodity Futures. *Journal of Applied Econometrics* 20: 405–422.

CHAPTER 5. SUMMARY AND DISCUSSION

In the preceding chapters, we propose a two-factor affine term structure model for the purpose of pricing commodity futures and options contracts in Chapter 2 and Chapter 3 respectively. Our model captures two key features on renewable commodities markets, price mean reversion and seasonality. Maturity effect and seasonality effect of futures return volatility is analyzed in Chapter 4. I summarize the main contributions of my dissertation in the following section.

5.1 Summary of Methods and Contributions

With the purpose of developing a method to estimate the long-term futures curve for agricultural futures, we generalize Schwartzs two-factor model, in Chapter 2, by allowing for both mean reversion in spot prices and seasonality. Given that one of the key issues in the development of longer-term futures is the confidence market players have in constructing long-term futures curves, a Bayesian MCMC algorithm is developed to estimate our model. Monthly lean hog and soybean futures data are employed to fit our model using the Bayesian algorithm. According to the the Bayesian deviance information criterion, two model innovations (price mean reversion and seasonality) are highly favored by the actual data set that we observed from the futures markets. The proposed theoretical model and empirical methods also provide a streamlined way to produce credible intervals for the projections of long-term futures curves, which are the key information needed for successfully construct the swap contract.

Based on the same affine term structure model, closed-form option pricing formulas are derived in Chapter 3. Our option pricing model incorporates mean reversion to long-run production costs that was found in lean hog and soybean markets, and as a result it provides option premia that are significantly lower than in the Black or Schwartz models. This is the key finding of Chapter 3 and it suggests that

the inappropriate use of these other models will result in overpricing of long-term options in renewable commodity markets. And, in fact, these markets suffer from a lack of trading for long-term options. Clear seasonal patterns are also found in agricultural commodity markets. Our option pricing model that incorporates seasonality also shows a decrease in the size of options premia.

In Chapter 4, we derive a term structure model of futures return volatility based on the futures pricing model that we proposed in Chapter 2. This model is employed to test the Samuelson hypothesis in the commodity futures market. Our model suggests that for a given commodity market the futures return volatility depends only on time to maturity. Therefore, we group 100 most recently expired contracts and calculate the return volatility on the futures prices with same time to maturity, instead of using single contract price to measure the return volatility. Compared to the existing models in the literature, our model has the following improvements. First, our model suggests that if the maturity effect exists, this effect is generally nonlinear. This is confirmed by the data set that we observed from energy and livestock market. Second, our theoretical model can also be utilized to explain why the maturity effect does not exist in certain markets such as silver and gold. Seasonal effect is also modeled and tested in our empirical model. It is found that seasonal effect is significant in grain and energy market and week in the metal and meat market. However, the maturity effect remains largely unaltered even after we control for seasonal effect in the futures return volatility.